

# Bio-electric Space Exploration

## Final Report

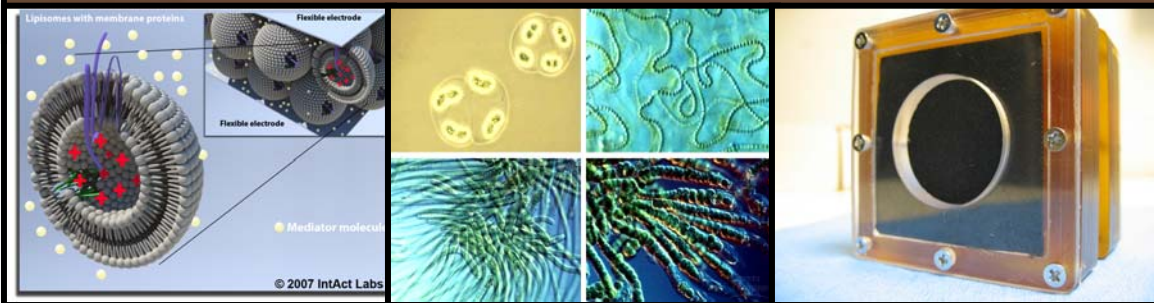
May, 2007

IntAct Labs LLC



PI: Matthew Silver  
Co-I: Kranthi Vistakula

NASA Institute for Advanced Concepts Phase I Grant (CP 06-01)  
September 2006 – April 2007



*- This page is intentionally blank -*

## Table of Contents

<b>1</b>	<b>INTRODUCTION.....</b>	<b>5</b>
<b>2</b>	<b>OUTREACH AND TEAM.....</b>	<b>7</b>
2.1	OUR TEAM .....	7
2.2	CONTACTS RELEVANT FOR POTENTIAL PHASE II EFFORT .....	7
2.3	SYNTHETIC BIOLOGY COMMUNITY .....	8
2.4	RESEARCH CENTER.....	8
<b>3</b>	<b>DATABASE.....</b>	<b>10</b>
3.1	SUMMARY OF RESULTS .....	10
3.2	DATABASE TOOL .....	11
3.3	DESIGN SPACE .....	13
3.4	CATEGORIES .....	13
<b>4</b>	<b>MOLECULE AND MECHANISM ANALYSIS.....</b>	<b>15</b>
4.1	PIEZOELECTRIC PROTEINS.....	15
4.1.1	<i>Prestin.....</i>	15
4.1.2	<i>Mechanosensitive Ion Channels .....</i>	18
4.1.3	<i>Summary of Piezo Electric Proteins.....</i>	20
4.2	PHOTO-ELECTRIC PROTEINS .....	20
4.2.1	<i>Overview of Photosynthesis.....</i>	21
4.2.2	<i>Photosystem II .....</i>	21
4.2.3	<i>Photosystem I.....</i>	22
4.2.4	<i>Rhodopsin.....</i>	23
4.2.5	<i>Biological Solar Cells.....</i>	23
4.2.6	<i>Optimization of Photo-Active Proteins.....</i>	25
4.2.7	<i>Photo-Active Protein Summary .....</i>	26
4.3	ELECTRICIGEN MICROBES AND MICROBIAL FUEL CELLS.....	27
4.3.1	<i>Introduction .....</i>	27
4.3.2	<i>Microbial Fuel Cells: Mechanism Overview.....</i>	28
4.3.3	<i>Literature Review: What has been built?.....</i>	30
4.3.4	<i>Microbial Fuel Cell Optimization.....</i>	32
4.4	ELECTROSTATIC ORGANISMS .....	33
4.4.1	<i>Introduction .....</i>	33
4.4.2	<i>Electrostatic Mechanism Analysis.....</i>	33
4.5	NEW MECHANISMS & MECHANISM-APPLICATION OVERLAP .....	35
4.5.1	<i>Photocells: Geobacter and Rhodopsin .....</i>	35
4.5.2	<i>Piezocells: Geobacter and Prestin .....</i>	36
4.6	MECHANISM SUMMARY .....	36
<b>5</b>	<b>EVALUATION CRITERIA.....</b>	<b>37</b>
5.1	POWER SYSTEM METRICS .....	37
5.2	SUPPLY SIDE: COMPARISON TO EXISTING SPACE POWER SYSTEMS .....	38
5.3	DEMAND SIDE: TAILORING METRICS TO APPLICATIONS .....	39
5.4	CONSIDERATIONS FOR MECHANISM-SPECIFIC COST BENEFIT ANALYSES.....	40
5.4.1	<i>Piezoelectric Proteins.....</i>	40
5.4.2	<i>Biological versus Conventional Solar Cells.....</i>	40
5.4.3	<i>Microbial Fuel Cells.....</i>	42
5.4.4	<i>Comparing Electrostatic Organisms .....</i>	42
5.5	EVALUATION CRITERIA CONCLUSION .....	43
<b>6</b>	<b>POWER SKINS BASED ON PIEZOELECTRIC PROTEINS.....</b>	<b>44</b>

6.1	INTRODUCTION AND APPLICATIONS.....	44
6.1.1	<i>Power Estimate</i> .....	45
6.2	POTENTIAL ARCHITECTURES.....	48
6.2.1	<i>Architecture 1: Power Skin Based on Synthetic Lipid Membranes</i> .....	48
6.2.2	<i>Power Skin Architecture 2: Living Power Skin</i> .....	52
6.3	EXPERIMENTS.....	53
6.4	CONCLUSION AND FUTURE WORK.....	55
<b>7</b>	<b>MICROBIAL FUEL CELLS IN SPACE: BIOELECTRIC CHAMBERS.....</b>	<b>56</b>
7.1	MISSION SCENARIOS AND HIGH-LEVEL POWER ESTIMATES.....	56
7.1.1	<i>Interplanetary Transit</i> .....	56
7.1.2	<i>Lunar Surface Operations</i> .....	57
7.1.3	<i>Mars Surface Operations</i> .....	57
7.1.4	<i>Upper Bound Power Estimates</i> .....	58
7.1.5	<i>Power Estimates for Mission Models</i> .....	61
7.1.6	<i>Systems Analysis</i> .....	62
7.2	DETAILED DESIGN CONSIDERATIONS: MFCs IN ADVANCED LIFE SUPPORT.....	64
7.2.1	<i>Microbe Selection</i> .....	65
7.2.2	<i>Detailed Waste Stream Models</i> .....	68
7.2.3	<i>Bioreactor Selection and Design</i> .....	71
7.2.4	<i>Materials Selection and Anode Design</i> .....	72
7.3	FUEL CELL GEOMETRY: A SIZING MODEL.....	73
7.3.1	<i>Architecture 1: Tubular Microbial Fuel Cells</i> .....	73
7.3.2	<i>Architecture 2: Reverse Tubular Fuel Cell (gravity compensation)</i> .....	75
7.3.3	<i>Fuel Cell Geometry Analysis Conclusions</i> .....	76
7.4	EXPERIMENTS.....	77
7.4.1	<i>Microbial Fuel Cell Test Chamber</i> .....	78
7.4.2	<i>Coupling Geobacter and Rhodopsin</i> .....	81
7.5	MFC CONCLUSIONS.....	84
<b>8</b>	<b>CONCLUSION.....</b>	<b>86</b>
	<b>APPENDIX-I: EXPERIMENTAL PROCEDURES FOR POWER SKIN.....</b>	<b>87</b>
	<b>APPENDIX II: DETAILED MFC EXPERIMENT REVIEW.....</b>	<b>94</b>
	<b>APPENDIX III: MICROBES IN ADVANCED LIFE SUPPORT.....</b>	<b>99</b>
	<b>APPENDIX IV: MATLAB CODE FOR SIZING MODEL.....</b>	<b>102</b>
	<b>BIBLIOGRAPHY.....</b>	<b>103</b>

# 1 Introduction

This report summarizes work completed by IntAct Labs under the NASA NIAC Phase 1 research grant (CP 06-01) titled “Bioelectric Space Exploration.” The goal for this project was to analyze the potential to use biological molecules and mechanisms as the basis for space power systems and to create conceptual designs and initial prototypes to validate specific end-applications.

In the first half of the research period (September through December) we took a broad look at the field of bio-electric energy across multiple scales in order to build a comprehensive database of molecules and mechanisms and set the groundwork for more detailed design of specific applications and prototyping. In addition to establishing the state of the art in various aspects of this nascent field, our background research identified specific technical hurdles to the successful exploitation of various biological mechanisms and molecules both on Earth and for space exploration. It also uncovered some exciting possibilities not discussed explicitly in the original proposal, which we have investigated further. For example, a major experimental endeavor undertaken in the second half of the project involved coupling two electrically active biological entities: the photo-active protein Bacterial Rhodopsin to the electricigenic microbe *Geobacter sulfurreducens*. This objective was chosen based on work done in the first half of the phase I contract.

In the second half of the research period (January through April) we down-selected two specific mechanisms for further study, moving from general survey of the bio-electric field to the design of end-architectures, computer models, power estimates, and laboratory experiments. For this detailed development, we chose (1) Power Skins, based on piezoelectric proteins, and (2) bio-electric chambers, based on microbial fuel cells powered by electrigen microbes.

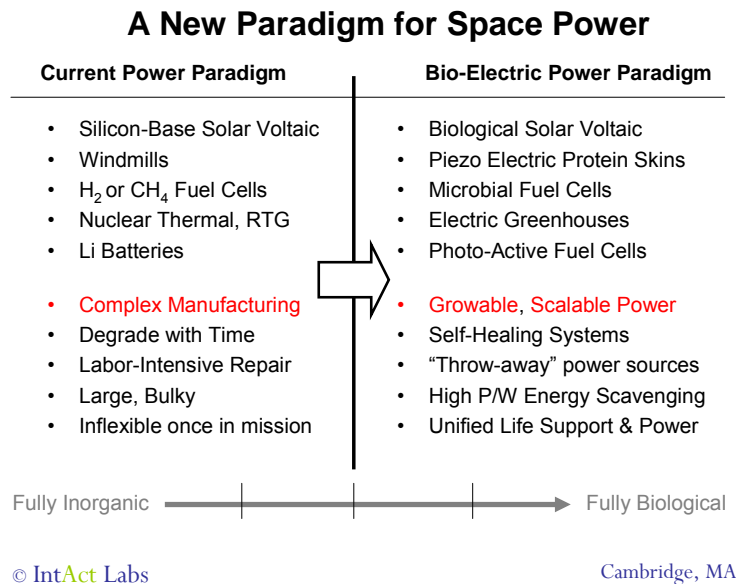


**Figure 1: A new paradigm for space power.**

As a whole, our research confirmed our initial claim that this nascent field has revolutionary potential for how we explore the universe. Biological systems exhibit extraordinary properties, both macro-scale and nano-scale, optimized over billions of years. Our current level of sophistication in biological and mechanical engineering is adequate to exploit these properties. Towards this end, we have identified specific components that can be applied to multiple systems, manufactured in tandem using a limited number of “biological factories.” With adequate development efforts, we believe these technologies could be deployed within the coming decade. Regardless of how such a project is carried forward, the era of biological machines and power sources based on synthetic biological processes has arrived. NASA, and the space exploration community at large, have much to gain from developing and employing such systems in order to help humans live more safely and sustainably on or off the Earth.

The following report is arranged as follows: Chapter 2 reviews outreach and team-related issues activities of the project. Chapter 3 describes the biological database we created and its implications for understanding the design space. Chapter 4 provides an in-depth examination of four main classes of electrically relevant biological molecules and mechanisms that we identified. Chapter 5 summarizes our thinking on down-selection metrics and comparisons to existing power systems. Chapter 6 presents our deeper analysis, models and experiments for the Power Skin concept. Chapter 7 presents our deeper analysis, models and experiments for the Bio-Electric Life-Support Chamber. Our concluding thoughts are presented in Chapter 8.

## 2 Outreach and Team

The topic of direct energy production from biological sources inspires and engages researchers and students in diverse fields. As importantly, a project as multidisciplinary as ours requires integration of diverse set of detailed technical knowledge. For these reasons, we established communication with a number of individuals who are leaders in fields relevant to bio-mimetic or bio-electric energy conversion. We believe these contacts and conversations position us to expand our research with outside team members in the future.

### 2.1 The Bio-electric Team

During the phase I effort we benefited from the help of people both directly and indirectly involved with the project. The project was lead by IntAct Labs. Payload Systems Inc. provided space systems engineering advice and aided with experiments and fabrication. Consultants at MIT provided important advice on feasibility and research direction.

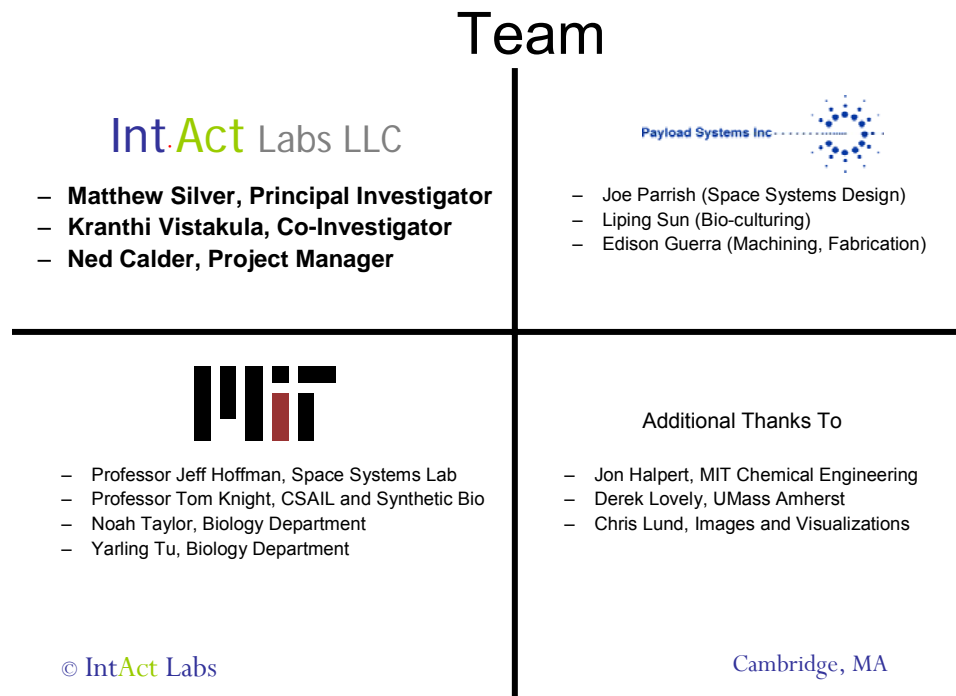


Figure 2: Bio-electric Space Exploration Team.

### 2.2 Contacts Relevant for Potential Phase II Effort

In addition to our core team, we spoke with experts in different fields relevant to the effort. The following researchers could be involved with further research in the area.

**Professor Derek Lovely**, *University of Massachusetts, Amherst*

Professor Lovely's research is focused on the physiology and ecology of novel anaerobic microorganisms. He is a recognized expert in the area of microbial fuel cells and also head of the Geobacter Project, a major research initiative funded primarily by the Department of Energy. Our conversation with Dr. Lovely has raised the possibility of collaboration during a potential phase II effort. We will explore this possibility later.

**Professor Bruce Rittmann**, *Arizona State University, Tempe Arizona*

Professor Rittmann's work focuses on engineering and microbiological systems. One of his substantive research interests is microbial fuel cells, for which he has conducted basic scientific research for NASA. We had the opportunity to meet with Dr. Rittman in person before the NIAC conference in Tucson.

**Dr. Bruce Logan**, *Pennsylvania State University, University Park, PA*

Dr. Logan is the Director of the Engineering Environmental Institute and the Hydrogen Energy Center at Penn States. He is a recognized expert on microbial fuel cells and waste remediation. We have spoken with Dr. Logan about potential collaboration under a NASA NIAC phase II project.

**MIT Undergraduate Outreach:** Intact Labs enabled undergraduates at MIT to participate in the project through the MIT Undergraduate Research Opportunities Program (UROP). Through this program, we encouraged young researchers to become involved in the area of bio-energy and space systems design.

## 2.3 Synthetic Biology Community

Our discussions with Dr. Tom Knight revealed synergies between our database efforts and those of the wider synthetic biology community. In particular, members of this community at MIT are actively building a registry of biological parts for use as building blocks of biological machines. Our discussions with members of this community informed our choice of citation management tools and database design.

## 2.4 Research Center

Direct biologically-based means of energy generation is an emerging field. We are laying the groundwork for this field by taking a broad looking at the research space. However, nascent research areas can benefit from a center of mass from which to stimulate other research in the field and provide the seed for the growing community. NASA has invested in a number of such efforts. One example is the 'University Space Engineering Centers', which are modeled on the NSF's Engineering Research Centers. There were originally nine (later reduced to eight) research centers based at universities that focused on specific areas of importance to NASA (e.g. Mars Mission Research Center at North Carolina State University). Broader engagements also exist. For example, the Ohio Space Grant Consortium, which is administrated by NASA but receives funding from Congress and contains both NASA centers (i.e. Glenn), industry,



and academia partners. We feel that the area of bio-energy may have enough potential to warrant this level of investment at some point.

## 3 Database

One of the four deliverables for this Phase I effort is a database of biological molecules and mechanisms with interesting electrical properties and potential application to space systems. Our hope is that this database will serve as the basis for continued research and development of a fully biological space and mobile power paradigm. In addition to condensing information from hundreds of scholarly articles, the creation of this database enabled us to better frame the design space for biological molecules and mechanisms. This section summarizes the results from the database effort. It begins with a summary of the database itself, and then addresses the broader issue of categorizing the design space.

### 3.1 Summary of Results

During our Phase I effort, we reviewed hundreds of scholarly articles to identify and evaluate molecules, mechanisms, microbes, and organisms with interesting electrical properties. The database can be accessed via the custom web-based tool that we developed at: <http://db.intactlabs.com>. Thus far, we have included a total of 63 entities. This includes: 6 piezoelectric proteins or ion channels, 20 solar-electric proteins or pigments, 6 thermo-electric proteins and ion channels, 24 microbes, 3 families of electrically interesting macro-organisms, and 1 microbial nano-wire. Where possible, these entities are classified according to their scientific taxonomy, potential end-applications, input characterization, output characterization, and other properties useful for exploitation.


One important finding from this effort is that the number of potentially interesting molecules, microbes, and organisms is vast. All of life runs, in one way or another, on electro-chemical reactions. We optimized our search by focusing on molecules or mechanisms that directly created a charge or a charge-separation which we believed could be exploited for space systems design. However, the task is not complete and there are surely many additional entities to be found.

In a related sense, the complexity of life-processes means that many molecules or microbes which may not directly create electricity can still have an important function within a broader-bioelectric paradigm. For example, we catalogued a number of *electrigen* microbes which can be used in microbial fuel cells. In nature, these microbes are quite often enmeshed in complex catabolic or anabolic networks in which the input and output of non-electricigen microbes are critical. These secondary microbes would still be beneficial to characterize if one were to design a microbial fuel cell for space applications. In this regard, the task of cataloguing electrically interesting molecules, microbes, and organisms, should be viewed as an ongoing process. This realization led us to create a web-based tool to continuously update the database through the Phase I period and beyond (see below).

A second interesting finding involves synergies between the function of many electrically active membrane-proteins. Classes of proteins such as piezoelectric, photo-electric, or

thermo-electric all respond to external stimulus (vibration, light, or heat, respectively) by creating potential differences across the lipid-membrane. highlights this fact with a subsection of the database (and limited descriptive categories). Many of these proteins are involved in sensing, indicating a highly developed sensitivity and efficiency.

## Database: High Level Mechanisms



Class/Genus	Description	Input	Output
Rhodopsins	Photo-Active membrane protein	Solar Radtion: 450-700nm, 560nm peak)	Electrochemical gradient, H <sup>+</sup> , Cl <sup>-</sup>
Prestin	Mechano-Sensitive membrane protein	Pressure, Vibration < 100 kHz	Electrochemical gradient Cl <sup>-</sup>
Transient Receptor Potential Proteins	Heat-Activated ion channel	Temperature activation threshold	Electrochemical Grandient, Ca <sup>+</sup>
<i>Geobacter</i>	Iron Reducing electrigen microbe	Acetate, aromatic compounds	CO <sub>2</sub> , electrons
<i>Rhodoferax</i>	Waste-Metabolizing electricigen microbe	Lactates, sugars	CO <sub>2</sub> , electrons
Geobacter Pili	Microbial Nano-Wire proteins	electrons	electrons

© IntAct Labs

Cambridge, MA

**Figure 3: Sample of the database. This example includes classes of proteins or genus of micro-organisms, each of which envelope multiple particular instantiations. In the full database, more categories were included to capture other relevant information, where possible.**

The common motifs and conserved mechanism are important because, as explained below, if we are able to develop an end-architecture which exploits the function of one of these proteins, it will also be applicable across the wide diversity of other proteins. The most promising end-architecture in this regard is the *Power Skin*, which we examine in more detail later in this report.

### 3.2 Database Tool

IntAct Labs created a custom database for this project and placed it online at: <http://db.intactlabs.com>. The database tool was designed to provide a concise, consolidated, annotated, web-accessible reference for scientists studying bio-mimetic energy. We recognized the need for such a tool during the course of our research, as we

identified numerous secondary molecules and organisms that had potential impact on the processes under investigation.

The database stores information about microbes, proteins, and macro-organisms and their properties with respect to power-generation. They are organized by potential application categories and mechanisms. Related information is tied to specific microbes or molecules. For example, we store the potential fuel inputs and outputs for a particular species of *Geobacter* bacteria, along with the maximum observed power yield. Users can access information about labs and researchers studying a particular molecule, and find relevant scientific publications.

The database was implemented using the MySQL database management system to define relationships between the various components (see Figure 4). To facilitate viewing these relationships and modifying database content, we created a web interface using the PHP programming language. From a web browser, a researcher can add a new molecule or microbe, or edit existing data. Molecules and microbes are associated with one or more applications and mechanisms. From the web interface it is possible to browse microbes and proteins by these categories, and to add new application categories or mechanisms. Molecules and organisms in the database may also be associated with reaction pathways that store a set of inputs and outputs, and a measure of observed energy production. These reaction properties can be modified through the web as new experiments are conducted and new inputs or environmental conditions are identified. The final set of information in the database ties microbes/molecules to outside resources. Each record in the database can be linked to several labs, researchers and publications, with contact information readily available online.

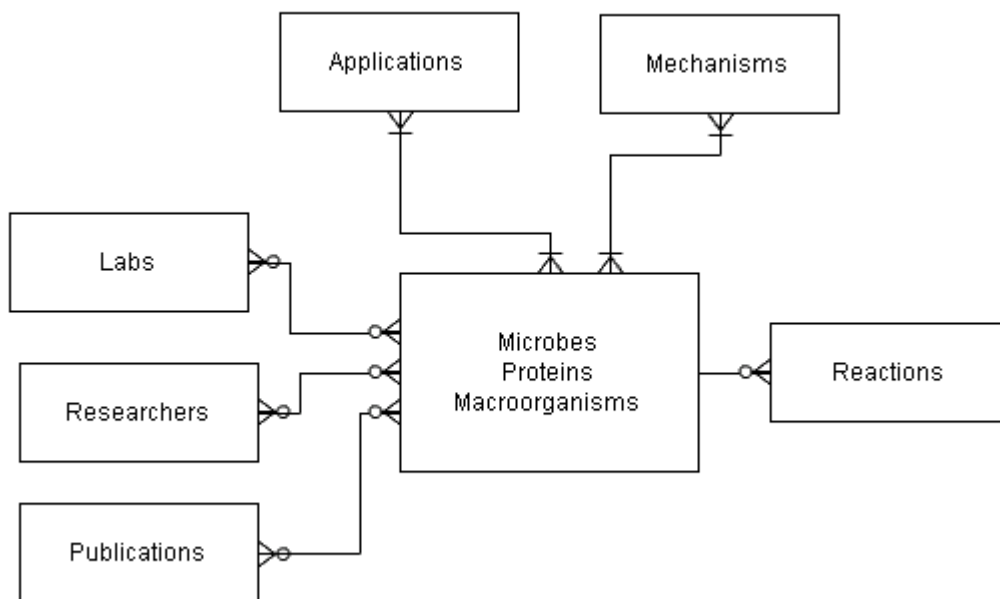


**Figure 4: Online Database Schematic**

### 3.3 Design Space

In order to get a sense of the design space we also catalogued specific molecules and mechanisms based on *energy input* and *mechanism-type*. Table 1 illustrates a sample breakdown, with energy sources on the left, and type of molecules on the top. Specific protein-types or end-applications fit at the intersection of these axes. We emphasize that this is not a complete breakdown of the space, but highlights how we thought about it.

**Table 1: Bioelectric Design Space. Green shows applications that have been prototyped. Yellow shows area that might be researched and prototyped.**

Design Space		Biological Systems ---Increasing Scale-->				
		Protein	Ion Channel	Microbe	Microbial Community	Tissue/Substrate
Energy Source	Vibration/movement	Piezo Proteins	Piezo Proteins	Pres/Geobacter	Pres/Geobacter	
	Wind	Piezo Proteins	Piezo Proteins	Pres/Geobacter	Pres/Geobacter	
	Solar	Enzyme Solar Cells		Rhodo/Geobacter	Rhodo/Geobacter	Photoactive Tissues
	Organic Chemical	Enzyme Fuel Cell		MFC	MFC	Macro Organisms

In Table 1, applications for which prototypes have already been created are highlighted in green. Applications for which underlying mechanisms have been identified—but no prototype built—are highlighted in yellow. White indicates a category for which we have not identified any specific molecules/energy sources. For example, “enzyme solar cells” are highlighted in green, because research at MIT has proven the feasibility of creating fuel cells using photosynthetic enzymes derived from spinach (enzyme solar cells), and a prototype has been built. There is a preliminary analysis, of more or less depth, for each of these application categories in this report, as it relates to space exploration.

Our proposal highlighted two specific areas of this design space with very strong potential. These were: the use of *Prestin* or *ion channels* to create *piezoelectric power skins*, and *microbial fuel cells* to construct *electric greenhouses* or *electric bio-chambers*. Table 2 shows the design space above, with these specific apps highlighted in Red.

**Table 2: Bioelectric design space, with proposal apps highlighted. Piezo proteins would be employed in power skins. Electrigen microbes would be employed in electric biochambers.**

Design Space		Biological Systems ---Increasing Scale-->				
		Protein	Ion Channel	Microbe	Microbial Community	Tissue/Substrate
Energy Source	Vibration/movement	Piezo Proteins	Piezo Proteins	Pres/Geobacter	Pres/Geobacter	
	Wind	Piezo Proteins	Piezo Proteins	Pres/Geobacter	Pres/Geobacter	
	Solar	Enzyme Solar Cells		Rhodo/Geobacter	Rhodo/Geobacter	Photoactive Tissues
	Organic Chemical	Enzyme Fuel Cell		MFC	MFC	Macro Organisms

As part of our database creation and preparation for down-selection, we have placed particular emphasis on the applications in red.

### 3.4 Categories

Through analysis of the database we identified four meta-categories of mechanism/fuel source combinations. These are listed in Table 3.

**Table 3: Four main application categories for biological energy production. Multiple organisms, micro-organisms, or molecules have characteristics that can be applied to each category.**

	<b>Application Category</b>	<b>Energy Source</b>	<b>Example Mechanisms</b>
1	Piezo Electric Mechanisms	Vibration, Wind	Prestin, MScL Ion Channels
2	Photo-Active Proteins and Cells	Solar Radiation	Bacterial Rhodopsin
3	Microbial Fuel Cells	Organic Matter and Waste	Geobacter, Geothrix
4	Electrostatic Organisms	Organics (sugars)	Electric Eels, Starfish

It should be emphasized that, given the overlap in some of these categories, work in one area may well prove valuable for the development of different classes of applications, either later in a potential Phase II effort. This potential overlap is further explored at the end of the next chapter.

## 4 Molecule and Mechanism Analysis

In order to down-select promising mechanism/architecture combinations, we conducted literature reviews and background analysis of the electrically interesting molecules and microbes identified above. The following section summarizes our findings from these investigations with a specific focus on how they impact NASA missions. It is divided into four main classes of molecules/mechanisms:

1. Piezo Electric Proteins
2. Photo-Active Proteins
3. Electrigen Microbes and Microbial Fuel Cells
4. Electrostatic Macro-Organisms

### 4.1 Piezoelectric Proteins

Proteins act as nano machines performing many actions. One such action is energy transduction. Piezo electric proteins are found in many forms in nature. Prestin is a mammalian piezo electric protein that transduces mechanical energy into ionic potential. Another such protein is Mechanosensitive ion channel present in E.coli. The latter have evolved to prevent cell rupture by transforming pressure into ions transport across the cell membranes. The following section reviews the state of knowledge about both Prestin and Mechanosensitive Ion channels. It is based on a comprehensive literature review.

#### 4.1.1 Prestin

The conserved gene of Prestin is the fifth member of the anion transporter family SLC26A5. The encoding gene —*Pres*— has 20 exons localized on the long arm of chromosome 7 the human. Prestin encoding cDNAs from various species (gerbil (AF230376), rat (AJ303372) and mouse (AY024359)) consist of:

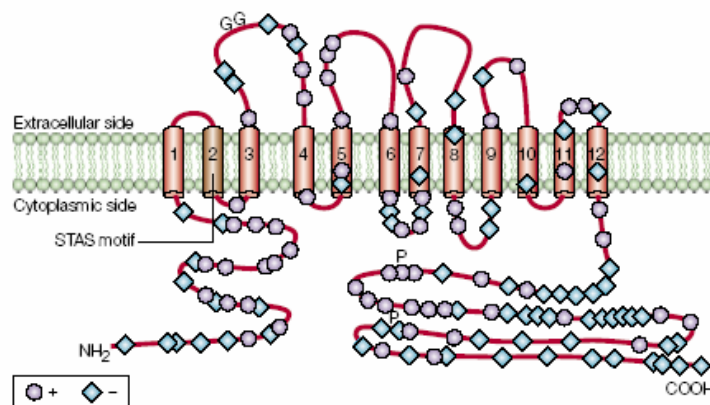


**Figure 5: Diagram of the membrane topology of Prestin. Positively and negatively charged amino acids are indicated using purple circles and blue diamonds, respectively. Amino-linked glycosylation**

sites (G) and phosphorylation sites (P) are also highlighted. The second membrane-spanning helix contains the highly conserved STAS motif (named after sulphate transporters and antisigma-factor antagonists), which is present in sulphate transporters through out the animal kingdom. (Peter Dallos: 2002)

2,232 nucleotides, and correspond to a polypeptide of 744 amino-acid residues with a molecular weight of about 80 kDa (Figure 5, Figure 6)[Zheng J 2000, Zheng J 2001, and Belyantseva I.A 2001] with primary sequences being 95 identical and minute variations occurring in the distal amino and carboxyl termini of the molecules. Kyte and Doolittle algorithm used by Zheng J to perform Hydrophobicity analysis indicated that Prestin is composed of up to 12 hydrophobic segments, which are long enough to span the plasma membrane as  $\alpha$ -helices or  $\beta$ -sheets. The cytoplasmic units [Belyantseva I.A 2001 and Ludwig J 2001] are mostly hydrophilic amino and carboxyl termini. The subunit stoichiometry of the functional Prestin molecule is unknown at present. Figure 6 shows the amino acid sequence of the protein.

```

1  mdhaeeneil aatqryyver pifshpvlqe rlhtkdkvpd siadklkqaf tctpkkirni
61  iymflpitkw lpaykfkeyv lgdlvsgist gvlqlpqqgla famlaavppi fglyssfyvp
121 imycflgtsr hisigpfavi slmiggvavr lvpddivipg gvnatngtea rdalrvkvam
181 svtllsgiiq fclgvcrfgf vaiylteplv rgfttaaavh vftsmkylf gvktkrysgi
241 fsvvystvav lqnvknlncv slgvglmvfg lllggkefne rfkeklpapi pleffavvmg
301 tgisagfnlk esynvdvvtg lplgllppan pdtslflhly vdaiaiaivg fsvtismakt
361 lankhgyqvd gnqelialgl cnsigslfqt fsiscslsrs lvqegtggkt qlagclaslm
421 illvilatgf lfeslpqavl saivivnlkg mfmqfsdlpf fwrtskielt iwlttfvssl
481 flglodyglit aviialltvi yrtqspyskv lgklpetdvy ididayeevk eipgikifqi
541 napiyyansd lysnalkrkt gnpavimga rrkamrkyak evgnanmana tvvkadaevd
601 gedatkpeee dgevkypiv ikstfpeemq rfmppgdvnh tvildftqvn fidsvgvktl
661 agivkeygdv giyvylagcs aqvndltrn rffenalpalwe llfhsihdav lgsqreala
721 eqeasappsq edlepnatpa tpea

```

**Figure 6: Amino acid sequence of human Prestin protein.**

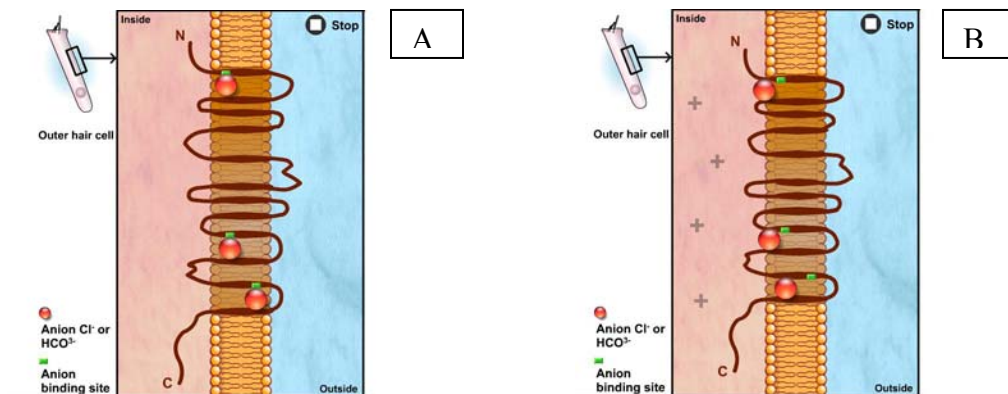
When scientists heterologously expressed Prestin in mammalian cell lines, the cells showed the characteristics of the outer hair cells. Zheng 2002 showed that expression endowed transfected cells (or excised patches of transfected cells) with non-linear capacitance (NLC), and this NLC had similar characteristics to those that were observed in outer hair cells [Zheng J 2000, Ludwig J 2001, and Oliver D, 2005]. Second, Prestin expressing cells were electromotile (generating motion in response to a transmembrane electric potential) [Zheng J 2000] with motility magnitudes approaching 0.2  $\mu\text{m}$ . Force measurements carried out with an atomic force microscope show that Prestin generates significant mechanical force independent of frequency (up to at least 20 kHz) [Ludwig J 2001]. The reciprocity of Prestin-mediated electromotility, generation of an electrical potential gradient from vibrational motion, was shown by Ludwig 2001 demonstrating that the protein indeed behaves as a biological *piezo-element* [Ludwig J 2001 and Santos-Sacchi J 2001]. Oliver and Zhen confirmed that functional properties of Prestin strongly support the concept of a single protein acting as an electromechanical transducer. The operation of the molecule apparently does not require any additional component, such as a specific membrane-lipid composition or the elaborate cytoskeletal network that is provided by the outer hair cells [Zheng J 2000, Ludwig J 2001, Belyantseva I.A 2001].



Subsequent work sought the mechanism of voltage sensing.

To verify the sensor, Kachar B 2001 neutralized all the charged residues that are not conserved between Prestin and SLC26A6, the SLC protein with the closest homology to Prestin. The resulting proteins were probed for NLC. As NLC was not abolished in any of these cases, the concept that charged particles that are extrinsic to the protein act as the voltage sensor was tested [Belyantseva I.A 2001, Oliver D 2001]. Neither cations nor external anions had any effect on NLC. However, NLC and, concomitantly, electromotility were reversibly eliminated by removing Cl<sup>-</sup> ions from the cytoplasm of cells containing either wild-type Prestin or any of the Prestin mutants tested [Oliver D 2001]. The half-activating Cl<sup>-</sup> concentration was 6 mM, matching the normal intracellular amount of this anion. Other monovalent anions were effective in promoting NLC: I<sup>-</sup> ≈ Br<sup>-</sup> > NO<sub>3</sub><sup>-</sup> > Cl<sup>-</sup> > HCO<sub>3</sub><sup>-</sup> > F<sup>-</sup>. Carboxylic acids could also substitute for Cl<sup>-</sup>, although their effectiveness is inversely proportional to their chain length, so the voltage required for moving butyrate across the plasma membrane is more than twice that necessary for translocating the halides, mentioned above, or formate [Oliver D 2001].

Prestin uses an extrinsic voltage sensor — monovalent anions — available in the cytoplasm. After binding to a site with millimolar affinity, these anions are released from the membrane bound protein in response to changes in the transmembrane voltage. They move towards the extra-cellular surface following hyperpolarization and towards the cytoplasmic side in response to depolarization (Figure 7). As a consequence, this translocation triggers conformational changes in the protein that ultimately alter its surface area in the plane of the plasma membrane. The area decreases when the anion is near the cytoplasmic face of the membrane ('short state'), and increases when the ion has crossed the membrane to the outer surface ('long state'). Prestin acts as an incomplete transporter; it swings anions across the membrane, but does not allow these anions to dissociate and escape to the extracellular space (Figure 7). When monovalent anions are not present in the cytoplasm, all Prestin molecules are in their 'short' state, as the outer hair cell is maximally contracted. Prestin in the lateral membrane of outer hair cells is packed in high density in form of 8-11 nm particles (Figure 5), each particle is assumed to have two protein molecules. The density of these particles is from 4000-6000 per sq micron. [Kalinec F 1992 and Forge A 1991]



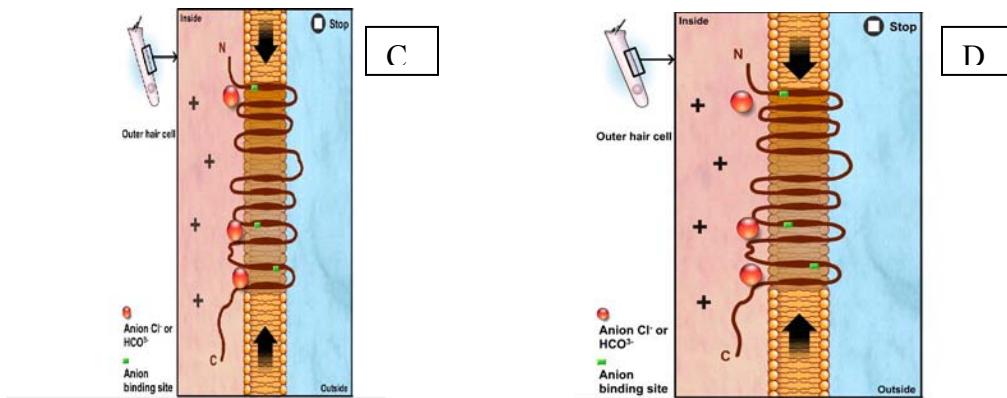


**Figure 7: Diagram showing the assumed mechanism of Prestin. A. Elongated state of the outer hair cells. Chloride ions (red balls) are in the anion binding site in the membrane. The cell is in resting potential state. (Animation modified from figure courtesy: G. Rebillard)**

Prestin is a new type of biological motor; it is entirely different from the well known and much studied classical cellular motors. It functions as a distinct biological actuator (unlike rotational motors like prokaryotic flagella and ATP synthase), directly converting voltage to movement. Prestin does not require ATP (unlike kinesin and myosin) to perform work nor does it carry ionic current [Zheng J 2002]. Prestin is a direct voltage-to-force converter, which uses cytoplasmic anions as extrinsic voltage sensors and can operate at microsecond rates [Dallos P 2002].

The remarkable properties of Prestin make it a candidate for future nanotechnology applications. Prestin ensembles could function as mechanical, voltage-controlled actuators at exceptional speeds. It is estimated that a single Prestin molecular assembly produces a force in the outer hair cells axial direction of about 2.4 PicoNewtons and a conformational displacement of around 1 nm. Prestin can also behave as a sensor of mechanical stress, or operate as a voltage-controlled capacitor in electrical nanocircuits and also to be used to electricity generator by converting mechanical energy into electrical energy. These properties of Prestin make it an ideal candidate to be used in the Power Skin Concept.

#### 4.1.2 Mechanosensitive Ion Channels

Mechanosensitive ion channels are classified into three categories: mechanosensitive channels of large conductance (MscL) that have approximately 3ns conductance, small conductance (MscS) that have approximately 1ns conductance and mini-conductance (MscM) that have approximately 30 ps conductance. The opening mechanism of the channels in the membrane is shown in Figure 5.

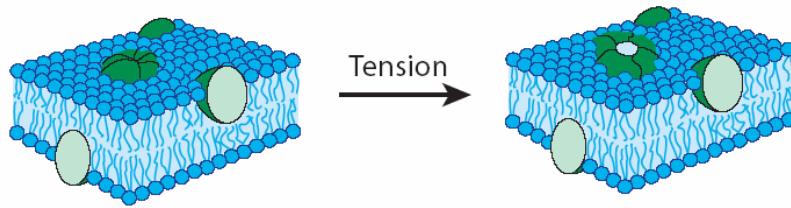


**Figure 8: The mechanosensitive channel of larger conductance gates in response to bilayer tension. (Image from Sukharev, 2001)**

The crystal structure of the MscL and MscS from *E. coli* were determined at high resolution by Rees et al and Sukharev et al. The structure and the opening mechanism of both of the proteins are show in Figures 6 and 7, respectively.

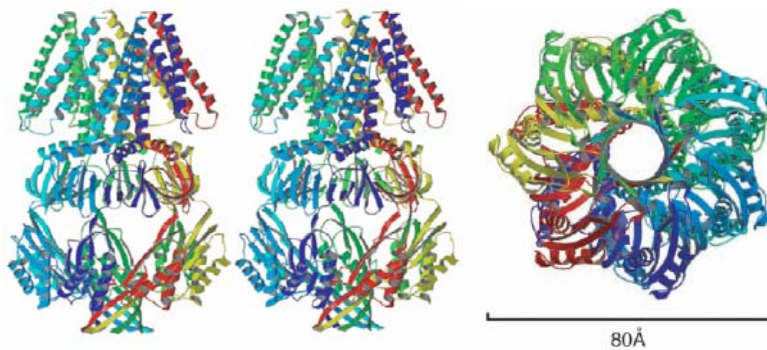


**Figure 9: Structure of MscS (Image from Sukharev, S, 2001)**

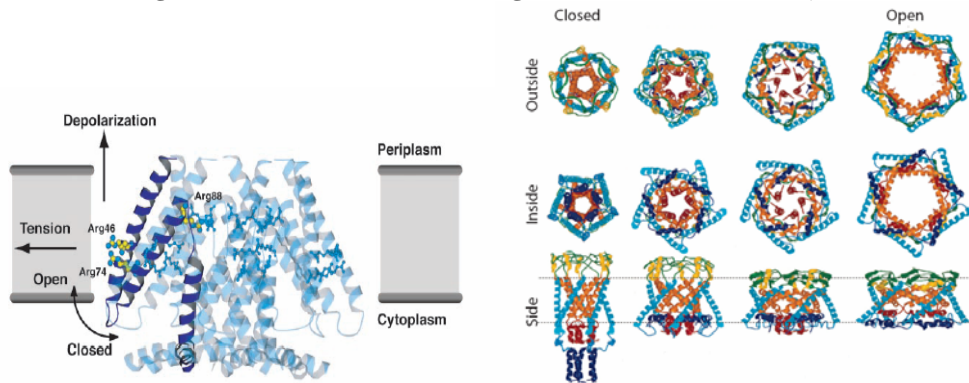


**Figure 10: Opening of MscS and MscL (Image from Sukharev, S, 2001)**

MscS and MscL ion channels in the *E. coli* have pore size of approximately 14 and 30 armstrong's respectively. The MscL and MscS are easily over expressed and purified in the E. Coli. Also, electro-physiology on isolated MscS and MscL proteins that were purified and reconstituted into lipid vesicles showed that MscS and MscL are necessary and sufficient to achieve channel activity in response to bilayer tension [Sukharev, S 2001, Sukharev, S 1994, Sukharev, S 1997, Sukharev, S 1999, Sukharev, S 1999b]. The tension required to open MS proteins has been quantitatively determined [Sukharev, S 2001] and plotted in Figure 8. The pressure that is required to open the MscS is

approximately half the pressure that is required to open the MscL [Kloda1 A 2001, Randal B 2002]. The amount of voltage that is generated [Sukharev, S 1999b] is shown in Figure 8 for both the proteins. Where  $P_o$  is the probability of opening of these proteins and pA is the applied pressure in mm of Hg onto the membrane. The amount of pressure required to open 50 percent ( $P_o=0.5$ ) of the channels for the MscS is 36 mm of Hg and for MscL is 75 mm of Hg.

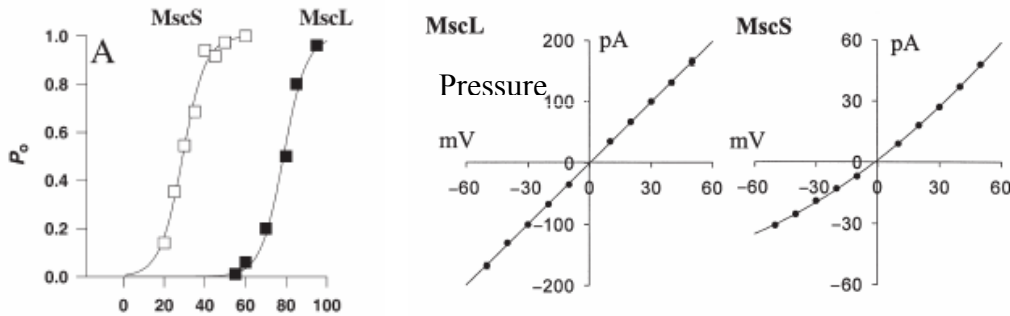


**Figure 11: Plots showing the opening pressure required to open the channel,  $P_o$  is the probability of proteins opened and voltage depolarization occurred due to applied pressure on the membrane (Image from Sukharev, S, 2001)**

The mechanism of opening and closing of these proteins has not been understood completely but they are shown to be functional in lipid bilayers, responding to external stimuli. Mechanosensitive ion channels respond to mechanical strain this property makes them interesting for Power Skin application.

#### 4.1.3 Summary of Piezo Electric Proteins

Piezo electric proteins are nano scale transducers that can be used in Power skin. The literature survey uncovered the vast amount of work has been done in understanding these proteins and the numerous scientists trying to understand these proteins. This work forms a solid basis on which to begin a transfer from science to engineering.

## 4.2 Photo-Electric Proteins

Due to the vast quantities of solar energy available on earth (and in the near solar system), scientists have long dreamed of harnessing photo-active properties of plants to create efficient solar cells. Very recently, preliminary biological solar cells have been built and science is finally on the cusp of exploiting photo-active proteins for various uses. Here we review important photoelectric proteins and their potential optimization.

The most important classes of proteins with photoelectric properties are those used in photosynthetic reactions, Photosystem I and II, and the rhodopsins, with several functions. The most obvious application for these proteins involves biological photovoltaic cells that convert solar energy directly into electricity. However, there are other applications can be imagined, including hybrid systems that combine microbial fuel

cells (see next section) with photoactive fuel cells or systems that use light energy to produce hydrogen or methane for use in traditional fuel cells.

#### 4.2.1 Overview of Photosynthesis

Photosynthesis is the process by which plants and phototrophic bacteria convert solar energy to chemical energy in the form of carbon dioxide and water fixed into carbohydrates. In plants, the process proceeds in a series of four steps:

- 1) Absorption of light;
- 2) Electron transport cascade starting with the formation of molecular oxygen from water; electrons from this process reduce  $\text{NADP}^+$  to NADPH, and movement of protons sets up a proton gradient;
- 3) Adenosine tri-phosphate (ATP) synthesis powered by the proton gradient; and
- 4) Carbon fixation using the energy from ATP & NADPH to form carbohydrates (Lodish et al., 2004).

At the heart of the photosynthetic process, there are two photosynthetic reaction centers, the photosystems I and II (PSI and PSII, respectively). They serve separate functions, but each is composed of a number of integral membrane proteins and associated light-harvesting protein complexes that contain pigments such as chlorophyll. When a photon strikes one of the light harvesting complexes, the energy induces a central pair of chlorophyll *a* molecules—called the “special pair”—to donate an electron to a primary acceptor molecule. The electron acceptor in the PSI and PSII reaction centers is different, as its subsequent path and function.

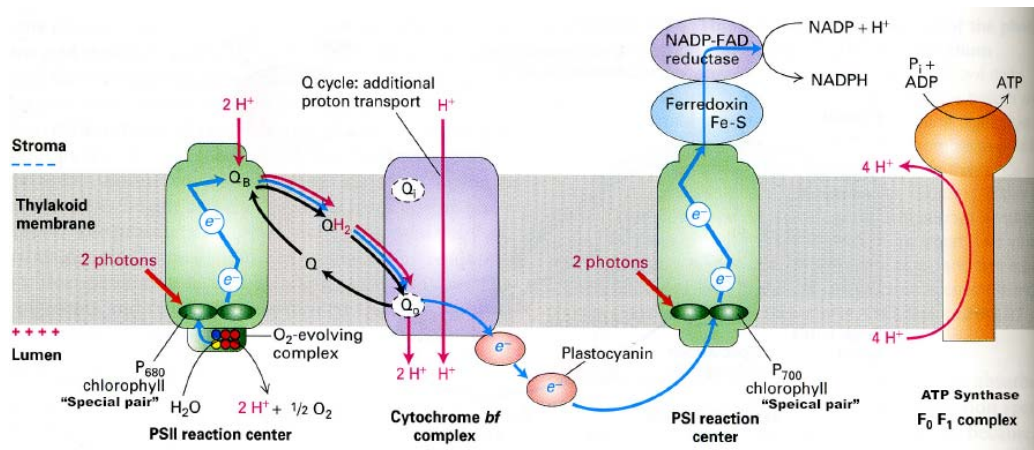


Figure 12: Photosynthesis schematic showing the flow of electrons and protons in the light reactions (Lodish, 2004)

#### 4.2.2 Photosystem II

With the capture of two photons by PSII, the special pair chlorophylls near the inner face of the thylakoid membrane donate two electrons to an acceptor called plastoquinone (Q), which quickly migrates across the membrane and picks up two protons, forming  $\text{QH}_2$

(Figure 12). This is the initial photo-induced charge separation that is central to the transfer of energy from light to chemical energy. With the aid of a Cytochrome *bf* protein complex, QH<sub>2</sub> is transported back toward the inner side of the membrane where it releases its two protons; due to the cyclic nature of plastoquinone operation, 2 protons are transported for each photon of light transmitted to the reaction center. Simultaneously, the ionized special pair chlorophylls strip two electrons from water, oxidizing it to protons and O<sub>2</sub> gas. These two reactions convert the transient charge separation produced by ionization of the special pair into a more stable proton gradient across the membrane; this proton gradient provides the energy for ATP synthesis by an enzyme complex called the F<sub>0</sub>F<sub>1</sub> complex (Lodish et al., 2004).

To summarize, PSII (and associated complexes) use energy from captured photons to set up a proton gradient for ATP synthesis and to split water to generate protons and O<sub>2</sub>. Note: in both PSII and PSI electrons are excited by photons and move through the protein individually; active sites at the oxygen-evolving complex, within cytochromes, and at electron transporter interfaces facilitate multi-electron transfers.

### 4.2.3 Photosystem I

PSI acts downstream of PSII, but performs a different function. As in PSII, in PSI the capture of two photons leads to ionization of the special pair chlorophylls by transfer of a pair of electrons to an acceptor (Figure 12). Through several intermediate carriers, the electrons are transferred to the primary acceptor, called ferredoxin. Ferredoxin then transfers its electrons to an enzyme called NADP-FAD reductase, to which it is bound on the outer side of the thylakoid membrane. NADP-FAD reductase is responsible for reducing the final electron acceptor, NADP<sup>+</sup>, to NADPH. Since reduced NADPH is eventually utilized for carbohydrate production by CO<sub>2</sub> fixation, the primary function of PSI is to drive generation of highly reduced NADPH for anabolic processes. PSII also drives carbohydrate synthesis indirectly, because ATP created by the proton gradient it sets up is also consumed by this process.

PSII acts before PSI because electrons are transferred from QH<sub>2</sub> to a protein called plastocyanin as it recycles to its neutral Q form; plastocyanin then diffuses in the thylakoid to the PSI reaction center, where it replenishes the electrons donated by the PSI special pair to ferredoxin. Photosynthesis is most efficient when it utilizes both photosystems, but each can function independently. In purple-membrane bacteria, only PSII is present, so photon capture drives only ATP synthesis by means of a proton gradient. PSI can also function independent of PSII because ferredoxin, the primary electron acceptor, can also donate electrons to quinone (Q), and so can utilize the cytochrome *bf* complex as well in a process known as cyclic electron transport. As with PSII, PSI drives only ATP synthesis in this case because it is no longer coupled to NADPH production. The purpose of cyclic electron transfer is to balance the levels of ATP and NADPH to meet cellular demand. The mechanisms and kinetics of the photosynthetic reaction centers have been reviewed in detail elsewhere (Lu et al., 2006).

#### 4.2.4 Rhodopsin

Rhodopsins are a class of structurally related cellular membrane proteins that perform two functions, signal transduction and/or ion translocation. Sensory rhodopsins, including the visual proteins found in the eyes of humans and all other animals, capture photons and initiate the signal cascade (resulting in visual perception in the case of those found in eyes). Ion-translocating rhodopsins are found in archaea and bacteria and include bacteriorhodopsins (BR), halorhodopsins, proteorhodopsins, and several other rhodopsin groups. These transmembrane proteins use light energy to pump ions across the membrane. In most cases, the target ion is a proton, and the pumping action is used to build up a proton gradient that is then utilized to synthesize ATP (Beja et al., 2000)

Rhodopsins consist of a single membrane protein with a covalently bound small pigment called *retinal*. When retinal is struck by a photon, it stereo-isomerizes, changing the protein's conformation and allowing a series of inter-protein proton exchanges resulting in the net transfer of one proton across the membrane, allowing the storage of energy in the electrochemical gradient. When the retinal relaxes back into the ground-state conformation, the protein conformation and residue protonation states reset completing the photocycle. The photocycle of this pumping action is on the order of a few microseconds, allowing for efficient action (Feng et al., 2006).

#### 4.2.5 Biological Solar Cells

The viability of biological photo-voltaics (BPV) has recently been demonstrated utilizing photosynthetic enzyme complexes, PSI and PSII, as well as bacterial rhodopsin. We review below the basic operation of a these BPVs, the power production characteristics and engineering challenges of these systems.

##### 4.2.5.1.1 Principles of Operation

In one instantiation of a BPV the electrons produced by PSII are captured and transferred to an anode. Lam et al. (2004) were one of the first groups to create a BVC using photosynthetic components. They suspended spinach thylakoids in a buffer solution with the redox mediator phenazine methosulfate. They then connected a load resistor to a cathode, where the electrons finally reduced ferricyanide Fe(III) into Fe(II). This configuration is represented schematically in Figure 13.

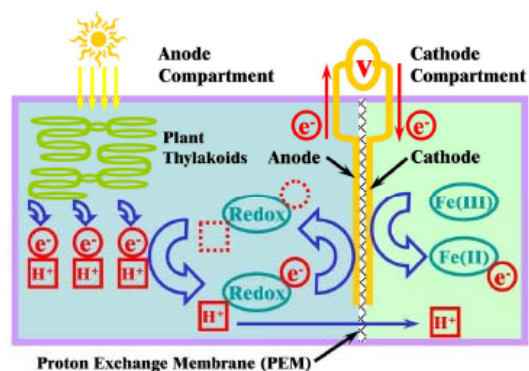


Figure 13: Schematic of a BVC (Lam, 2006)

For this configuration, they achieved a power density of 5.4pW/cm<sup>2</sup> at a current of 1uA/cm<sup>2</sup>. As indicated in Figure 14, there is a trade-off between voltage and power which could be tailored for the application.

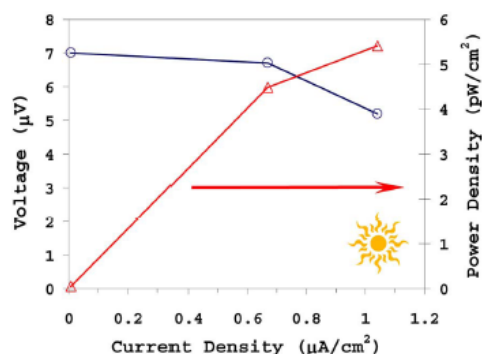


Figure 14: Power and Voltage Trade-off (Lam, 2006)

The light to power conversion efficiency produced by Lam et al. (2006) was approximately 1%. They note a number of reasons for low efficiency. First, there was slow electron transfer from the diffusive biocatalysts (redox electron mediators) used to the electrode in the anode chamber. This might be mitigated by mediator selection and electrode material and nanostructure optimization. Second, the sensitivity of the biocatalysts and mediators to oxidation by O<sub>2</sub> reduces the total power output. They calculated that an optimal BVC based on photosystem proteins could produce a maximum current of 9.6mA/cm<sup>2</sup> (Lam et al., 2006).

Other researchers have produced BPVs based on plant photosystems. Baldo et al. (2004) demonstrated a BPV containing PSI with efficiencies of approximately 20%. They utilized histine tags to orient the proteins for maximum light absorption. The system created by Lam et al. (2006) required flushing of the proteins, whereas Baldo et al. (2004) were able to stabilize the proteins using surfactant peptides for multiple weeks. This represents one of the most significant engineering challenges for a viable BPV system for space applications. The possibility for biological assembly and full self-replication remains on the horizon and is an enticing solution to this problem.



#### **4.2.5.2 *Bacterial Rhodopsin in a Biological Solar Cell***

There has been relatively little work on the development of a bacteriorhodopsin (BR) based solar cell. Some groups have demonstrated rudimentary BR solar cells (Bertocello, 2004). They deposit thin films of BR on an electrode and then measure the performance. They report currents of approximately 2nA and potential voltages of 50mV.

#### **4.2.6 Optimization of Photo-Active Proteins**

Developing a BPV requires using proteins and protein complexes that were evolved to function in different environments and optimized for different constraints. It may be possible to optimize BR and photosynthetic complexes specifically for power production in space environments. This would require use of mutagenesis techniques and selection for desired properties.

##### **4.2.6.1 *Optimization of Rhodopsins***

Modification of BR would involve structural changes in the protein or amino acid sequence, leading to changes in the optical and photochemical properties. Desired modifications might include altering the kinetics of the pumping action, the wavelength of photons that induce pumping, or the orientation of the protein within the membrane (Wise et al., 2002). Some modification is possible by simply altering the environmental conditions (temperature, pH, salinity, etc.) though these changes are limited in their scope and specificity (Hoffman et al., 1994). Recent advances in protein engineering have developed techniques that are able to create specific, targeted changes in protein behavior. Modifications of visual rhodopsins have been attempted with some success, but they have not been used extensively with bacterial rhodopsins, and have not been used to optimize these proteins for power production (Hampp, 2000; Wise et al., 2002); technologies for optimization are detailed below.

##### **4.2.6.2 *Retinal Analogs***

Functional rhodopsin complexes consist of a small *retinal* molecule coupled to the opsin peptide. The retinal molecule is integral in determining the optical and photochemical properties of BR, so by using chemicals that closely mimic the structure of retinal (such as all-*trans* retinal or 3,4-dihydro-retinal) it is possible to change the properties of the complex, especially the excitation wavelength (Feng et al., 2006).

##### **4.2.6.3 *Random Mutagenesis***

Using chemical mutagenesis agents or X-ray irradiation, random mutations in the gene encoding a protein can be induced. While the majority of these mutations will encode a protein that is less functional or entirely non-functional, a small fraction may encode proteins that are better suited a particular function than the original. By screening for improved proteins, mutagenesis may be carried out in several steps to create a protein that performs much better than the native one. Coupled with appropriate means to select

for improved function, this “directed evolution” mutagenesis strategy mimics the natural process of evolution toward a desired goal.

#### **4.2.6.4 Site-Specific Mutagenesis**

Site-specific mutagenesis is a controlled version of the random mutagenesis. By using the crystal structure of the protein to find the active sites, or by observing where the most productive mutations are found during random mutagenesis, it is possible to target mutations to key regions of the protein by PCR or other techniques. As with random mutagenesis, most mutations will have deleterious effects on function, but a smaller number of candidates usually need to be screened to find proteins with improvements in the desired function.

BR is an excellent candidate for this powerful technique for several reasons: it consists of a single small protein; there are dozens of structurally related molecules in the family with different properties; and the crystal structures and active sites of the protein are very well characterized.

#### **4.2.6.5 Optimization of Photosystem I and PS II Proteins**

While similar techniques can be used to optimize PS I and II, modification of components involved in photosynthesis is more difficult than in the case of BR. They consist of a number of intimately complexed proteins, and modification of each would most likely have to occur in tandem. However, once these challenges are overcome, the highly evolved photosynthetic system probably has enormous potential to be used in (or indirectly inspire) very efficient photovoltaic cells. For example, PS II has better than 95% efficiency in converting captured light energy to an initial charge separation, so engineering PS II to bypass later steps and use this charge separation to drive current instead could be tremendously rewarding (Esper et al., 2006).

Since efforts to create photovoltaic cells based on photosystem proteins have focused on immobilizing them on membranes or chemical scaffolds, the most rapidly rewarding engineering involving these proteins will likely center around modifications to make them more stable when immobilized (Lu et al., 2006). However, investigation into *in vivo* (using living organisms) biological solar cells should continue since the benefits of these systems are tremendous.

### **4.2.7 Photo-Active Protein Summary**

Light has been the primary source of energy on the earth for billions of years; during this time, organisms have evolved very efficient mechanisms to harness this energy and convert it to electrical potential and chemical energy. For this reason, many researchers are looking to biological systems for tools and inspiration to harvest the huge quantities of energy. These need not be direct photovoltaic systems, as some groups have proposed using light-harvesting molecules complemented by enzymes that produce hydrogen gas (Esper et al., 2006).

Rhodopsins are a group of simple membrane proteins used by cells as an auxiliary energy source when other sources are not available. Its small size and simplicity make it a good initial target for engineering to tailor it for photovoltaic applications, and it would work well in a complex with other proteins for the same reasons. However, its simplicity might be a drawback in that its efficiency to convert light to chemical energy is limited. In contrast, the large, multi-protein complex (PS I and PS II) involved in photosynthesis present more difficult targets for engineering approaches, but they have become highly efficient at light harvesting through millions of years of evolution. With the correct modifications, photosystem proteins could form the backbone of excellent biological photovoltaics.

Other photoactive proteins, especially fluorescent proteins such as green and red fluorescent proteins (GFP and RFP, respectively) and are well understood and have been extensively engineered. These proteins, though very useful in imaging, have dubious applications for photovoltaic cells.

### **4.3 Electricigen Microbes and Microbial Fuel Cells**

#### **4.3.1 Introduction**

Electricity production from micro-organisms, harnessed through fuel-cell type mechanisms, is not new. However, recent discoveries and advances in microbiology, biotechnology, and synthetic biology have enabled the development of much higher-power systems with potentially revolutionary implications for space-power production and advanced life support. Coupled with other bio-energy systems and bio-based materials production, microbial power production could form the basis for long-term, sustainable power production on a space vehicle, the Moon, on Mars, or beyond.

Electricity production in microbial cultures was first observed almost 100 years ago by Potter (1910, 1911). Early studies suffered from lack of understanding of underlying processes and limited efficiency due to the use of fermentation processes, but recent discoveries have created a resurgence of interest in the potential for microbial fuel-cells to generate power. These include the discovery of *Geobacter*, *Rhodeferax*, and *Desulfuromonas* genera of microbes with the capability to oxidize organic compounds and directly transfer electrons to electrodes. Especially important is the species *Geobacter sulfurreducens*, and recent studies by Dr. Lovley at University of Massachusetts, Amherst have advanced the understanding of their unique electron transfer mechanisms. C-type cytochromes, OmcS, and other proteins form long pili attached to the outer cell membrane that act as microbial nanowires, capable of transferring electrons directly to the anode even when lacking direct contact with it (Lovley, 2006). This finding identifies a strong candidate for optimization in fuel cells.

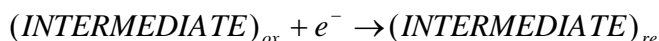
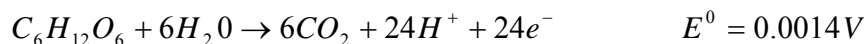
NASA examined the potential to use microbial fuel cells as part of advanced life support in long-haul spaceflights during the 1960s (Rohrback, 1962). These studies were discontinued because the underlying processes were not well understood and the relative

advantages of solar cells at the time. Given the recent advances in knowledge regarding the fundamental principals of microbial fuel cells, it seems appropriate to revisit the issue for NASA.

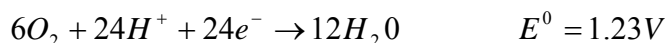
### 4.3.2 Microbial Fuel Cells: Mechanism Overview

Biological and microbial fuel cells (MFCs) convert chemical energy, in the form of carbohydrates and organic molecules (alcohols, acetates, etc.) directly into electrical energy. They do this by exploiting chemical reactions associated with microbial metabolism to channel electrons otherwise captured by electron receptors in the microbes' environment. For example, the respiration process of *Geobacter* sp. includes the transfer of electrons to Fe<sup>+</sup> and Mn<sup>+</sup> in their environment, creating reduced metal deposits. A microbial fuel cell captures these electrons at the anode and induces current to flow by keeping the cathode in an reducing environment at a lower potential.

For example, in microbial catabolism, carbohydrate can be oxidized initially without participation of oxygen, and electrons are taken up by an enzyme active site as follows:



However, in a microbial fuel cell the first step of this process occurs in an anodic chamber, and the second step of the process is carried out by reduction reactions at a cathode. The electrons are diverted to the electrode either by direct transfer along the bacteria's hair-like extrusions (pili) or through electron shuttles. Once deposited at the anode, the electrons pass through an outer circuit, eventually combining with an electron sink (e.g. molecular oxygen) in the following reaction:



Similar reactions involving acetates or other organic compounds can be exploited to create electric current. These depend on the specific type of fuel cell—whether enzymatic, indirect to anode, direct to anode, or a fuel-producer for traditional fuel cells (e.g. hydrogen or methane). Figure 15 illustrates this process.

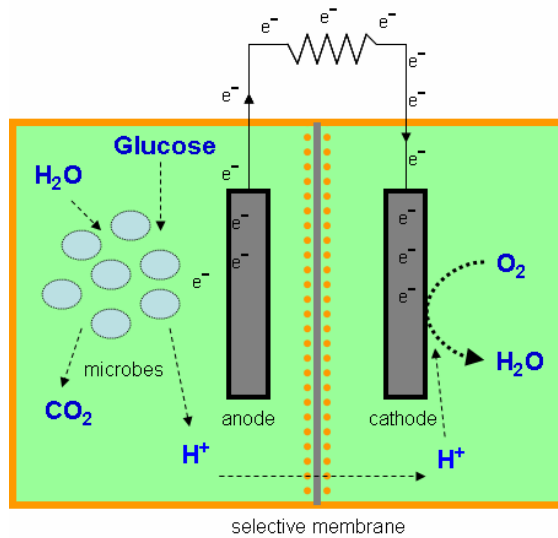


**Figure 15: Schematic of an MFC running on glucose. © IntAct Labs**

Microbial fuel cells are thus functionally similar to chemical fuel cells. Both include a space for reactants and two electrodes separated by a membrane or electrolyte. Some advantages of microbial fuel cells over chemical fuel cells included the following:

1. Unlike chemical fuel cells they operate at ambient temperature and pressure.
2. They employ neutral electrolytes and do not need expensive catalysts such as platinum
3. They can be powered by, and hence remediate, organic wastes

#### **4.3.2.1 Indirect Microbial Fuel Cell with Electron Shuttles**

In indirect microbial fuel cells, microbes use electron shuttles to transfer electrons to the electrode. Figure 13 illustrates this process.

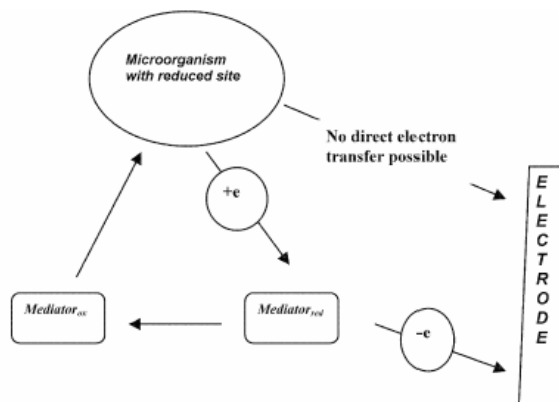


**Figure 16: Indirect Microbial Fuel Cells.**

Indirect microbial fuel cells suffer from the fact that they are based on fermentation processes, which from a practical standpoint are slow. Another weakness is that in a

flow-through process the concentration of electron shuttles is constantly being reduced, thereby lowering power production until concentration is restored. These draw-backs have limited the applications of indirect microbial fuel cells. There may be advantages to using microbial fuel cells with electron shuttles if they incorporate direct microbial communities.

#### **4.3.2.2 Direct Microbial Fuel Cells**

Until recent discoveries of organisms with direct electron transfer capabilities, it was thought that all microbial fuel cells functioned via the operation of “electron shuttles,” which carry electrons from inside the microbe (or on the outer membrane surface) to the electrode. Recent work has discovered a new class of anaerobic bacteria capable of direct transfer of electrons to anodes. Families of microbes called “electricigens,” which include organisms such as *Geobacter* and *Rhodospirillum rubrum*, can reduce organic wastes with direct electron transfer to the anode, obviating the need for electron shuttles, and making them applicable for flow-through waste remediation systems such as those used by NASA. Here are the names and details of some species of interest:

- ***Desulfuromonas***: oxidation of acetates, alcohols and aromatic components in a saline environment.
- ***Geobacteraceae***: Family of bacteria; oxidation of acetates, alcohols and, aromatic components in a non-saline (fresh water) stream.
- ***Rhodospirillum rubrum***: oxidation of sugars
- ***Geothrix***: This family of bacteria, which has shown to power sediment fuel cells, has been found highly concentrated on the anode of fresh-water fuel cells

#### **4.3.2.3 Microbial Fuel Production**

Microbes can create fuel for use in chemical fuel cells. For example, some bacteria are capable of converting carbohydrates such as glucose to hydrogen through a multi-enzyme process. In the current prototypes hydrogen production is still below theoretical values for various reasons. Researchers are actively trying to employ genetic engineering or evolutionary pressure techniques to increase H<sub>2</sub> production (Esper et al., 2006). A rigorous analysis evaluating the energy efficiency of direct microbial fuel cells versus microbial fuel production has not been performed. As discussed below, a combination of the two may be advantageous.

#### **4.3.3 Literature Review: What has been built?**

Power output generated by microbial fuel cells currently range from 0.01 W/m<sup>2</sup> to 4.3 W/m<sup>2</sup>. Output varies between bacterial species and fuel cell design. For instance, pure cell cultures containing only a single species generally yield higher power output, but mixed communities may be more suited for bioremediation purposes because of the heterogeneous nature of the growth medium.

The highest power seen so far has been  $4.31\text{W/m}^2$ , generated by Rabaey et al. (2004) through simulated evolution of a mixed bacterial colony over 71 days. Mixed culture inoculums were placed in a Plexiglas biofuel cell using graphite rod electrodes with ferricyanide electron acceptors and anaerobic, granular, methanogenic sludge from a local potato-processing factory electron donor. The sludge was mixed with nutrient broth and replaced every two weeks, and the bacterial culture that resulted was analyzed for efficiency. At the initiation of the 71-day enrichment period, electron recovery was only 4% with maximum power density of  $0.65\text{W/m}^2$ , but efficiency rose over time to 81% with power density of  $4.31\text{W/m}^2$ . The genetic composition of the resulting culture showed a prevalence of facultative anaerobic bacteria, such as *Alcaligenes faecalis* and *Enterococcus ganllinarum*, with a strong presence of *Pseudomonas aeruginosa* species as well. *P.aeruginosa* can produce its own electron shuttles, such as phenazine pyocyanin (Rabaey et al., 2005), eliminating the need for the addition of exogenous compounds to the system. However, Cheng et al. (2006) suggest that ferricyanide is impractical for wastewater treatment because it must be externally regenerated. Still, this experiment is evidence that evolutionary pressure on bacterial cultures can also be used to harness higher power outputs over time.

Despite this high power generated by *P. aeruginosa* in Rabaey's experiments, bacteria that require electron shuttles are generally considered less efficient because of the increased internal resistance that the shuttling process creates. The *Geobacter* and *Rhodoferrax* genera have been the subject of most recent interest, since they transfer electrons directly to the anode of the fuel cell. Other genera like *Shewanella* and *Clostridium* also connect directly to the anode but produce far lower outputs ( $0.003\text{mA/m}^2$  compared to  $4\text{-}8\text{mA/m}^2$  for *Geobacter*) and lower electron extraction efficiencies (0.03-0.04% compared to 95% for *Geobacter*) (Bond and Lovley, 2003). It has been shown that the bacterial pili in *Geobacter sulfurreducens* offer electrical conduits between bacteria, creating a "nano power grid" such that a direct connection between an individual bacterium and the anode is unnecessary (Reguera et al. 2006). Cell viability remained steady with increasing distance from the anode, and direct linear increase in current related to increased biomass is observed. This suggests that the constraint of maximal surface area may be relaxed to some extent in species exhibiting pili. *Geobacter* power outputs have recently been observed at an average of approximately  $3\text{ W/m}^2$  [D. Lovley, personal correspondence].

Surface and anode composition likely play a large factor in determining power output of *Geobacter sulfurreducens*. Chaudhuri and Lovley (2003) increased the power output for *Rhodoferrax ferrireducens* by using different types of graphite electrodes. Replacing graphite rods with graphite felt increased current production threefold, and replacing that with porous graphite foam increased current again by 2.4-fold (Chaudhuri and Lovley, 2003).

A variety of other methods have been tested to improve power output within microbial fuel cells. The elimination of salt bridges and oxygen diffusion into the anode has become a standard, as Min et al. (2004) charted the large power loss incurred by both of

these issues. Min et al. (2004) used test inoculums of *Geobacter metallireducens* in fuel cells with either proton exchange membranes or salt bridges as proton conductors. They discovered a drop from  $40 \pm 1 \text{ mW/m}^2$  to  $2.2 \text{ mW/m}^2$  in fuel cells using salt bridges. The same group noticed a rise in Coulombic efficiency from 19% to 47-55% when dissolved oxygen flux into the anode was decreased by nitrogen gas sparging or the addition of oxygen scavengers like L-cysteine. Dissolved oxygen in the anode has varying effects on the efficiencies of different species of anaerobic bacteria.

Different chambered setups also displayed different responses to distance alterations between the anode and cathode. Decreasing the distance between electrodes from 4 to 2 cm in a single-chamber fed-batch system actually increased power output from 720 to  $1210 \text{ mW/m}^2$  (Liu et al., 2005). However Cheng et al. (2006) decreased the distance from 2 to 1 cm in the same system and found a decrease in power output from 811 to  $423 \text{ mW/m}^2$ . It was suggested that this resulted from decreased activity of the bacteria and not from decreased internal ohmic resistance, which would have otherwise increased power. Cheng et al. (2006) then replaced occasional glucose input with continuous flow through the anode to increase the power value to  $1540 \text{ mW/m}^2$ .

Similar alterations to fuel cells seem to have variable results based on the specific system used, and each application may demand a different combination of design parameters for optimal operation. While mixed bacterial communities are slightly less efficient than single species cultures, they are necessary when heterogeneous bio waste or sludge is used for fuel. Individual species themselves have tradeoffs: certain species may produce a larger power output, but the constant replenishment of electron shuttles they require offsets these gains. Thus, it can be seen that the optimization of a single fuel cell will require consideration of each aspect of the system in conjunction.

#### **4.3.4 Microbial Fuel Cell Optimization**

##### ***4.3.4.1 Simulated Evolution***

Maximum power levels to date have been created using evolutionary pressure. This involves creating an environment which selects for high-energy output, and then letting bacteria in a culture evolve with this environment. Simulated evolution has the potential to simultaneously improve all factors controlling power output, including increased respiration rate, a larger range of food molecules consumed, and even improved symbiosis among within communities of microbes. Microbes are ideally suited for simulated evolution because of their rapid division and immense numbers. Hyper-mutation can even be induced by periodically irradiating the cultures with DNA-damaging X-rays; while this strategy may kill a large proportion of cells, the survivors will have increased genetic diversity that will likely spur faster evolution.

##### ***4.3.4.2 Directed Engineering***

Another strategy to improve power output is by designing microbes with faster metabolism and growth through biological engineering. For example, one might



exchange key metabolic genes in a microbe with those of a microbe that has a higher respiration rate, or conducting rounds of directed mutagenesis and selection for improved versions of metabolic enzymes. This is also known as metabolic engineering, and constitutes an important frontier for microbial fuel cell research.

#### ***4.3.4.3 Simulating and Optimizing Metabolic Pathways***

Metabolic optimization might also be accomplished with computational simulations. Models of the *Geobacter sulfurreducens* metabolic paths have been created and are being used to test optimization strategies. Such “systems models” can be very powerful as a way to determine direction of bio-engineering or simulated evolution. Creating a systems-model of different aspects of a microbial fuel cell, specifically for space applications, might be an efficient and effective method for optimization.

#### ***4.3.4.4 Anode Composition***

Increasing the anodic surface area per unit volume is clear way to increase power output. This can be accomplished either through the creation novel materials or engineering the fuel cell geometry. We are investigating possible materials and have created a Matlab model to analyze fuel cell geometries. The most important design goal is to create anode surfaces with an ideal pore size for both bacterial colonization and nutrient exchange. Researchers have examined the use of porous graphite foams, graphite brushes, reticulated surfaces, electrode gravel, and other means of increasing surface-area of electrode per volume.

## **4.4 Electrostatic Organisms**

### **4.4.1 Introduction**

Some organisms, known as electrostatic organisms, create very strong voltages to stun prey. We have analyzed the mechanisms employed by electrostatic organisms, and identified researchers working to exploit these mechanisms to generate electricity.

### **4.4.2 Electrostatic Mechanism Analysis**

All cells are surrounded by lipid membranes that are selectively permeable to different ions based on the ion channels and pumps they contain. Using a variety of mechanisms, cells can induce ionic gradients across their membranes that store electrical and chemical potential energy. This energy is used in ATP synthesis and movement of larger molecules. Multi-cellular organisms use ionic gradients across electrically excitable membranes as the basis for neural signaling, and in a highly analogous process, certain species are able to generate pulses of over 500V in dedicated electric organs. Such species, termed electrostatic organisms, total around 200 described species. Though not closely related, these species all use a common mechanism to generate pulses of electric

charge: an electric organ comprised of modified muscle cells, called electrocytes, which discharge in unison like capacitors in series.

In resting electrocytes and neurons, there is a potential difference across the membrane measured at -85 to -90mV, inside negative; additionally, potassium is concentrated within the cell and sodium is much higher extracellularly. These two gradients of positive ions afford reservoirs of selectively mobile charge that allow membrane voltage to change. In response to a nerve impulse or electric stimulus, the voltage difference across the membrane decreases, and voltage-gated Na<sup>+</sup> channels open, allowing a rapid influx that increases the membrane voltage to the point where it reverses polarity briefly. After a delay, voltage-gated K<sup>+</sup> channels then open, creating an exhaust for positive charge and restoring the negative voltage inside.

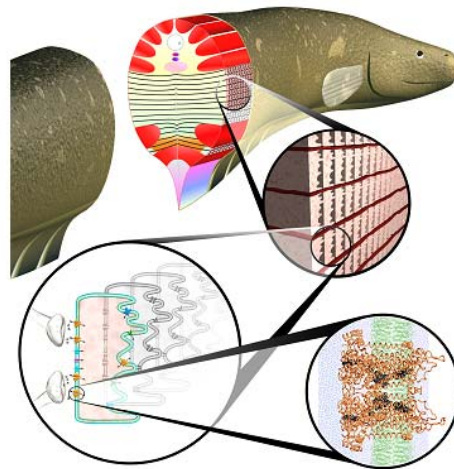


**Figure 17: Electrocytes in Eels**  
(courtesy: National Center for Design of Bio-mimetic Nanoconductors)

In neurons, the membrane has a uniform distribution of voltage-gated channels, so the signal propagates down the length of the neuron to allow signaling. However in electrocytes, voltage-gated sodium channels are present only the enervated face of the flattened cells. When the membrane polarity inverts on this face, it aligns with the polarity on the opposing membrane face, allowing current to flow rapidly across the cell. Thousands of electrocytes in series are excited synchronously to produce a discharge large enough to stun or kill prey.

Because electrogenesis is the result of individual electrocytes discharging in series, the voltage generated depends both on the potential difference across individual electrocytes at the time of discharge and the number of cells in series. Many electrogenic species have distinct electric organs (or distinct regions within the electric organ) with a variance in the number and density of electrocytes to facilitate discharges with a wide range of voltages and frequencies. Low-voltage discharges in the range of a few to several tens of volts are used for communication and for navigating by electro-location. High-voltage pulses are used for hunting prey or for defense, and can top 500V in the electric eel

(*Electrophorus electricus*). The potential across individual electrocytes is determined by the membrane potential, and seems to be fairly constant at 50-100 mV in all species.

The frequency of discharge is determined by the excitation of the enervated electrocyte face, and is limited only by the speed of activation and inactivation of excitable ion channels. The time constants of activation and inactivation for these channels are on the order of a few milliseconds, but the channels of other excitable cells may be even faster, allowing the engineering of even higher frequency discharging electric organs. Voltage and frequency of discharge seem inversely correlated, as low-voltage discharges can top 800 Hz in some knifefishes (family Gymnotidae) while the strongest *Electrophorus* discharges may take several seconds between pulses.

The electric organ's use of excitable membranes to produce power provides an excellent model for a biologically-based power source or energy storage device. Since the mechanism used is very similar to that used in the nervous systems of many animals, there is a wealth of knowledge that can be applied toward the understanding of this unique system. Most important are the individual excitable channel proteins that are present in the electrocyte membrane, which are common in the membranes of other excitable cells. This similarity is extremely advantageous for designing a power system whose characteristics are determined by the kinetics of these channel proteins, because hundreds have been discovered, their genes sequenced and their molecular structures characterized. Engineering of excitable channel proteins is not a new undertaking and to do so for an electric system of this type would begin with a large base of knowledge.

Several groups have begun to design power systems modeled after the electrocyte. Most prominently, the National Center for Design of Bio-mimetic Nanoconductors has proposed to build an implantable retina using excitable membranes that would self-assemble on a nano-porous silicon scaffold. Designing an energy storage device based on excitable channels in a lipid membrane is attractive for several reasons. It could be designed to self-assemble or repair minor damage, and discharge could be controlled with tiny inputs of power relative to the storage capacity. Additionally, the extremely thin membrane (under 10 nm) would make possible the storage of huge amounts of charge in a very small amount of space.

## **4.5 New Mechanisms & Mechanism-Application Overlap**

As discussed above, while conducting our initial research we identified mechanisms which span multiple categories. This overlap may prove valuable for future research.

### **4.5.1 Photocells: *Geobacter* and Rhodopsin**

It may be possible to synthesize novel devices by combining photosynthetic proteins (i.e. bacterial rhodopsin) and microbes with electron transfer capabilities (e.g. *Geobacter*). Since rhodopsin is a cell-wall protein that functions as an electron pump, expressing rhodopsin in *Geobacter* could couple photo-induced charge separation with electron

transfer through the pili of *Geobacter* directly to an electrode. We have carried out experiments towards this end (see below).

#### **4.5.2 Piezocells: *Geobacter* and Prestin**

We have proposed to investigate the development of power skins based on piezo electric proteins such as Prestin. One difficulty in using proteins on surfaces involves stabilizing the protein for extended periods of time. However, in a similar vein to the concept described above, this instability may be overcome by placing Prestin within the cell wall of a micro-organism like *Geobacter*; it also might be possible to use the electron transfer capabilities of *Geobacter* pili to harness power generated by Prestin.

### **4.6 Mechanism Summary**

These initial findings confirm the scientific feasibility of using biological mechanisms to create power, and also demonstrate some interesting synergies in different aspects of energy production. The latter may themselves prove to be very fruitful research projects. The potential to use photosynthetic or piezoelectric proteins in conjunction with bacteria designed for microbial fuel cells, for example, clarifies the “grand vision” of creating diverse space power systems from a limited number of standard biological parts. These preliminary findings have validated the revolutionary potential of pursuing this line of research. It has also highlighted the benefit of taking a multi-disciplinary approach which integrates fields beneath an umbrella in which information can be shared.

## 5 Evaluation Criteria

For NASA to extract value from the database we created, a set of *down-selection criteria* must be developed to identify molecules and mechanisms with potential to impact NASA and which mechanisms warrant further investment. We have begun developing down-selection criteria for this purpose.

Down-selection criteria are composed of two components. The first is based on the molecules and mechanisms themselves and includes questions such as:

- To what depth and extent is the fundamental science understood?
- What is the potential impact of exploiting this molecule or mechanism?
- What are the major hurdles involved with exploiting this molecule or mechanism?
- How long would it likely take to develop a prototype?

The second component focuses on applications. Once applied to a specific application, a biology-based power system will have distinct benefits and costs when compared to other power-systems. These relative comparisons will determine how each system can have the most impact and how it is superior to existing systems. In some cases benefits may drive the decision to pursue the technology. We must gather application-specific information and quantify the distinctive costs and benefits for each potential system, in order to make informed and rigorous comparisons to existing power systems. This cost-benefit analysis should be carried at a broad level for each potential mechanism/application combination and then more thoroughly once conceptual design has been completed.

### 5.1 Power System Metrics

We review here relevant metrics by which to evaluate power systems. Many different types of power systems exist, each with advantages and disadvantages. The final choice of a power system depends on trade-offs that are application and/or mission specific, against metrics selected specifically for that application. We have identified a number of important metrics for characterizing power systems which are outlined below with comments where necessary.

#### 1) *Power and Energy*

- a. Energy: ‘Energy’ includes both the total amount of energy available to the system and also the rate at which energy is available for conversation. For example, in the case of a microbial fuel cell used on a spacecraft the source of energy might be human waste in the form of brines. The total energy would be dependent on the amount of brines produced (e.g. proportional to the number of astronauts) while the rate would energy availability would depend on other variables (e.g. other limiting rates in the processing steps).
- b. Range (W): Max to min power, both estimated and observed.
- c. Specific Power (W/kg)

- d. Specific Cost (\$/W)
- e. Efficiency
- f. Storage

**2) Environmental/Spacecraft Constraints**

- a. Zero/micro-gravity
- b. Radiation hardness
- c. Thermal requirements
- d. Lifetime

**3) Operational Issues**

- a. Maintenance Requirements
- b. Deployment sequences
- c. Safety
  - i. Required reliability (manned vs. non-manned missions)
  - ii. Human safety requirements
  - iii. Impact on extra-terrestrial environments

**4) Availability**

- a. Technology Readiness Levels: We are attempting to map all of our molecules/mechanism/application combinations onto NASA’s canonical technology readiness levels. This provides NASA with the capability to easily assess the time and resources necessary to develop these technologies given their own classification scheme.
- b. Associated Technical Challenges: For innovative power systems that are not commercially available, we are identifying the greatest challenges to their realization. Power systems often require a number of inter-dependant technologies and one of our goals is to identify technological hurdles that might slow or stop the progress of a given system, regardless of the potential upside of other components.
- c. System Availability: This metric addresses how long it takes from conception to design to develop a system for a given application.

**5.2 Supply Side: Comparison to Existing Space Power Systems**

We have compiled a set of characteristics for other major power systems for the purpose of comparison. Table 4 shows accepted values ranges for some of the different metrics identified above for common space power systems and Table 7 shows a critical metric for battery systems.

**Table 4: Comparing existing power systems by metric. (\* indicates system used on the space shuttle)**

<b>Design Parameter</b>	<b>Photovoltaic</b>	<b>Solar Dynamic</b>	<b>Nuclear Reactor</b>	<b>Hydrogen Fuel Cell</b>	<b>Radio-isotope</b>
Power Range (kW)	.1-300	10-300	100-10,000	.2-50 7-12*	.1-10

Specific Power (W/kg)	25-250	9-15	2-40	275 60-100*	5-20
Specific Cost (\$/W)	700-2500	1000-2000	400-700	-	16,000-200,000
Efficiency	14-23%	17%	20%	-	3-10%
Radiation Hardness	Low-medium	High	Very high	-	Very high
Storage	Batteries	Integral thermal	None	Hydrogen	None
Shadowing Sensitivity	High	High	None	None	None
Safety	Minimal	Minimal	High	Medium	Medium
Lifetime (years)	20	-	-	-	25
System Availability	6-12 months	Not commercial	Not commercial	Custom	Custom

**Table 5: Comparison of common batteries with potential application in space**

Battery	NiCd	NiMH	Lion	Sodium Sulfur
Specific Energy Density (W-hr/kg)	25-35	30	70	140

It should be noted, however, that many of the applications we are investigating have advantages along dimension not normally considered for existing power systems. This includes manufacturability, potential to be self-healing, synergies between diverse applications (solar, fuel cell, etc). These kinds of benefits hold the potential to enable wholly new mission architectures, potentially unimaginable with existing systems.

### 5.3 Demand Side: Tailoring metrics to applications

The benefit and cost of a specific power system depends on the requirements created by the mission and by the application. For example, the optimal power system on a deep-space, unmanned satellite is different from the optimal power system on a permanent Martian Base. Part of controlling for applications involved collecting information on typical power loads in space systems. Table 6 below illustrates estimated power loads for various subsystems on a lunar outpost.

**Table 6: Estimated power loads for a lunar based (courtesy: )**

	System	Expected Power Demand (kW)
Baseline	Housekeeping	5
	Habitat lighting	.05
	Life support	16

	Communications	1
	Scientific instrumentation	2
	Habitat heat	0
Peak	Crew-discretionary	17
	EVA floodlights	2
	Rover charging	3
	ISRU testing	10
Remote	Science instrumentation	1

## 5.4 Considerations for Mechanism-Specific Cost Benefit Analyses

### 5.4.1 Piezoelectric Proteins

Piezoelectric proteins should be compared against the known piezoelectric characteristics of existing materials. Piezoelectricity is a property of materials in which mechanical displacement and electric displacement are coupled. The Gibbs free energy of these materials is given by the equation below [Ikeda 1990].

$$G(E, F) = G(0, 0) + 1/2 c_{11}E^2 + c_{12}EF + 1/2 c_{11}F^2$$

Where E is the electric field and F is the force applied. The most important coefficient is  $c_{12}$  which is piezo electric coefficient. This coefficient represents the electromechanical coupling in the piezo electric material. Another important coefficient is the coupling coefficient  $k$ , it represents the fraction of mechanical energy converted into mechanical energy or vice versa.  $k$  is given by the following equation [Ikeda 1990]

$$k = c_{12}^2 / c_{11} c_{22}$$

K. H. Iwasa made measurement of piezoelectric properties of Prestin containing cells and found that  $c_{12}$  value for these cells is around  $25\mu\text{C}/\text{N}$  [K. H. Iwasa, 2001] which is four orders greater than the best known piezoelectric material.  $k$  value for Prestin containing cells was around 0.3 and the best known piezoelectric material has a value of 0.76. Iwasa concluded high inertia as the reason for lower value of  $k$  irrespective of a very high piezo electric coefficient.

The Piezoelectric properties of Prestin are many orders higher than the best known piezoelectric materials. The bottle neck in harnessing these properties is the mechanical compliance of the membranes. We are working on reducing the compliance of membranes in developing our architectures for the power skin.

### 5.4.2 Biological versus Conventional Solar Cells



Photovoltaic systems are currently capable of producing 10 KW of power, efficiencies have increased by a factor of 2.5 and specific power (power to weight) has decreased by a factor of 5 since the originally developed in 1958. Nevertheless, PV still account for 10-20% of a spacecraft's weight and 10-30% of the cost (Allen, SDIO). There is thus much research into further improvements of PV technologies. In addition to the canonical goal of greater efficiency at lower weight and cost, research into traditional PV technology is addressing a number of mission specific challenges including temperature robustness, radiation hardness, and other issues.

Analysis of the viability of biological solar cells must take into account competitive technologies, both alternative power systems and solar cells constructed from non-biological materials. While a real cost-benefit analysis demands more knowledge of the end-goal and functioning of a biological solar cell, we have begun to identify metrics and questions that must be addressed. The

#### ***5.4.2.1 PV Characteristics and Metrics***

There are number of different metrics with which to compare solar cell performance and overall ability to impact NASA missions. Efficiency is the most common metric used, but there are a number of other importance variables. Another important characteristic is weight, which is a direct proxy for other important variables such as cost. Weight must include not only launch weight but also the drag weight, i.e extra mass incurred from the fuel necessary to balance torque produced from solar cell support structures. Packaging is a related variable that affects system design and complexity. To characterize the importance of weight and packaging, in addition to individual solar characteristics, we are examining the support structures necessary for different technologies.

Other variables that require consideration are: space radiation/plasma environment, lifetime, operation and survival temperatures, deployed stiffness, on-orbit accelerations, on-orbit voltage sun tracking capabilities, transfer orbit power, deployed area, dimensional stability and survivability from auxiliary environments.

#### ***5.4.2.2 Inorganic Solar Cells***

Inorganic solar cells represent the most common class of photovoltaic devices. Originally inorganic PVs were entirely made up of silicone with efficiencies around 10%. However new materials, mostly GaInP, GaAs and Ge based solar cells are capable of efficiencies nearing 30%. Today, production of solar cells is split almost equally between silicon and gallium based solar cells. In addition to the choice of material, efficiency gains have been realized by the developing designs based on two, three or four junctions, as opposed to the traditional single junction devices. Most research is concentrated on the addition of fourth and fifth junctions (which have been demonstrated by the Fraunhofer Insitute for Solar Energy Systems), the use of more optimal band gaps grown in cells where the lattice matching constraint is relaxed, and lastly new, novel materials including amorphous silicon, cadium telluride and copper indium gallium selenide. These new approaches will push the efficiency of inorganic solar cells above the 30% mark.

### 5.4.2.3 Organic Solar Cells

Another area of research is in organic PVs. Many materials being studied (e.g. phtalocyanines, dyes, conducting polymers (polythiophenses, polycarbazoles, polyphenylenes and poly (6-20) have demonstrated the potential to act as PVs (Bertoncello, 2003). Organic PVs are created when an electron donor-type polymer is mixed with an electron acceptor, forming a ‘bulk hetero-junction’. Much of the research in this area focused on better understanding the charge transport complex. One of the potential benefits of organic PV materials is that fabrication is less costly and less energy consuming, although efficiency are not as high as inorganic materials (Bertoncello, 2003).

### 5.4.3 Microbial Fuel Cells

Microbial fuel cell must be compared against alternative methods available to exploit organics. MFCs use the cathode reaction as the electron sink for an oxidation reaction instigated by microbes. However, other possible sinks are available, in particular methane ( $\text{CH}_4$ ) and Hydrogen ( $\text{H}_2$ ) both of which are useful in space and can even generate electricity through traditional fuel cells. These alternatives may or may not compete with the direct electricity production. Methane and Hydrogen are often produced from biomass or organic wastes via fermentation processes, which do not fully reduce the organic compounds, and produce significant amounts of secondary organics, such as acetate ( $\text{C}_2\text{H}_4\text{O}_2$ ) or Butyrate ( $\text{C}_4\text{H}_8\text{O}_2$ ) depending on the specific process [Logan 2004]. These secondary organics can be further exploited by organisms in a microbial fuel cell in a synergistic process. These considerations highlight the need for *systems-level design* of various biological waste-treatment/energy production capabilities, which can be used to inform and optimize component designs.

A secondary set of system-level considerations involves synergies between Microbial Fuel Cells and alterative methods for biological energy production. As noted above, it may be possible to use similar organisms for MFCs and solar-electric and piezoelectric power generation. This has important consequences for in-space manufacturing. This design-goal will affect the design and optimization of a microbial fuel cell for space applications and, by extension, their relative benefits and costs compared to alternative power systems

### 5.4.4 Comparing Electrostatic Organisms

The underlying mechanisms of charge storage and discharge utilized by electrostatic organisms may have multiple uses in a biological power paradigm, including as ultra-capacitors or charge storage devices. Similar to microbial fuel cells, the benefits and costs of such systems should be weighed at systems level, where the full advantages of biological systems can be evaluated, in addition to the component level. In the absence of an obvious end application it is of course difficult to provide an initial characterization of such a cost-benefit analysis. In part for this reason, we decided not to down-select the

mechanisms from electro-static organisms for further study in our Phase I project. The basic mechanisms, however, should not be ruled out for further study.

## **5.5 Evaluation Criteria Conclusion**

A full cost-benefit analysis of a given bio-electric technology depends critically on the end-architecture developed. Still, it is possible to rank different biological mechanisms based the relative ease of developing an end application from it, and the potential impact of that end application. In this regard, we have identified piezoelectric proteins coupled into “Power Skins” as well as Microbial Fuel Cells, as the most promising technologies for further investigation during the Phase I research period. We should also stress that the full benefit of using biological power sources will be realized on the system-level, rather than the application level. That is, the true end-goal should be the development of biological paradigm in which multiple applications are synergistic and can be fabricated from similar underlying parts. This paradigm will exhibit multiple benefits at the systems level not present at the application level, such as the ability to flexibly manufacture technologies based on specific needs and synergies with other critical functions such as advanced life support.

## 6 Power Skins based on Piezoelectric Proteins

This chapter summarizes our more detailed analyses of Power Skins. We provide preliminary end-architectures, estimate total power output as a function of various environment and system parameters and describe progress on experiments designed to validate the basic mechanism.

Power Skins are envisioned as thin skins which harness the transduction potential of piezoelectric proteins to scavenge vibration and generate power for sensors or other devices. In the course of our investigations, we found two aspects of this concept particularly interesting: First, if power skins were based on self-assembling biological molecules like lipids and proteins, one could envision growing them when needed in space, for specific applications. This notion of “on demand” and “throw away” power systems built in part from in-situ materials has the potential to greatly increase mission flexibility.

Second, while investigating the range of electrically active proteins described above, it became apparent to us that many such proteins function in a similar way—namely, by creating a charge separation across a lipid membrane through the separation of ions. This parallelism is extremely interesting. It suggests that if Power Skins could be developed to function based on the action of one kind of protein, the underlying architecture could be altered to accommodate many kinds of proteins. By extension, the range of stimuli that could be scavenged for energy increases substantially. From our review alone, one could envision power skins that scavenge vibration, sunlight, or temperature gradients. This also raises the possibility of “mixed” power skins, grown with different ratios of such proteins for use in specific environments.

### 6.1 Introduction and Applications

In order to power a device, Prestin must be expressed, localized, and oriented in a lipid-bilayer so that an electric potential can be established from vibrational stimulation. Subsequently, the potential difference created must be harnessed. We have developed some preliminary models and architectures to accomplish these tasks. Once the architectures have been developed and implemented, many applications are envisioned; skins could be incorporated into astronaut suits, cover structures, or stand-alone as an energy production facility. Further, skins could be integrated with biological sensors, to create a unified power-producing sensing surface. Electrically active proteins have the benefit of a high power to weight ratio, making them affordable to transport per Watt produced. These proteins also have the benefit of working on the nanometer length scale, allowing remarkable efficiency and a wide range of implementation magnitude (from microsensors to power plants).



**Figure 18:** A space suit, modeled after the *Biosuit*, covered with a power skin and sensors. Sensors can be placed at random on the suit and draw power from the skin itself.  
(image by Chris Lund © IntAct Labs)

### 6.1.1 Power Estimate

Power generated by a skin containing Prestin is dependent on total surface area, vibrational energy, and the characteristics of the proteins itself. We have taken three approaches to estimate the amount of power that can be generated. The first one is calculating total power that is available in the wind and assuming a 45% efficiency of Power skin. Total energy in the wind can be calculated by using

$$P = 1/2 * \rho * A * v^3$$

Where P is the power in the wind,  $\rho$  is the density of the wind, A is the surface area of the Power skin, and v is the velocity of the wind. Martian winds have similar wind velocities but low air density which is around  $0.22 \text{ Kg/m}^3$ . The total power that is available in the Martian wind with wind velocities of 10m/s (very conservative estimate) and a area of  $1\text{m}^2$  is 1.1 W. At 45% efficiency half a watt of power can be generated using Power skin. Figure 16 shows the power output by varying velocity of the wind and area of the Power skin. These the results show that if the area of the surface is increased the power produced in the order of 10 of watts. By covering a Martian base a close to 100 watts of power can be generated.

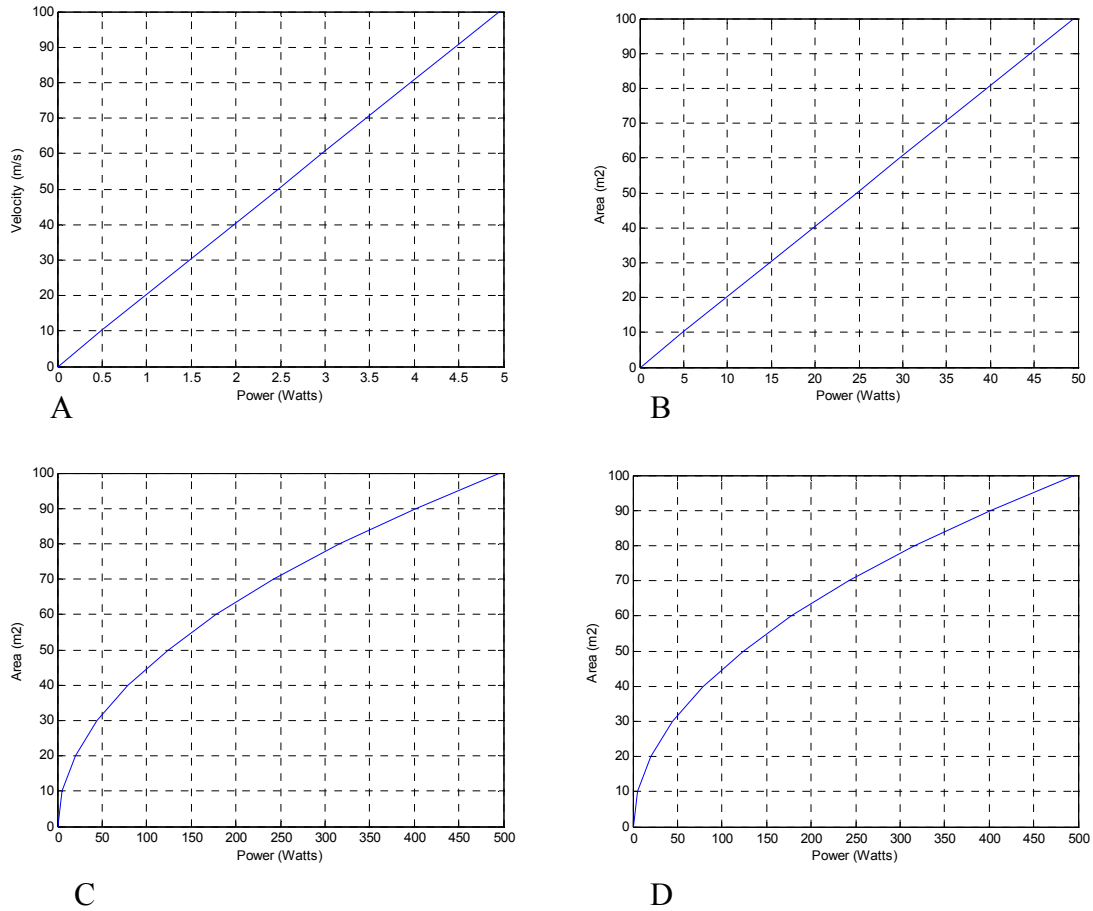


**Figure 19: Power output by varying different parameters like the velocity of the wind and the area of the Power skin. A) The output power generated by power skin (constant area of 1m²). B) The output power generated by power skin (constant velocity of 10m/s). C&D**

The second approach we used to estimate the power calculations by considering that fact that most structures vibrate at their natural frequency and these vibrations can be harnessed by Power skin. A lumped element model as created by [Roundy 2002] of this is shown in Figure 17 below:

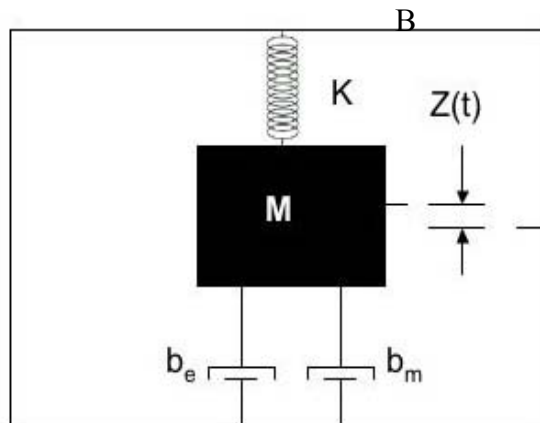


**Figure 20: A lumped element model adapted from Roundy 2002**

The total power generated is given by the following equation

$$P = \frac{m\zeta_c\omega_n\omega^2(\omega/\omega_n)^3Y^2}{(2\zeta_T\omega/\omega_n)+(1-((\omega/\omega_n)^2))^2}$$

Where  $m$  is mass of the system and  $\omega$ 's are natural and damped frequencies. Calculations done by [Roundy, 2002] show that the power available is around 0.1W by considering 120Hz vibrations with acceleration of 2.25 m/s<sup>2</sup>.

The third and final approach utilizes experimental results from the Peter Dallos lab at Northwestern University which measured the piezoelectric properties of Prestin containing cells. We have extrapolated those results linearly to Prestin following the widely accepted assumption that the piezoelectricity of these cells is from Prestin. The results of their measurements are published in [S. Sacchi, 2001] Their measurements showed when a 2KPa tension is applied to cell membrane of Prestin containing cells, the resting potential changed by 65mv and a charge displacement of 0.96 Pico coulombs. The power generated is given by the following equation

$$P=V*Q*F$$

Where  $V$  is the change in the resting potential of the membrane,  $Q$  is the charge displaced across the membrane and  $F$  is the frequency at which the charge is displaced across the membrane. At 3000 Hz the amount of power generated is ~38 microwatts/mm<sup>2</sup>. Below Figure 18 shows the variation of the power with change in frequency.

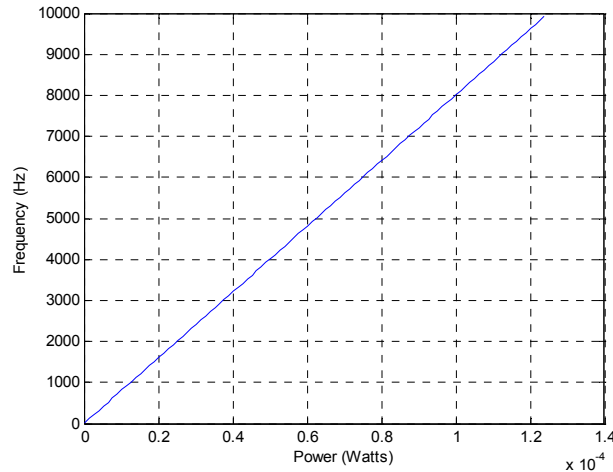


**Figure 21: Variation of power with the variation of frequency at which pressure is applied.**

These calculations bring us to a conclusion that sufficient mechanical energy is available that can be harvested and Prestin is capable of converting it into useful electrical power.

## 6.2 Potential Architectures

We have developed two related architectures to realize the power-skin concept. The first architecture is built around proteins embedded in synthetic lipid bilayers sandwiched by electrodes. The second architecture uses specially designed living organisms such as *E. coli* or *Geobacter* designed to house and maintain energy scavenging proteins. Movement of the cell wall of such microbes will create ionic potential difference that can be harnessed. Both architectures offer distinct advantages and disadvantages and we believe both should be pursued and tested before down-selection. The synthetic system is based on fully known production methods and the artificial membrane can be designed to have less compliance than the living membranes. We expect this feature would raise the efficiency of this architecture in comparison to the second architecture. The second architecture, based on living organisms, would involve novel fabrication and maintenance methods, increasing the uncertainty and possibly lowering efficiency. However, the use of living organisms provides a powerful and simple method for maintaining the proteins over long periods of time. It also raises the possibility of fabricating power on-site by growing microbes. We describe both architectures in more depth below.

### 6.2.1 Architecture 1: Power Skin Based on Synthetic Lipid Membranes

Our first architecture is developed around a synthetic lipid membrane in which Prestin is embedded. The membrane will be sandwiched between electrodes, and the ionic potential gradient will be harnessed using standard methods. Additional electronics such as maximum power point tracking (MPPT) chip or some related mechanism can be used to smooth the signal. The end product is a series of chips (estimated size 2x2 cm) connected in mechanically and electrically in series. Initial prototypes for this architecture will use rigid electrodes, but we will later use flexible electrodes.

For this architecture we have developed two principal variants: 1a. The central membrane is a flat lipid bilayer embedded with proteins sandwiched by electrodes, and 1b) Proteins are embedded within synthetic liposomes sandwiched between electrodes. Both of these variants are described below.

#### 6.2.1.1 Architecture 1a: Flat Lipid Bilayer Tethered to a surface

The first variant of architecture 1 involves using a flat lipid bilayer rather than liposomes. There are three principal aspects of this architecture: (1.) The lipid bilayer is tethered to a gold electrode by low molecular weight spacer groups such as peptides or polyoxyethylene groups. (2.) Proteins are embedded in the flat bilayer during assembly of this flat bilayer. (3.) The gold electrode is connected to another electrode and a fluctuating potential difference is harvested. *These basic steps have all been realized independently in the laboratory by different researchers.* Our plan is to integrate them into a final product. These three aspects are described below.



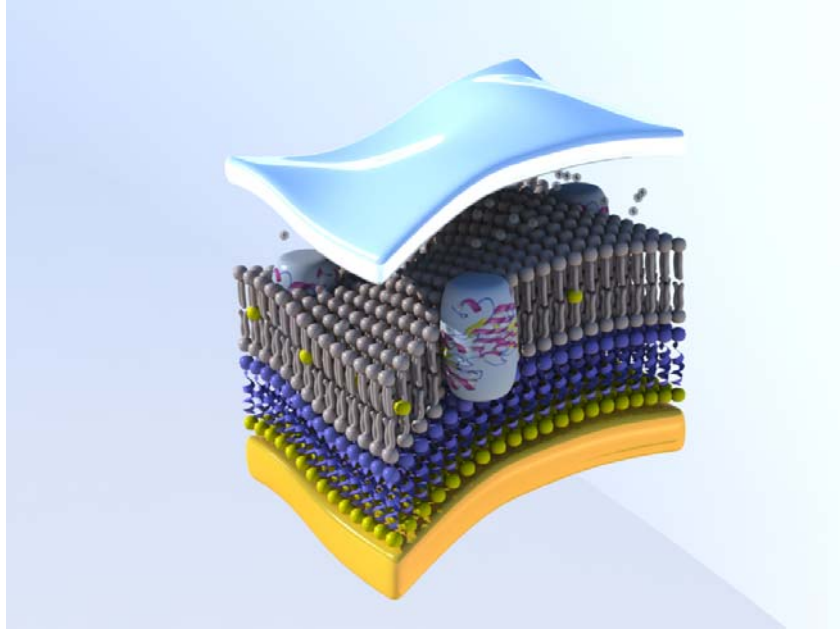


**Figure 22: A model of a membrane that will be used in developing the Power skin. Gold Electrodes on the bottom, platinum electrode on the top. (Image by Chris Lund © IntAct Labs)**

First, a bilayer must be formed and tethered across a surface. This can be accomplished using the *vesicle fusion* method in which vesicles are fused onto self-assembled monolayers of spacer peptides. In the process developed by Lingler [Lingler, S 1997], the spacer peptides are terminated by a sulfur functionality to be anchored to a gold surface by covalent bonds. Spacer groups provide an aqueous compartment between the lipid bilayer and the gold film and at the same time to tether the lipid bilayer covalently to the spacer peptide. To create this latter covalent bond the free COOH terminal is activated in situ. The Lingler method is illustrated below (Figure 23).

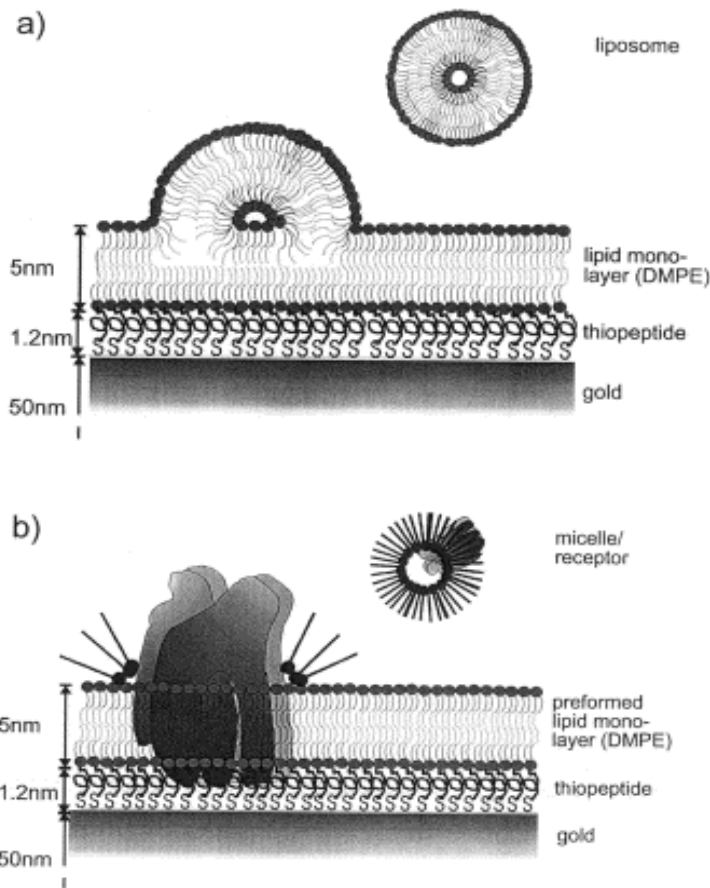


**Figure 23: Vesicle Fusion (Lingler 1997)**

Our architecture will be derived from the Lingler method. However, we will use a porous gold substrate, rather than a gold substrate, to increase the ionic flow. Also, rather than use the space peptide described above, we will use a relatively hydrophobic pentamer of alanine which is functionalized with terminal sulfur group followed by more hydrophilic peptide. For the bilayer to be electrically active, Prestin must be embedded in it. This is accomplished by using vesicles which contain Prestin during the process of bilayer assembly.

Second, this bilayer must be sandwiched by electrodes and the potential difference harvested. As noted, initial prototypes will use rigid gold and/or platinum electrodes. Later architectures will use flexible electrodes (likely coated in gold). These will create chips of approximately (2x2 cm). The chips will be coupled mechanically as well as electrically. Mechanical coupling will enable mechanical energy to be transferred from one chip to another on a skin. Electrical coupling should be in series. The output will be fluctuated ionic potential that can be smoothed using a maximum power point tracking (MPPT) chip or related electronic system.

### **6.2.1.2 Architecture 1a: Synthetic Liposomal Encapsulation**

The same basic principals can be used to create a variant of architecture 1, in which the driving proteins are encapsulated in liposomes instead of flat lipid bilayers. Instead of vesicle fusion onto the substrate, the vesicles are attached to the substrate by using surface chemistry techniques. A layer of liposomes sandwiched in electrodes may be more robust than a solid skin, but would likely be less efficient. Liposome architecture would therefore be most useful where stress levels are high on the membrane. The circular structure of the liposome can absorb shock without significant deformation. The liposomes will be sandwiched between two layers of flexible electrodes as shown in Figure 24. A third electrode in a reference solution provides a reference voltage to create the potential difference.

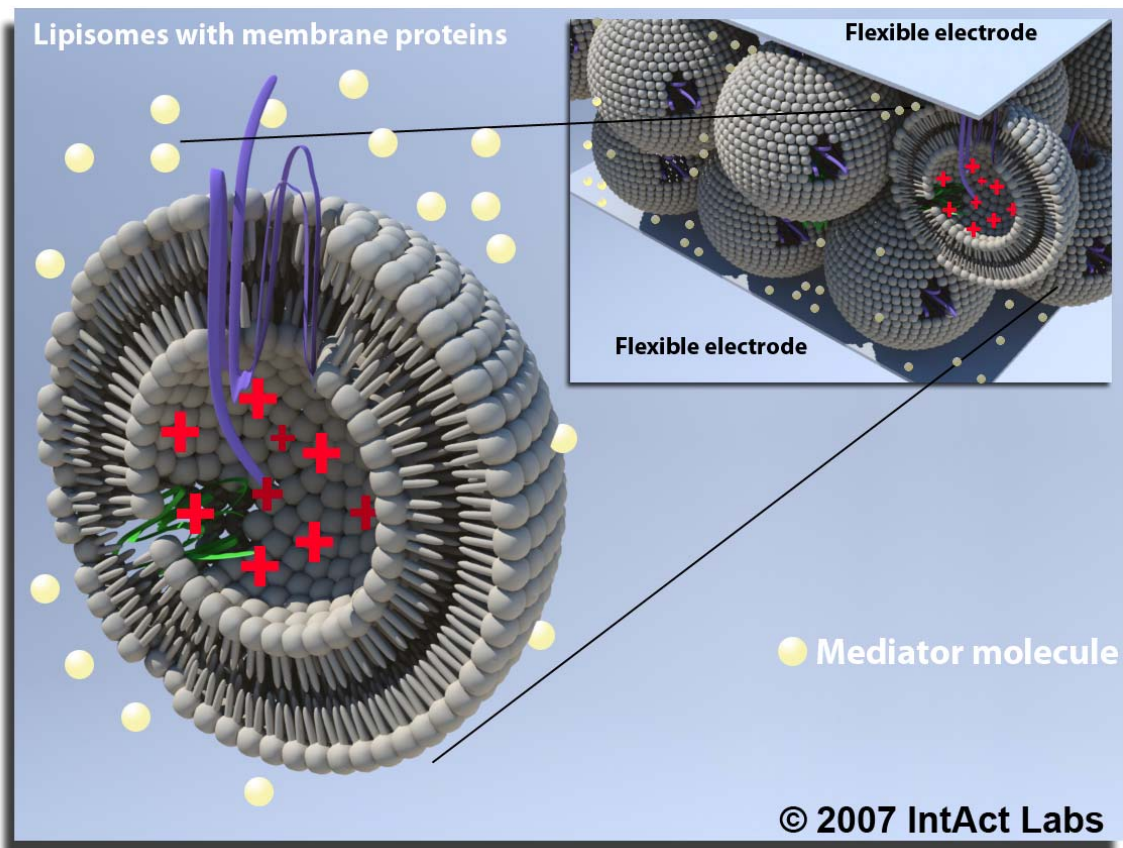


**Figure 24: Liposomal model of the membranes with Prestin. When conformed charge builds up inside or outside of the liposomes. Another compartment would house an electrode, connected to one of the electrodes in this picture. Potential difference between these electrodes would be harnessed.**

© IntAct Labs

### 6.2.1.3 Making the Skin Flexible and Robust

Whether a flat bilayer or liposomal layer is used, our end goal is a flexible robust skin. As noted, in a first prototype, we will use rigid electrodes—the gold surface comprising one electrode and the other being platinum electrode. In later prototypes these electrodes

should be made flexible. This can be accomplished using thin gold coating on a flexible membrane.

Flexibility introduces the need to make the lipid bilayer more robust. Robustness can be introduced by cross linking the lipids using a covalent bond like ester bonds or disulphide, or by introducing structural membrane proteins. This notion is shown in Figure 25. Ester bonds/disulphide bonds are shown in yellow. Disulphide would increase the rigidity and robustness of the membrane, however, it should be noted that this could decrease efficiency slightly.

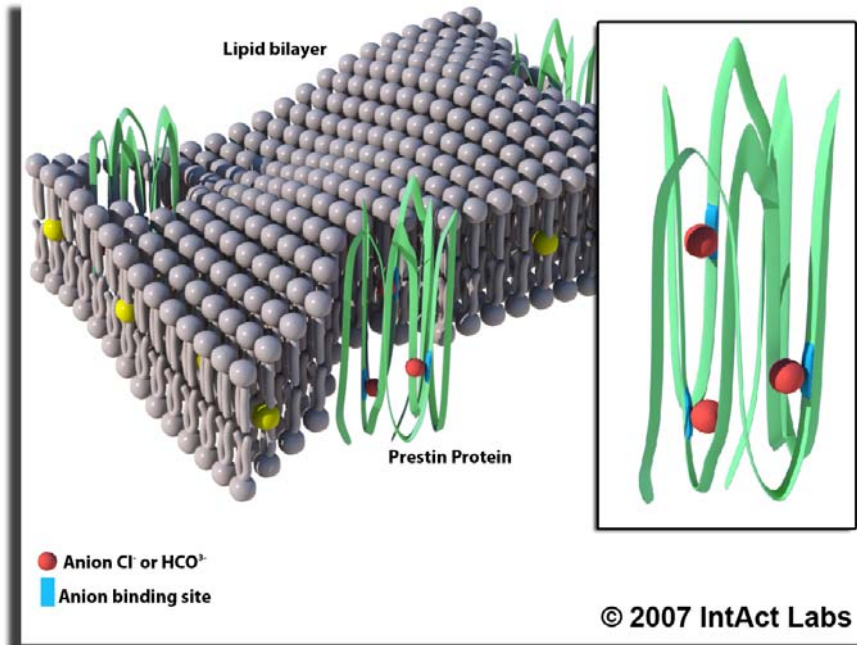


**Figure 25: Artist conception of a more robust Power Skin membrane in which cross-linked lipids are incorporated along with Prestin. (Picture by Chris Lund © IntAct Labs 2007)**

## 6.2.2 Power Skin Architecture 2: Living Power Skin

The second architecture uses biological cells as the central membrane structure. We propose to express Prestin in E Coli or Geobacter while genetically engineering them to minimize their metabolism and other functions. Genetic engineering changes can be done by inserting required gene in to a vector and inserting the plasmid into the cell and replacing unwanted gene with required gene. The end result in this case would be a layer of living cells with over-expressed Prestin (or related electrically active protein such as heat-activated ion channels) sandwiched between an electrode and an insulating sheet. The electrode would be linked to a reference electrode.

Power generated by this concept is difficult to model or assess a priori. The architecture introduces the problem of maintaining living cells. However, this issue also opens the door to tremendous potential advantages. For example, in the right environments, one could imagine growing power on-site, or using colonies to perpetually scavenging power

where food sources are present. This architecture begins to link the Power Skin concept with the notion of a flat, portable microbial fuel cell. The effort to use living cells in the architecture would therefore be carried out within the context of the Mobile MFC effort.

### 6.3 Experiments

Experiments are ongoing in the process of creating a sensor using Prestin. We acquired the full length Gerbil Prestin gene of from Peter Dallos lab in Northwestern University. Figure 22 shows the full length gene inserted in pGEM-72 with cloned BamH I and Apa I restriction enzymes sites.

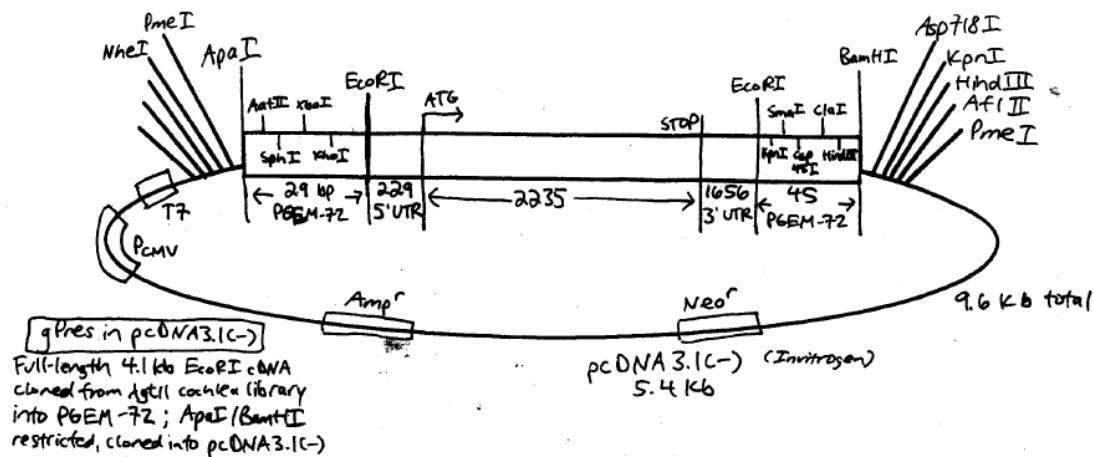


Figure 26: Full length pGEM-72vector (Peter Dallos lab, personal correspondence)

In order to test the electrical properties of Prestin in a sensor we created the following protocols:

1. PCR extraction of Prestin coding region from pGEM-72 vectors
2. Insertion of N terminal Histidine tag attached Prestin coding region with EcoR I and Xho I restriction enzyme sites in pET 28a Vector.
  - a. PCR amplification of the pET 28a Vector
  - b. PCR amplification of Prestin coding region
  - c. Restriction Digestion of both amplified pET 28a Vector and Prestin gene with both EcoR I and Xho I.
  - d. Ligation of pET 28a vector and Prestin Gene
3. Expressing the Plasmid in a chemically competent cells
4. Purification of Plasmid
5. Expression of this plasmid in Rosetta Gami E.Coli strain
6. Purification of Expressed Prestin using Histidine tag
7. Attachment of the protein to the substrate

### 6.3.1.1 Experimental Design

Prestin gene was inserted into pET28A vector, shown in figure 23, in the coding region of the pET 28a vector in between the EcoR I and Xho I site. The designed primers are

Forward Primer : GTTTCTGAATTCTCCTTCTTAAAGTTAAACAAAAT  
 Reverse Primer : GTTTCTCTCGAGCACCACCACCACCACCTG

The primers are designed with restriction enzymes sites that are used when the Prestin gene is inserted into the Vector. The Prestin gene and the pET 28a vectors were amplified by PCR. The formation of the right PCR products was confirmed by Agarose gel electrophoresis. The amplified PCR products were then later restriction digested with the

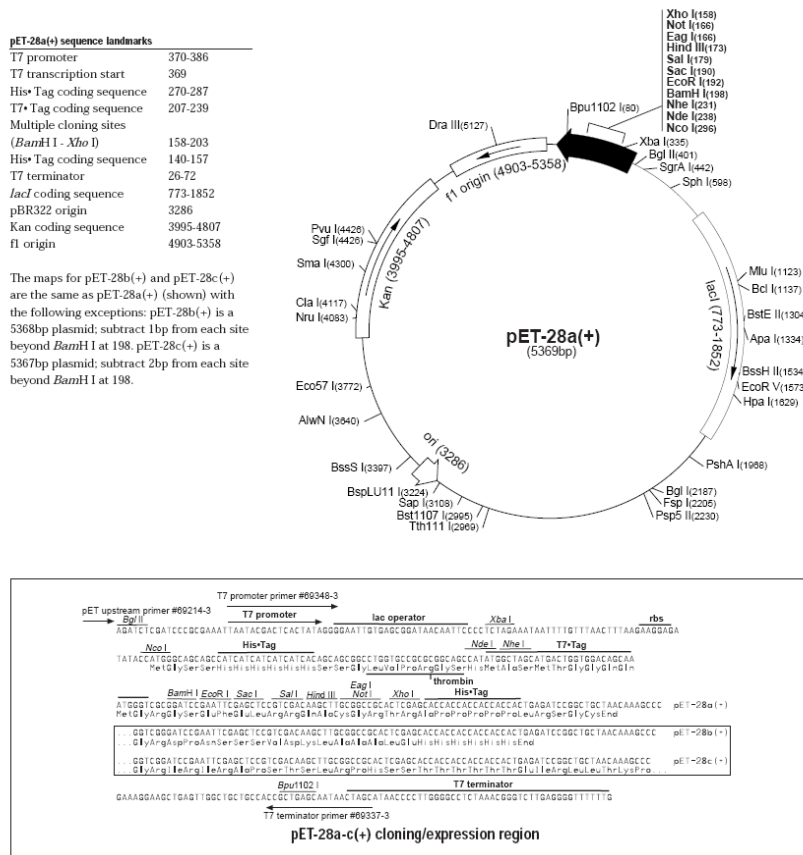


Figure 27: Vector map of pET 28a (Image courtesy: Novagen)

restriction enzymes for 12 hours at 37°C and heat kill the enzymes at 80°C for 20 minutes and the formation of the right products was again verified by Agarose gel electrophoresis. These cut pieces of Prestin gene and pET 28a were then later ligated using T4 ligase for half an hour at room temperature and another half an hour at 18°C and the enzyme was later heat killed at 80°C for 20 minutes. This was again verified by Agarose gel electrophoresis. This ligated product was later then transformed into chemically competent cells by heat shock at 42 °C and later grown in Kanamycin plate. Single

colonies were then grown in Kanamycin broth. The grown cells were lysed and the plasmids were extracted. Currently the Plasmids are in the process of being sequenced.

Once the sequencing results confirm the right sequence of Prestin and pET 28a, the DNA will be transformed into Rosetta gami strain for the protein expression. The protein will be purified and affixed on a substrate for the sensor fabrication.

## **6.4 Conclusion and future work**

Power Skins are envisioned ultimately as “growable,” self-healing skins capable of harnessing the transduction capability of highly sensitive membrane proteins that are identified and classified by IntAct Labs. We envision that the skins will be optimized for specific environments by varying the ratios of such electrically-active proteins. During phase I we created a plasmid with Prestin gene that can be expressed in E.coli, estimated power outputs that can be theoretically generated by using power skins, and developed conceptual architectures for potential implementation. Further work will entail detailed conceptual designs and characterization of the device as well as experimental validation of fixing substrates to electrodes and maintaining structure, functionality, and stability of the proteins.

## 7 Microbial Fuel Cells in Space: Bioelectric Chambers

Microbial Fuel Cells can be coupled with advanced life support functions to simultaneously create power and remediate wastes in space. Further, it may be possible to “grow” fuel in the form of algae or other biomass using in-situ resources on Mars (H<sub>2</sub>O, CO<sub>2</sub>, Nutrients) and possibly the Moon (H<sub>2</sub>O). The microbes used in such applications, such as *Geobacter sulfurreducens* may also be exploited in other bio-electric applications, thus creating synergies in a broader bio-electric paradigm. Together, these applications could radically alter the design of space systems, increase mission flexibility, and open new pathways for creation of electricity in space.

This chapter analyzes the design constraints, opportunities, and challenges associated with creating Microbial Fuel Cells for space applications. First, a set of mission scenarios and high-level architectures are created, in order to develop requirements for the use of microbial fuel cells. These scenarios are used to derive an upper-bound estimate for the amount of electricity that may be produced in a given mission using MFCs. They are also used to create a systems dynamics model using Vensim® to evaluate the effects of using feedback loops and in-situ resources in the fuel cell system. Next, more specific challenges associated with designing MFCs for integration with advanced life support are analyzed. These design challenges include the need to select and control microbes, the need for detailed models of waste streams, bio-reactor selection and design, and anode design and materials selection. After this, a sizing model for microbial fuel cells assuming stylize architectures is created using Matlab. Finally, we present and discuss two experiments conducted to validate the discussion: (1) a MFC running on *Geobacter Sulf*, and (2) genetic alteration of *Geobacter sulf*. using the photo-electric protein Bacterial Rhodopsin.

### 7.1 Mission Scenarios and High-Level Power Estimates

As part of our evaluation of the broad efficacy of Microbial Fuel Cells (MFCs) for advanced space exploration applications, we have developed a suite of application architectures and performed a systems analysis of those architectures. This section describes the application architectures and provides the results of our systems analysis.

#### 7.1.1 Interplanetary Transit

Interplanetary transit missions (the term “interplanetary” is used here with some license, as we also include lunar transits) are characterized by the following design-driving parameters:

- Short (days) to medium (months) duration
- Power is critical and highly constrained. Solar power and/or nuclear (radioisotope/fission) power may be available
- Surface area and volume (interior and exterior of vehicle) is highly constrained



- Crew metabolic processes must be supported and an organic waste stream from crew metabolism will be available
- Other organic sources (e.g., biomass) are TBD
- Other than pre-positioned stores and crew metabolic waste, there is no other organic source

The interplanetary transit application would likely involve a MFC bioreactor that processed crew waste and trash to recycle the waste/trash and to provide ancillary power for particular systems (e.g., ECLSS). If a greenhouse is provided for augmentation of the crew diet, etc., there may be additional biomass contributed by that system. However, it is unlikely that additional volume or surface area, either internally or externally, would be allocated specifically to support a biomass generation function; instead higher-energy-density systems such as batteries and/or radioisotope systems would be utilized.

### **7.1.2 Lunar Surface Operations**

Lunar surface operations are characterized by the following design-driving parameters:

- Short (days) to long (years) duration
- Power is critical and constrained. Solar power may be available, subject to a 14 Earth day - 14 Earth night diurnal cycle, except for a few specific locations which receive either complete sun or complete shade. Nuclear (radioisotope/fission) may be available.
- Surface area and volume on interior of the Lunar base is constrained, but surface area and volume on exterior is relatively unconstrained
- Crew metabolic processes must be supported and a waste stream from crew metabolism will be available
- Other organic sources (e.g., biomass) are TBD
- No environmental source of hydrogen, oxygen, or carbon
- Other than prepositioned stores and crew metabolic waste, there is no other organic source

The Lunar surface application would likely involve a MFC bioreactor that processed crew waste and trash as in the interplanetary transit application described above. However, the available external surface area surrounding the Lunar base and the abundant solar flux during the 14-day sunlight cycle could additionally be utilized to support a greenhouse for biomass production. (Note: There is a major constraint relating to carbon availability, see discussion in Section 7.1.6 below.) Therefore, the size of the MFC could be tailored to meet the power level required.

### **7.1.3 Mars Surface Operations**

Mars surface operations are characterized by the following design-driving parameters:

- Medium (months) to long (years) duration
- Power is critical and constrained. Solar power may be available, subject to reduced solar insolation (approximately 40% that of Earth) and potentially strong

seasonal influences depending on latitude. Nuclear (radioisotope/fission) may be available.

- Surface area and volume on interior of the Mars base is constrained, but surface area and volume on exterior is relatively unconstrained
- Crew metabolic processes must be supported and a waste stream from crew metabolism will be available
- Other organic sources (e.g., biomass) are TBD
- Carbon is available via atmospheric CO<sub>2</sub> and frozen CO<sub>2</sub> at the poles, and may also be a constituent of the Martian regolith
- H<sub>2</sub>O may be available in the form of ice at the poles and/or subsurface water at other latitudes

The Mars surface operation application would likely involve a MFC bioreactor that processed crew waste and trash as in the interplanetary transit and Lunar surface applications described above. As with the Lunar surface application, the available external surface area surrounding the Mars base could be utilized to support a greenhouse for biomass production. . And as with the Lunar surface application, the size of the MFC could be tailored to meet the power level required. The abundance of atmospheric CO<sub>2</sub> and the potential use of Martian regolith as a growth medium make the Mars surface application attractive for MFCs.

#### **7.1.4 Upper Bound Power Estimates**

Our systems analysis addressed the organic decomposition of human waste, trash, and biomass into cellulose and complex carbohydrates that are, in turn, used as feedstocks for microbial conversion to energy in the MFC.

We must first establish exactly how much electricity is theoretically available from organic wastes. The most important waste streams currently produced in space include human solid and liquid wastes, waste biomass from food, and waste biomass from a potential greenhouse. These waste streams are composed of diverse and variable organic compounds. In this section, we begin a simplified model of waste streams and fuel-cell technology to determine the maximum theoretical energy available.

Recent NASA studies have used the following organic waste estimates for a six person crew on various missions:

**Table 7: Waste Model for a six person crew [Source: Solid Waste Processing and Resource Recovery Workshop, Engineer Director, Crew and Thermal Systems Division 2001 CTSD-ADV-474]<sup>1</sup>**

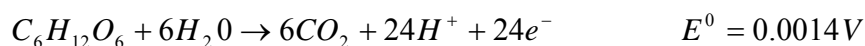
<b>Units are kg/day (based on 6 person crew)</b>					
<b>Waste Component</b>	<b>Transit, Packaged Food &amp; Salad Crops</b>	<b>Independent Exploration, salad crops grown</b>	<b>Exploration Mission, Low carbohydrate diet</b>	<b>Extended Base, All plants menu</b>	<b>Extended Base, All plants menu</b>
Dry Human Waste	0.720	0.720	0.720	0.720	0.720
Inedible Plant Biomass	1.691	2.247	5.450	7.503	13.820
Trash	0.556	0.556	0.556	0.556	0.556
Packaging Material	7.908	4.721	2.017	1.493	0.408
Paper	1.164	1.164	1.164	1.164	1.164
Tape	0.246	0.246	0.246	0.246	0.246
Filters	0.326	0.326	0.326	0.326	0.326
Miscellaneous	0.069	0.069	0.069	0.069	0.069
<b>Waste Stream Sub Total</b>	<b>12.68</b>	<b>10.05</b>	<b>10.55</b>	<b>12.08</b>	<b>17.31</b>

Biomass can be roughly modeled as complex carbohydrates such as cellulose and associated structural proteins such as lignin [Logan 2004]. The organic content of human solid waste is roughly 50% biomass and 50% bacteria [NASA ALS studies]. We can assume that the usable organic chemicals in trash, paper, tape, and similar packaging materials is in the form of cellulose. We make the high-level assumption that the dry-mass of each waste stream is composed the following organic compounds:

- Human Solid Wastes: 50% Cellulose, 50% Dead Bacteria
- Human Liquid Wastes: 50% Urea, 50% Uric Acid
- Inedible Biomass/Roots: 75% Cellulose, 25% Biopolymers (ie structural proteins such as Lignin)
- Greenhouse Biomass: 75% Cellulose, 25% Biopolymers
- Paper, Trash, Tape, etc: 75% Cellulose, 25% Unusable Polymers

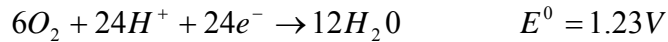
Ignoring, for the moment, the bacteria present in the solid wastes, NASA's estimates for a six-person crew on an exploration mission with some plant production and a low carbohydrate diet would produce 7.68 kg/day of complex carbohydrates such as cellulose.

Cellulose (C<sub>6</sub>H<sub>10</sub>O<sub>5</sub>)<sub>n</sub> is a polysaccharide composed of chains of glucydes. We can approximate this with Glucose: C<sub>6</sub>H<sub>10</sub>O<sub>6</sub>. The oxidation of Glucose to CO<sub>2</sub> yields 24 electrons:



<sup>1</sup> Inedible plant biomass is calculated from the BVAD diet as Inedible Biomass/Average Consumption x Mass of Grown Food and plus 10% of the Packaged Food to represent table scraps.

If the electrons are made to pass through an outer circuit, eventually combining with an electron sink (e.g. molecular oxygen) the following reaction occurs:



If we use the atomic weight of cellulose, which is slightly less than glucose, each mol of the cellulosic waste stream has a molar mass of 0.164156 kg/mol, or 6.09 mol/kg. Assuming this is fully oxidized via the glucose oxidation, every kilogram of waste would produce  $6.09 \times 24$  mol of electrons, or 146.2 mol of electrons. Using Faraday's constant (96,487 Coulomb/mole of electrons), this represents approximately  $14.1 \times 10^6$  Coulomb/kg of charge for cellulose/glucose in the waste stream. Assuming this charge is released continuously during the day, this results in 163.2 Amps of current per kilogram throughout the day.

In order to do work this charge must pass through the electric circuit at a voltage. While the idealized potential difference of the stoichiometric equation above is 1.23 V, experimental MFCs running on Glucose to date have operated at a maximum of about 900 mV [Neissen 2004]. Therefore let us assume 1 Volt potential difference. One volt is equal to one joule/coulomb, so at 1 V difference, this is  $14.1 \times 10^6$  joules per kilogram of waste or a total of  $10.7 \times 10^7$  joules/day based on the above estimate of organic waste per day. This is the equivalent of **29.7 Kilowatt-hours** of available energy a day.

We can compare this number to alternative power technologies, such as solar arrays on Mars. NASA has estimated that the surface of mars receives the approximately 3 kW-hr/m<sup>2</sup> per day of incident solar radiation [<http://powerweb.grc.nasa.gov>]. Assuming 20% efficiency of solar arrays, 29.7 kW-Hours a day is the equivalent of **49.5 m<sup>2</sup> of solar arrays**. In addition to the logistical problem associated with bringing and deploying such solar arrays, this represents about **44.6 kilograms** of extra mass on the surface of mars (Using NASA estimates of 0.9 kg/m<sup>2</sup>).

#### **7.1.4.1 Uncertainties in Estimating Power Content**

The number, **29.7 Kilowatt-hours** is, of course rather rough and must be refined using more detailed models. It is an upper bound first because the polarization of a fuel cell will cause the potential difference to drop as charge is transferred through an external circuit. Second, there are number of additional losses incurred by the operation of the cell, including energy absorbed by the organisms for growth (though this is only on the order of 5% of the total energy for many organisms [Lovely, 2006]). Finally, the total power will depend on the reaction rates, which may or may not be spread evenly across a day.

Additional uncertainties might add or remove power from the estimate. The exact amount of organic waste produced is uncertain. Also, the potential difference across the circuit might be increased if certain techniques are used. Finally, and most importantly, more detailed models of the exact molecular content of the organics is needed, as well as more specific reactions.

To take one example, the content of the Bacteria in solid waste could itself be considered fuel. Bacteria are composed of widely varying organic molecules, principally the elements Oxygen, Hydrogen, Carbon, and Nitrogen. Some empirical studies have identified the relative amount of these elements by weight, under different growing conditions for various bacteria. If we assume that the bacteria is principally *E. coli* which, under normal growing conditions with mixed culturing medium, can be modeled with the following ratios  $C_{4.16}H_8O_{1.25}N$  [Rittman2001, Ch. 2] These contents can be used as fuel as well.

### 7.1.5 Power Estimates for Mission Models

Based upon our analysis of the energy content in the human waste stream, we applied the following basic power estimates:

- A **single crewmember** produces a waste stream (including trash) that yields approximately **0.8 kg/day of complex carbohydrates** (assuming that the waste stream is completely reduced in one day), which can provide approximately **100W continuous power from a MFC**
- **One kg of algae biomass** yields approximately **150W continuous power from a MFC** (again, assuming that the biomass is completely reduced in one day). It should be noted that the production of 1.0 kg of algal biomass daily requires approximately 40 m<sup>2</sup> of sun-exposed surface area for growth (based on a growth estimate of 25 g/m<sup>2</sup>/day for high-productivity algal biomass), and 1.5 kg of CO<sub>2</sub> as an input, but yields 1.0 kg of O<sub>2</sub> as a beneficial byproduct.

Table 8 shows the key parameters associated with two mission models. The first, entitled “NASA Model”, is for a six-person crew with some biomass production, and is commonly used by NASA for exploration mission analysis. The resulting MFC system can provide approximately 1200W continuously. The second, entitled “6kW Output”, is sized for a six-person crew and the amount of biomass is adjusted to provide 6kW continuous power production. 6 kW was chosen as a representative power requirement for an advanced ECLSS system for a six-person crew.

**Table 8: MFC Power Output and Areal Size for Two Mission Concepts**

	<i>NASA Model</i>	<i>6kW Output</i>
<i>Human waste + other (kg)</i>	0.4	0.4
<i>Plant Biomass (kg)</i>	4.1	33.6
<i>Paper, etc. (kg)</i>	3.2	3.2
<b>Total Cellulose (kg)</b>	7.7	37.2
<b>Power Output - Human (W)</b>	579	579
<b>Power Output - Biomass (W)</b>	659	5421
<b>Power Output (W)</b>	1238	6000
<b>Areal Size - Solar Arrays</b>	45	370
<b>Areal Size - Algae (m<sup>2</sup>)</b>	164	1346
<b>Areal Size - Switchgrass (m<sup>2</sup>)</b>	1492	12279

If algae is used as the biomass material, then approximately 1300 m<sup>2</sup> of area is required. (This is roughly the size of two football fields.) If Switchgrass (a popular biomass material due to its relatively rapid growth rate) is used, approximately ten times the area of algae is required. In comparison, solar arrays would require approximately one quarter of the algal area to achieve the same power production levels.

### 7.1.6 Systems Analysis

When developing a system to serve a specific MFC architecture or mission application, it is essential that the complete system be modeled, including required inputs (e.g., H<sub>2</sub>O, CO<sub>2</sub>) and by-products. For example, the lunar and Mars surface exploration scenarios appear, at first blush, to be very similar. However, if biomass production is required to satisfy the energy requirements, then a source of carbon, hydrogen, and oxygen is needed to form the inputs to the biomass system. Based on these system models, surpluses and deficits of key elements may be identified.

We created a systems level model using VENSIM® modeling software. This model incorporates waste streams described above as well as the feedback loops created if certain key elements, such as CO<sub>2</sub>. It also includes the potential to create “fuel” by growing biomass in the form of algae on a planetary surface. Of course, algal growth requires a source of CO<sub>2</sub>, some nutrients, and sunlight.

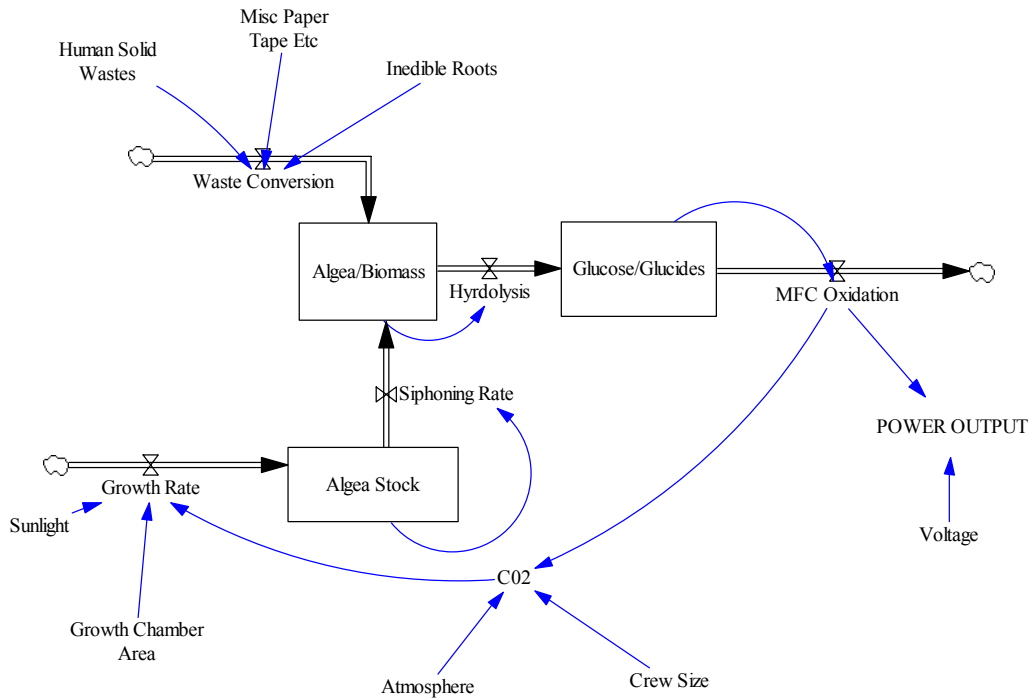


Figure 28: VENSIM systems dynamics model of MFC power production in space.

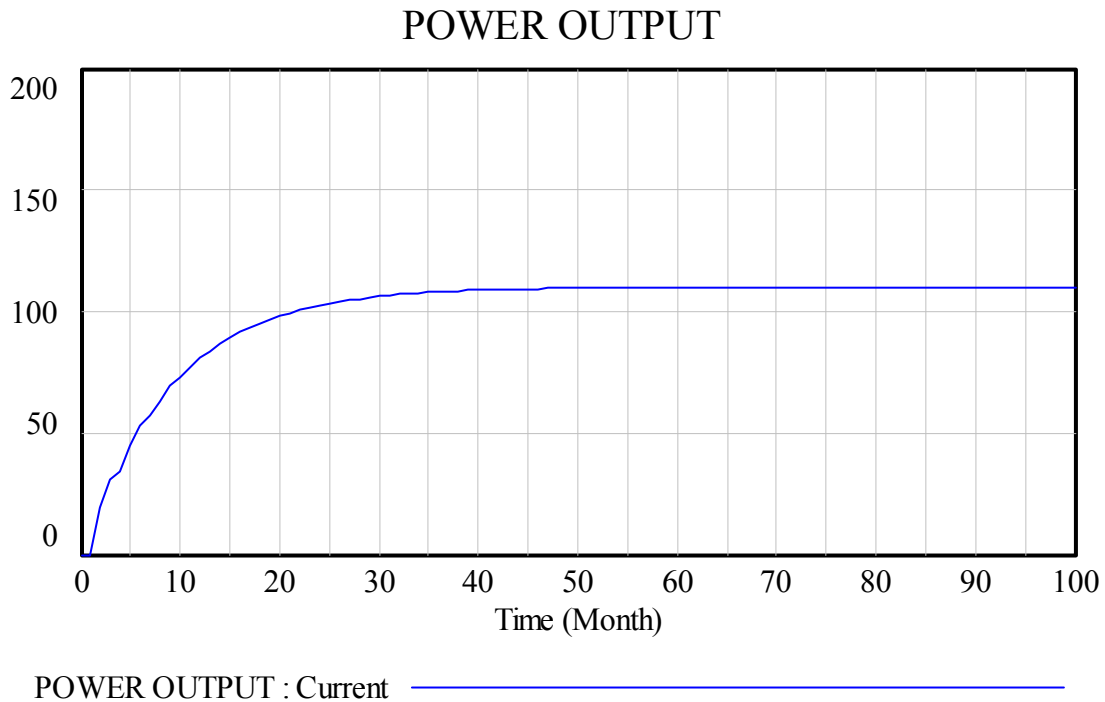


Figure 29: Power Output Estimate in KW-Hours per day, under one run of the model. This estimate assume that extra algae is grown as feedstock and fed into the fuel cell. This feedstock uses CO2 from the crew and Mars atmosphere as feedstock.

In the lunar environment, accessible carbon is almost non-existent and hydrogen and oxygen may be available in the form of water ice, but only in a few isolated locations and, furthermore, this hypothesis has not been conclusively proven. The lack of readily accessible carbon is a significant negative factor for biomass production on a lunar surface mission, and therefore any application of MFCs requiring significant biomass appears to be limited. Solar power is competitive, given the high solar insolation during the day cycle, and the 1/6g ambient gravitational load may enable a lightweight solar array approach.

In the Martian environment, however, carbon is readily accessible through atmospheric CO<sub>2</sub> – in fact, although the ambient surface pressure at Mars is but a small fraction of that on Earth, the concentration of CO<sub>2</sub> in the Martian atmosphere is such that the partial pressure of CO<sub>2</sub> (ppCO<sub>2</sub>) is approximately six times that of Earth, so a greenhouse environment consisting of Martian atmosphere (at appropriate pressure and temperature to sustain liquid water media) could be superior to that on Earth. Note that the solar insolation level on Mars (590 W/m<sup>2</sup>) is roughly 40% that on Earth (1370 W/m<sup>2</sup>), so some accommodation must be made for this factor. ***On Mars, the reduced solar insolation likely makes solar arrays less attractive in comparison to a biomass production system and associated MFC bioreactor.***

The Vensim model has been developed to iteratively test these kinds of assumptions, and can serve as a powerful analytical tool for the purpose of further design and testing of MFCs in space.

## **7.2 Detailed Design Considerations: MFCs in Advanced Life Support**

A microbial fuel cell system for space, whether on a space vehicle or a surface outpost, would carry out both waste remediation and electricity production. The development of MFCs in space must therefore integrate advances from two established fields: Advanced Life Support and Fuel Cell Systems. We have conducted a thorough review of the use of microbes in NASA advanced life support (Appendix A). This section reviews some of the more detailed design considerations that must be addressed to develop a microbial fuel cell system.

Our initial research has identified four principal, interconnected areas, which must be addressed to design a functioning MFC in space: (1) Selection and Optimization of Microbes (2) Characterization of Waste Streams (3) Bioreactor Design (4) Anode and Materials Selection. Each of these categories is inter-dependant, which means that successful design of an MFC will be an exercise in highly multidisciplinary optimization.



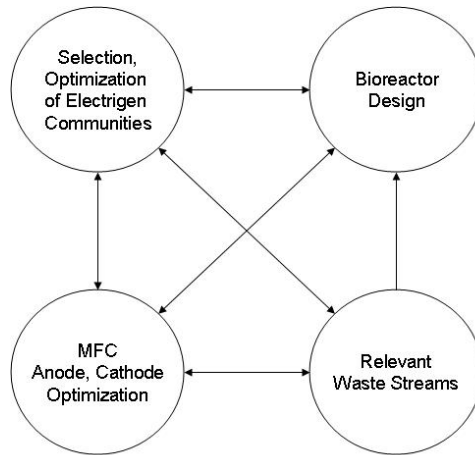


**Figure 1: Four areas that must be developed and integrated to create a dual function ALS power generation system.**

In this section, we analyze each of these four categories. We conclude with a preliminary calculation of power outputs as a function of the fuel cell geometry.

### 7.2.1 Microbe Selection

There are three main options for organism-selection: (1) single strain, (2) multi-strain microbial community already present in the waste-stream, and (3) tailored microbial community. Each of these options presents a unique set of benefits, limitations, design challenges, and optimization strategies. To our knowledge, fuel cell designs have been built to exploit either single strains or bacteria already extant in the waste stream, but there has been no attempt to create a custom microbial community. Building tailored communities may not always be possible, and would probably necessitate pre-treating and a highly-optimized fuel-cell architecture.

#### 7.2.1.1 Single Strains

Microbial Fuel Cells running on single bacteria strains have the advantage that they are easy to work with and allow for controlled experimentation and operation. Many researchers have therefore developed single-culture fuel cells using microbes from families such as *Geobacter*, *Clostridia*, *Rhodospirillum rubrum*, and *E. coli*.

While single-strain MFCs are advantageous for purposes of design and experimentation, each of these microbes can only metabolize a limited number of organic molecules and, therefore, they are not ideal for remediation complex organic wastes. As noted in the first status report, the maximum power density obtained from single-strain MFCs to date is on the order of 2.5-3.5 W/m<sup>2</sup>. Two different mechanisms that reported these power densities used the hydrogen-producing bacteria *Clostridia* to reduce starch, and the iron-fixing bacteria *Geobacter*:

- **Strain:** *Clostridia*
- **Fuel:** Complex Carbohydrates

- **Power Density:** 2.6 W/M<sup>2</sup> [Neissen, et al 2004]
- **Strain:** *Geobacter*
- **Fuel:** Acetate
- **Power Density:** 3.6 w/M<sup>2</sup> [Lovely, Phone Conversation]

### 7.2.1.2 *Multi-Strain Communities of Micro-Organisms Present in the Waste Stream*

To date, all MFCs designed to reduce waste have used microbial communities already present in the waste stream. This is partly necessary due to the high bacterial diversity in the waste itself, and has a number of obvious advantages including ease-of-use and the possibility of reducing a wider range of organic molecules through complex microbial catabolism.

Microbes in the waste stream can be cultured because the presence of an anode with a potential difference introduces an electron sink for the bacteria and causes changes in the make-up and metabolism of the microbes in the stream itself; microbes that can take advantage of the higher energy pathway made possible by the oxidation reaction available in the cathode chamber reproduce more quickly, and the community of organisms evolves towards using the anode electron sink. Generally, experiments with waste remediation slowly increase power output over time. As noted in Status Report I, the maximum density power obtained for such simulated evolution is higher than in single cell systems, at 4.3 W/m<sup>2</sup>; however, this experiment took time to create these conditions and has certain disadvantages [Rabaey et al. 2004].

For space applications, there are issues with using microbes present in the waste-stream. Most importantly, the relatively high power density obtained by Rabaey et al was the result of rather long culturing periods in a batch system which enabled evolutionary pressure to act over time. The resulting catabolic pathways relied on electron shuttles which, while efficient, would be washed away during a flow-through system [Cheng et al, 2006]

Similarly, it is difficult to predict exactly which microbes will be present at any given time and it would be difficult, though perhaps not impossible, to produce a flow-through system with a steady mix of specific microbial communities. Using microbes extant in the stream makes modeling and thus optimization very difficult because fermentation/reduction processes and pathways carried out in microbial communities is highly variable, depending on the feedback mechanisms in the environment and issues such as voltage differences at the anode and availability of various electron sinks. Many microbes have the ability to switch between aerobic and anaerobic respiration depending on environmental factors, and molecules that hinder efficient electricity generation—such as methane—may build up in the chamber.

Finally, using only bacteria extant in the stream eliminates the possibility of modifying certain microbes to increase power output.

### 7.2.1.3 Creating Highly-controlled, Tailored Communities

There are various strategies to overcome the problems associated with designing MFCs around single-strain or native-microbial communities. The first may be to use a hybrid system, in which highly-optimized single-strains are grown and fixed in a biofilm, which is exposed to the waste-stream. This strategy could make use of the architecture described in Status Report I, which used modified Membrane Biofilm Reactors. The second strategy may be to destroy the bacteria extant in a waste-stream in some way, and then flow the resulting waste and dead bacteria through highly controlled and tailored communities of organisms. These two strategies could be related, of course, in that the tailored organisms might be optimized themselves.

Creating highly-tailored microbial communities demands catabolic engineering. How would this work? To take a simple example, let us return to the highest power levels achieved by two very different organisms in a single strain MFC. These were:

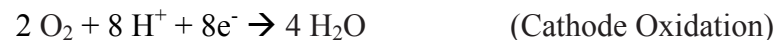
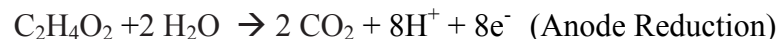
- **Strain:** *Clostridia*
- **Fuel:** Complex Carbohydrates
- **Power Density:** 2.6 W/M<sup>2</sup> [Neissen, et al 2004]
  
- **Strain:** *Geobacter*
- **Fuel:** Acetate
- **Power Density:** 3.6 w/M<sup>2</sup> [Lovely, Phone Conversation]

These organisms carried out specific, well understood reactions, in order to create electricity. *Clostridia* can create *hydrogen* from starch (or glucose) via fermentation processes that create acetate:



The hydrogen produced from this reaction is ionized by a polymer-coated platinum anode as in a standard hydrogen fuel cell.

The remaining product is Acetate. *Geobacter* can reduce acetate to carbon dioxide with the anode as an electron sink for an oxidation reaction at the cathode:



Using a cascading compartment with *Clostridia* and *Geobacter* would therefore, in theory, enable the complete oxidation and exploitation of glucose present in the waste-stream, with higher total power output than either of the single-strain systems. Further, each organism could be optimized for its reaction.

Given the sheer magnitude of microbial diversity, with many microbes able to reduce various organic molecules, it is relatively clear that full oxidation pathways can be developed. The first challenge would be to create metabolic and catabolic network models of the possible reactions and reaction rates, as a function of microbe. Once these were developed, the challenge would involve controlling the communities. This would involve eliminating or killing microbes extant in the waste, and controlling communities of single strains. The latter might be achieved through specialized sub-chambers and biofilms or through the exploitation of feedback mechanisms in microbial species. Based on our research and conversations with leading researchers in the field, we believe this represents the most critical frontier in the development of high-power and efficient microbial fuel cells for waste remediation.

#### **7.2.1.4 Cell Growth and Storage Considerations**

Using any biological source in space, especially one based on live microbial cultures, demands consideration for cell growth and storage. Practical questions include how often filters inside bioreactor must be refurbished and how to effectively control cell growth, thereby keeping a colony of microorganisms sustainable.

Cell source preparation for in-space operation of a MFC based on membrane biofilm reactors (MBfR), as opposed to on the ground, may represent an issue. On the ground, source cells can be prepared and delivered to the bioreactor, such as the MBfR, without consideration for culture space and culture environment and maintenance requirements. However, in space it would be critical that they are stored adequately. One basic question in this regard is whether to grow the microorganisms in space or simply to launch enough source cells.

The first option is to bring a small number of micro-organisms and grow them in space, which raises the question of where and how they shall be grown: in liquid or dry format, with/without temperature control, etc. Currently, for experimental purposes, microbial cells are launched in dry format without stringent thermal control requirement before they are used.

A related, but critical consideration associated with the practical development of an MFC system involves controlling microbial source cell growth. One promising solution to this problem may be to capture source microbial cells at the *self assemble* but not *self replicate* stage. This can be accomplished using an optical density meter which can monitor cell growth and therefore hopefully determine when to stop source cell growth.

#### **7.2.2 Detailed Waste Stream Models**

We have begun to collect more detailed data on the waste streams expected in a NASA missions. These included organic contents of soluble components from crop residues, inedible biomass, paper waste, trash, food remains, and human solid wastes (feces, urine

solids, shower/hand wash solids, and sweat). Soluble organics can be taken as primarily carbohydrates for bacteria. The NASA model presented above presents the following estimates:

**Table 9: Human Component (Dry Weight)**

	Kg/(person•day)	lb <sub>m</sub> /(person•day)
Feces	0.03	0.07
Urine	0.06	0.13
Shower/Hand Wash	0.01	0.02
Sweat	0.02	0.04
<i>Total</i>	<i>0.12</i>	<i>0.26</i>

**Table 10: Inedible Plant Biomass (Dry Weight)**

	Kg/(person•day)	lb <sub>m</sub> /(person•day)
Protein	0.25	0.56
Carbohydrate	0.29	0.64
Lipids	0.07	0.16
Fiber	1.09	2.41
Lignin	0.11	0.24
<i>Total</i> <sup>2,3</sup>	<i>1.82</i>	<i>4.01</i>

**Table 11: Trash**

	Kg/(person•day)	lb <sub>m</sub> /(person•day)
Clothes/Towels	0.0007	0.0015
Toilet Paper <sup>4</sup>	0.0230	0.0507
Pads/Tampons <sup>4</sup>	0.0035	0.0077
Menstrual Solids <sup>4</sup>	0.0004	0.0009
Paper <sup>4</sup>	0.0650	0.1433
<i>Total</i>	<i>0.0926</i>	<i>0.2041</i>

**Table 12: Packaging Material Trash<sup>5,6</sup>**

	Kg/(person•day)	lb <sub>m</sub> /(person•day)
Snack Packaging	0.060	0.132
Food Containers <sup>7</sup>	0.470	1.036
Plastic Bags <sup>7</sup>	0.060	0.132
Food Remains <sup>8</sup>	0.100	0.220
Frozen	0.050	0.110
Refrigerated	0.020	0.044

<sup>2</sup>Hanford, A. J. (1999) "Baseline Values and Assumptions Document."

<sup>3</sup>The inedible plant biomass values here are upper limits. In other words, these values reflect a life support system architecture in which all food is supplied from crops grown on site.

<sup>4</sup>Cellulosic

<sup>5</sup>Grounds, P. (1991) "STS-35 Trash Evaluation Report," NASA TM SP4-91-041, 12 March 1991.

<sup>6</sup>The packaging material values here are upper limits. In other words, these values reflect a life support system architecture in which all food is prepared before launch and supplied in individual serving packages.

<sup>7</sup>Polyethylene

<sup>8</sup>The composition is 25% protein, 51% carbohydrate, 8% lipid, and 16% fiber.

Ambient	0.410	0.904
Beverage <sup>9</sup>	0.128	0.282
Straws	0.020	0.044
<i>Total</i>	<u>1.318</u>	<u>2.906</u>

**Table 13: Paper Trash**

	Kg/(person•day)	lb <sub>m</sub> /(person•day)
Wipes	0.14	0.309
Tissues	0.02	0.044
Facial Tissues	0.03	0.066
Waste	0.004	0.009
<i>Total</i>	<u>0.194</u>	<u>0.428</u>

**Table 14: Tape**

	Kg/(person•day)	lb <sub>m</sub> /(person•day)
Masking	0.002	0.004
Conduit	0.004	0.009
Duct	0.035	0.077
<i>Total</i>	<u>0.041</u>	<u>0.090</u>

**Table 15: Filters**

	Kg/(person•day)	lb <sub>m</sub> /(person•day)
Air <sup>10</sup>	0.0244	0.054
Prefilters	0.03	0.066
<i>Total</i>	<u>0.0544</u>	<u>0.120</u>

**Table 16: Miscellaneous**

	Kg/(person•day)	lb <sub>m</sub> /(person•day)
Teflon	0.011	0.024
PVC	0.0005	0.001
<i>Total</i>	<u>0.0115</u>	<u>0.025</u>

### 7.2.2.1 Feces

Of the dried feces, 1/3 (or about 1/12 of the whole) is dead bacteria. Another 1/3 of the remaining quarter is indigestible food, such as cellulose (C<sub>6</sub>H<sub>10</sub>O<sub>5</sub>)<sub>n</sub>. Some acetic acid bacteria are known to synthesize cellulose.

### 7.2.2.2 Urine

The main constituents of urine are water, salts and urea (CON<sub>2</sub>H<sub>4</sub> or (NH<sub>2</sub>)<sub>2</sub>CO). Urea is one of the three nitrogenous waste products. The other two are creatinine and uric acid. Urea is an organic compound of carbon, nitrogen, oxygen and hydrogen, with the above chemical formula. Creatinine is a breakdown product of creatine phosphate in muscle,

<sup>9</sup>Grounds, P. (1991) "Beverage Pouches," NASA TM SP4-91-081, 4 June 1991.

<sup>10</sup>ECLSS Architecture Description Document, Volume 2, Book 2, Revision A, ISS air filters (2.15 kg each, 29 total)

and is usually produced at a fairly constant rate by the body (depending on muscle mass). Uric acid (or urate) is an organic compound of carbon, nitrogen, oxygen and hydrogen with the formula  $C_5H_4N_4O_3$ .

- Urea:  $CON_2H_4$  or  $(NH_2)_2CO$
- Uric acid (or urate):  $C_5H_4N_4O_3$

### 7.2.3 Bioreactor Selection and Design

Microbial Fuel Cells employ bio-reactors which enable microbes to grow and reduce wastes. Various reactors exist, such as continuous stirred tank, fixed-film bioreactors, and the more recent membrane biofilm reactors (MBfR), but our research has indicated that significant work has not yet gone into optimizing such reactors for use in an MFC.

One classical reactor is the stirred tank bioreactor (STBR). These have the advantage of ease of automation, and a uniform and controllable cell culture environment. However STBRs rely on a clear liquid and gas phase separation. Under microgravity, it will be difficult to achieve the clear phase separation. Without external force, liquid and gas phase under microgravity tends to form a group of small liquid/gas mixtures. This mixture is generally detrimental to cells themselves. In addition, this will not satisfy the MFC requirement for phase separation.

Traditional perfusion-based cultures such as hollow fiber bioreactors provide wide operational flexibility. Specifically, they provide a clear phase separation, and this phase separation is gravity independent. We have therefore estimated that a MBfR, with proper membrane selection, might suit space applications well.

The MBfR is comprised of a membrane of porous fibers in a cylinder through which gas can be funneled and filtered. As the gas diffuses through the membranes, it serves as an electron donor for growth of a naturally occurring biofilm on the outside of the hollow fibers, which in turn reduces or destroys oxidized contaminants in the water. The membrane fibers have microporous inner and outer layers and a nonporous layer sandwiched between the inner and outer layers. Hydrogen is introduced inside the fibers, which are sealed on one end to prevent direct escape of the hydrogen gas. When hydrogen gas is fed through the fibers, a biofilm grows at the intersection of the fibers and the water. As waste-water flows past the biofilm, it is cleaned or treated by the microbes.



Figure 30: *Natriegens* biofilm growing on a silicone membrane in a MBfR (source: [www.ucd.ie](http://www.ucd.ie))

MBfR use autotrophic biological reduction processes to reduce oxidized contaminants, such as nitrate, perchlorate, chlorinated solvents, organics, or other contaminants

depending on the micro-organisms used. MBfR have the advantage that they are flexible, relatively simple to construct, and gravity independent. Creating a microbial fuel cell using the architecture of a membrane biofilm reactor may enable new uses for microbial fuel cells and potentially increase total power output substantially.

#### **7.2.4 Materials Selection and Anode Design**

Anode-microbe interaction plays a critical role in the efficiency with which electrigen microbes reduce organic compounds. Common anode materials include graphite and iron. One area of active investigation involves the interaction of the microbes with the anodes themselves. A critical determinant of fuel cell efficiency is the total surface area of the anode. One promising method to optimize an anode that we have identified involves using surfaces created by nano-particles with fractal geometric structures. A fractal surface would greatly increase total surface area per unit volume, and may facilitate the creation of a biofilm. *Experimentation with fractal anode structures constitutes a potential direction for future research.*

Fabrication of the anodes based on carbon nano-tubes, gold nano-particles, or similar materials with fractal properties will depend slightly on the specific instantiations—for example, whether in a microbial fuel cell based on membrane biofilm reactor architecture or a more traditional microbial fuel cell. It will also depend on the specific application—for example, whether in a space system, in an industrial setting, or for use in off-grid electricity production in a developing country. Generally, however, these materials can be introduced into a traditional fuel cell or a fuel cell based on membrane biofilm reactors using standard techniques in nano-fabrications.

Anodes with fractal surface area might be created from Gold nano-particles, Carbon nanotubes, or similar materials. Gold nano-particles are easily created and harvested using commercial techniques. Carbon nano-tubes can be created in any number of methods and applied to an anode surface. This includes procedures such as the precipitation of nanoparticles onto polymeric and inorganic particles dispersed in aqueous solutions, either directly onto the cores or by direct surface reactions utilizing specific functional groups on the cores that induce the coatings. Another method involves controlled assembly of a nano-composite layer on a surface using the LbL method based on colloidal templates. Such methods have been used to create particles with shells but can also be used to coat a larger surface. Further, it may be possible to integrate the surface materials directly with bio macromolecules by employing gold colloids which bind to proteins, and placing this protein-colloid layer between microorganisms and the anode surface. In general, latest advances in nano-surface engineering can be employed to create a surface with fractal geometric structure and thus high surface area in a given space.

While increasing surface area is an obvious way to increase power-output, this alone may not be the most important factor. Some microbes, such as those in the Geobacter family, may be capable of creating extended pili, which function as electrical conductors that can transfer electrons at a distance. In this case, a thicker biofilm on the anode may do as



much to increase power output as a large total surface area. These kind of trade-offs must be carried out experimentally.

### 7.3 Fuel Cell Geometry: A Sizing Model

In order to estimate rough power levels, we conducted a preliminary analysis of the power output of microbial fuel cell architectures, using representative fuel cell geometries. In addition to estimating power levels, the Matlab models presented below will serve as the basis for more detailed modeling and optimization during conceptual design.

#### 7.3.1 Architecture 1: Tubular Microbial Fuel Cells

Our first architecture assumes a microbial fuel cell comprised of a series of tubes within a square frame, through which organic waste can flow. This is modeled after standard with Solid Oxide Fuel Cells, which have cathode on the inside, anodes on the outside and an electrolyte separating the two (Figure 31). In a Tubular Solid Oxide Fuel Cells oxygen flows through the tubes serving as an electron receptor, and oxidized chemicals are in contact with the outside of the tube.

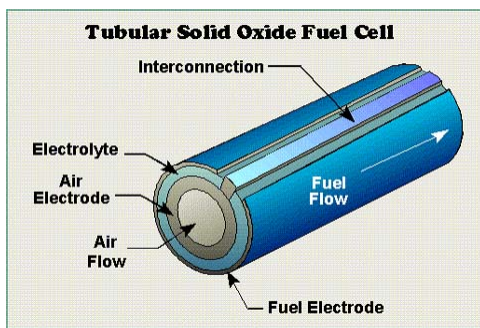
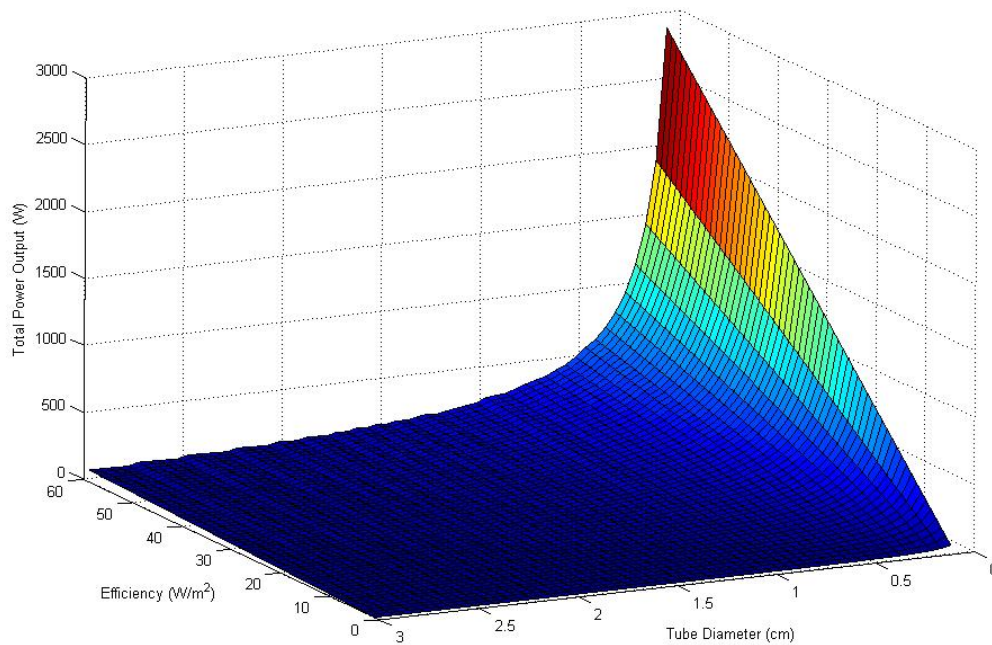


Figure 31: Solid Oxide Fuel Cell (courtesy: <http://americanhistory.si>)

For our preliminary design we assumed multiple tubular fuel cells placed in a square container through which organic matter flows. Using this geometry we can estimate total power output as a function of the tube size and the efficiency (watts/m<sup>2</sup>) of a MFC, in a fixed volume. For the initial calculations we conservatively assume that the total volume is 25 cm cubed (or about 1 foot cubed).

We can estimate total power output using a range of densities from 0 to 60 w/M<sup>2</sup>. As noted, ranges of power outputs in the literature are about 3-4 W/m<sup>2</sup>, however, bio-engineering strategies might be employed to raise this level. Another unknown given this design is how small the tubes can be made. We therefore varied the tube diameter from 1mm to 3cm.



**Figure 32: Total power output of a 25 cubic centimeter MFC. We vary tube diameter and MFC efficiency.**

Our first results demonstrate a theoretical maximum power output of roughly 2.9KW assuming  $60 \text{ W/m}^2$  efficiency and a tube size of 1 millimeter. Of course, this makes the assumptions that each tube can be as small as 1 millimeter, and that these tubes are packed at maximum density, without hindering the flow of matter, oxygen flow or electron depletion rates. However, the results are encouraging in that they demonstrate that it may be possible to convert nearly the maximum amount of electro-chemical energy in the fuel itself into electricity if the tubes can be made small enough. Further, the relevant scale sizes, given potential efficiencies, is well above nano or micro-meter scales, which increases the possibility of constructing tubes of this size.

Figure 33 presents a snapshot of Figure 32, focused on the ranges that would likely be used, at least in the next few years—tube diameter range of 1mm to 1cm and efficiencies of 1 to  $10 \text{ W/m}^2$ .

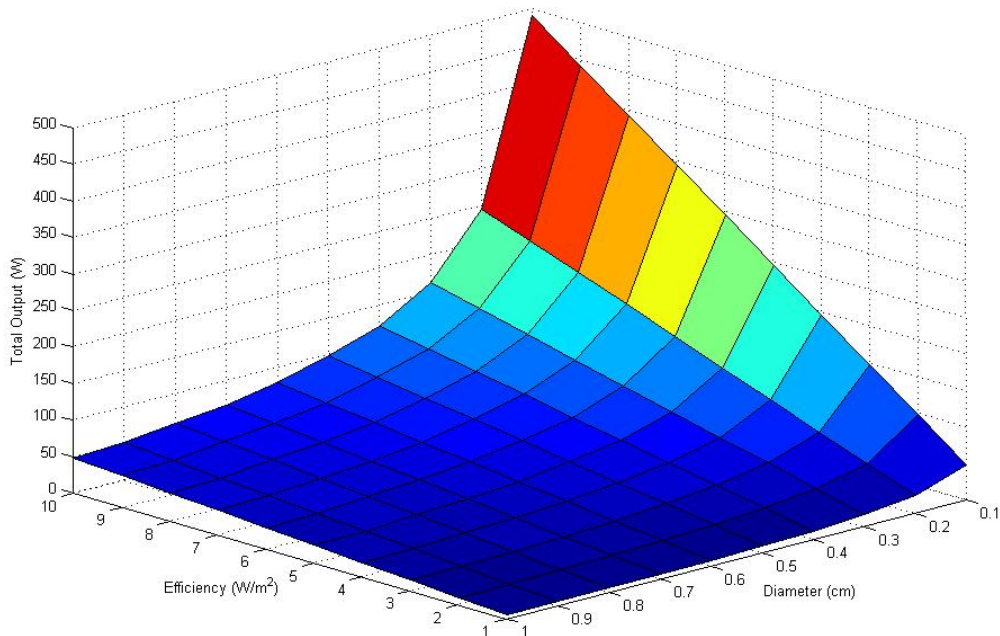


**Figure 33: Total Power Output of an MFC at a smaller range of tube diameters and efficiencies.**

These calculations illustrate that the maximum power output, based on 1mm tube diameter and efficiency of 10 W/M<sup>2</sup>, is 490.8 Watts. This drops significantly as the tube size is increased, falling dramatically to 162.3 Watts at 3mm diameter. These variations are, of course, purely due to the number of tubes that can be packed into the given space, but they illustrate well that making the fuel cells small enough can have dramatic impact on total power output. It should also be noted that, as would be expected, total power varies linearly as the efficiency increased. Given a 1mm diameter tube, the power output varies linearly from 49.1 Watts to the maximum 490.8 Watts, as the efficiency rises from 1 W/m<sup>2</sup> to 10 W/m<sup>2</sup>.

### 7.3.2 Architecture 2: Reverse Tubular Fuel Cell (gravity compensation)

We have assumed in these calculations a fuel cell in which air/oxygen is pumped through tubes, and organic materials and wastes flow around the tubes. This configuration may not be acceptable or practical in a zero-gravity environment, due to well-known flow and surface tension problems. One simple alteration may be to reverse the anode and cathode—that is, flow organic material through the inside of the tubes and flow air around the outside.

Figure 34 presents the results of this reverse tube-cell architecture. We conservatively assume for this model that tubes themselves have a thickness of 0.5 cm, so even in the theoretical extreme of given a tube with zero inner diameter, the tubes will still have a total diameter of 0.5 cm— this means that the total surface area of the anode is smaller and the number of tube is fewer.

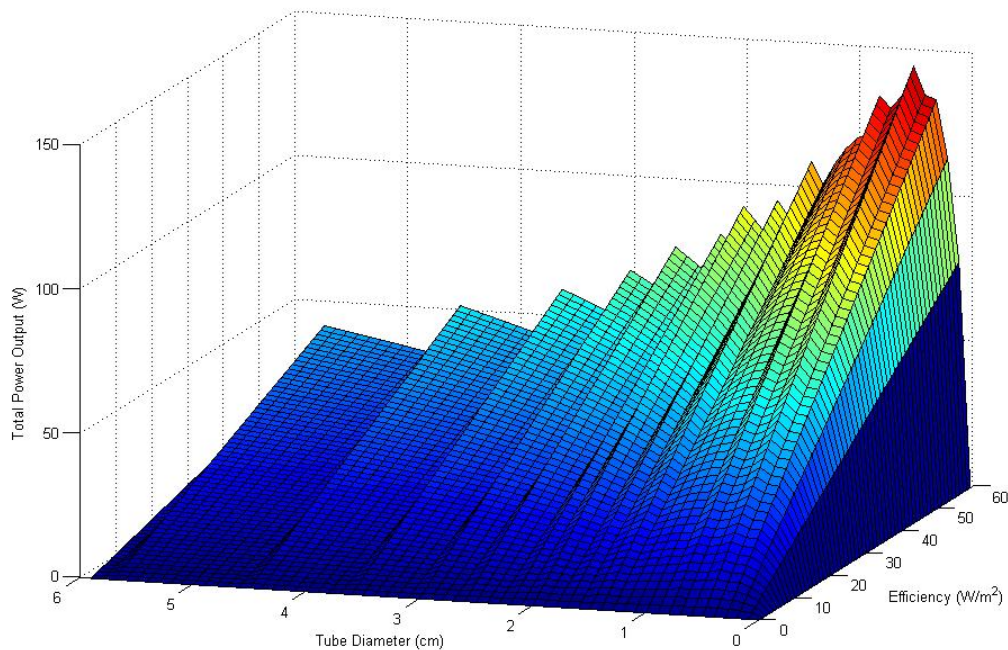


**Figure 34: Total Power Output as a function of tube *inner diameter* (cm) and MFC efficiency (W/m<sup>2</sup>). This assumes an MFC composed of several tubes within a square box 25cm cubed (roughly 1 foot cubed). The tubes themselves are assumed to have a thickness of 0.5 cm.**

The maximum power created is here is 144.8 watts assuming a very optimistic 60 W/m<sup>2</sup> of power density. Result in Figure 34 follows a jagged contour because the number of tubes allowed in the box is rounded down, and thus while the total power output rises as the diameter rises, it drops dramatically whenever a tube is removed from the box. Given our geometric assumptions, this same phenomenon actually affects the other results above. It is less pronounced because total power output is higher and total free surface area is less dependant on the number of tubes (since each tube accounts for a larger fraction of anode surface area).

This is one potential change in fuel cell design that must be contemplated in order for the MFC to operate in zero or reduced gravity. However, other geometries are possible. This is discussed below.

### 7.3.3 Fuel Cell Geometry Analysis Conclusions

This analysis demonstrates the critical importance that geometry of the fuel cell will have on total power input and provides rough estimates for maximum and minimum power levels in a roughly cubic-foot area. A first lesson is that if the tubes can be made sufficiently small, we may be able to achieve something close to extracting the maximum energy from the organic chemicals. This raises the question of how to create a fuel cell of

this size and indicates an important potential direction for the preliminary design of the fuel cells.

We should note that, in some ways, these estimates are optimistic. For example, we assume that the tubes are packed closely together. Practically, this may not be achievable. A lower packing density will decrease total surface area and thus reduce maximum power output. On the other hand, we have assumed that our anodes are completely smooth. As discussed above, it may be possible to increase the surface of the anode without geometrical changes, or to roughen the surface in some other way, to increase surface area per volume. Also, it is not clear yet that efficiencies on the order of 60 W/m<sup>2</sup> can be achieved, and this will depend on advances in bioengineering. However, even at power outputs seen today (3 W/m<sup>2</sup>, according to Dr. Lovely) a one foot square fuel cell with 1mm tubes could generate up to 147.2 Watts.

These models have also raised specific questions for further research:

1. Do we need air to flow through the middle of the tubular fuel cell, or can each rod function as an anode, all attached to an exterior cathode? This depends on the depletion rate of molecular oxygen at the cathode, and is an open empirical question. Would this be different if we use a MBfR instead of a tube?
2. Can we use carbon nano-tube fibers to create a mesh of microtubules, either across the fuel cell compartment, or on a fixed anode surface?
3. Biofilm growth: How does a biofilm grow on the tubes, as a function of surface roughness?
4. Geometric Optimization: What are some other methods for geometric optimization? This demands further simulation.

While some of these questions have been addressed in the literature, others demand empirical observations and further simulation.

## 7.4 Experiments

We have conducted two experiments to begin laying the groundwork for the use of MFCs in space. Researchers have recently investigated the electrical properties of *Geobacter sulfurreducens* (In particular Derek Lovley, UMass Amherst) and some have focused on increasing power output through mixed cultures (for example, Bruce Logan at Penn State University). Relevant experiments are summarized in the Appendix. However, no significant work has been done to optimize fuel cell chambers for space exploration or to genetically alter bacteria for the purpose of developing a space-power paradigm. Further, *Geobacter* is considered a more efficient electrogenic species because it forms a “nano power grid” of conductive pili (Reguera et al. 2004) to the anode, eliminating the need for electron shuttles, which increase internal resistance. As stressed throughout this report, the application of MFCs to space power in the context of a broader space power paradigm has revolutionary implications. We therefore conducted experiments focused

on (1) optimizing chambers and (2) genetic engineering of *Geobacter sulfurreducens* as a step towards creating such systems for space applications.

## **7.4.1 Microbial Fuel Cell Test Chamber**

### ***7.4.1.1 Experimental Goals***

In our first experiment we built single-chamber batch mode fuel cells in order to accomplish three major goals:

First, we sought to validate the power output numbers achieved for *Geobacter sulf.* using state-of-the-art MFCs. Second, we wanted to quantify the power output fluctuations as a function of novel anodes. Chaudhuri and Lovley (2003) achieved power variation through alterations in the anode surface area between graphite rods, graphite felt, and graphite foam. Our design investigates the effects of different anode material, where power output is compared between gold plated anodes and the control graphite anodes, where gold is almost three orders of magnitude more conductive than graphite. Third, we used the chambers to test the effect of our genetic experiment (see below). This involved measuring electricity production of the standard DL1 strain of *G. sulfurreducens* against a strain we mutated by expressing the photo-electric bacteriorhodopsin protein from the species *Halorubrum*.

### ***7.4.1.2 Chamber Design***

The fuel cells were single-chamber, batch-mode systems derived from those of Liu *et al.* (2004). The chambers themselves were made of 1/8" thick polycarbonate tubing, with electrodes clamped on either end between a 5/8" thick polycarbonate sheet and a 1/8" thick polycarbonate cover. Connection points were sealed with O-rings and reinforced with RTV118 silicon sealant. The dimensions of the chamber were 1 1/4" diameter and 1 1/2" length, holding a volume of approximately 30mL. Copper foil was used at either end to create an electrical connection to the graphite that would extend outside the cell for measurement purposes. Two sampling ports were added through which fluid could be added and the chamber could be purged of oxygen. A photograph and diagram of the chambers can be found in Figure 35.

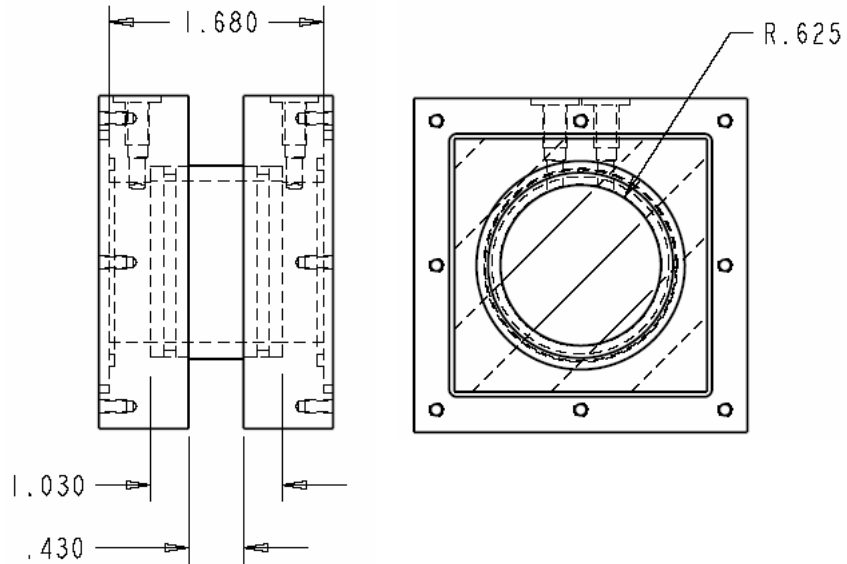


Figure 35: Fuel Cells Schematic Diagram. © IntAct Labs

## Cathodes

The cathodes were designed to be air-breathing, such that the oxygen used to close the electron loop came directly from the air, and were made from Nafion 117 proton exchange membrane (PEM) hot pressed onto carbon cloth. The PEM was designed to allow only the exchange of protons between the inside and outside environments, allowing the inside of the chamber to remain oxygen free, while the electrons combine protons and molecular oxygen outside to form water. The conducting carbon cloth was a high temperature E-TEK ELAT GDE microporous layer with  $5\text{g/m}^2$  Pt catalyst coating for extra reactivity (fuelcellstore.com)

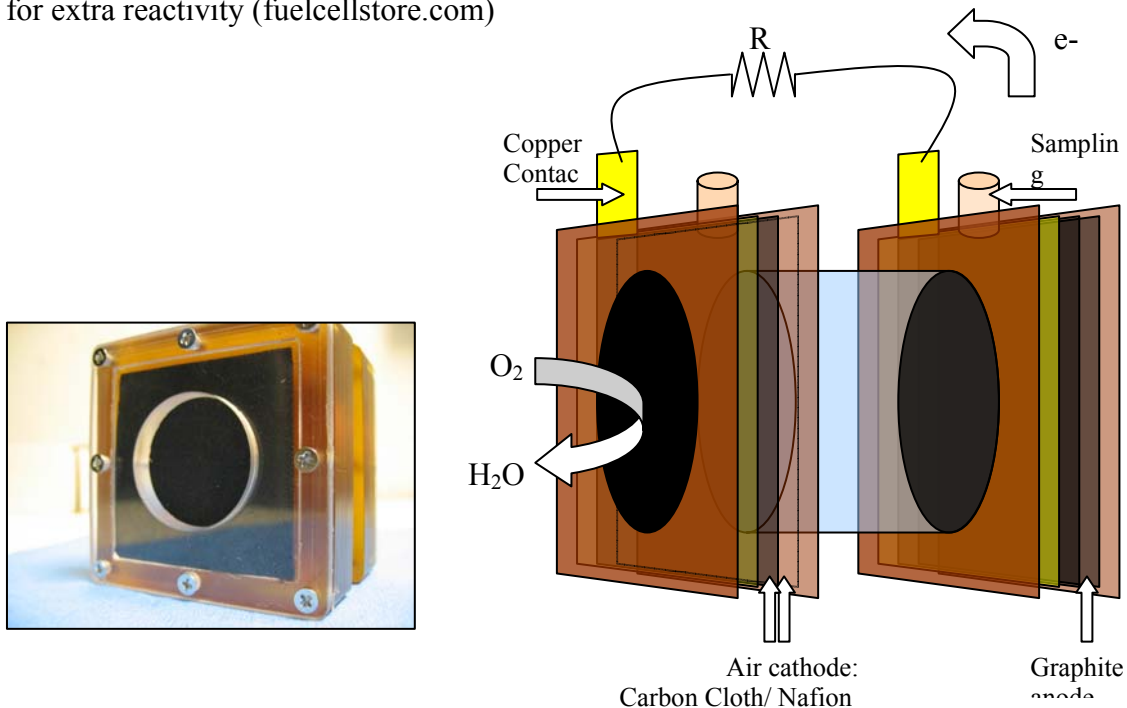


Figure 36: Photograph and diagram of the microbial fuel cell built at IntAct Labs with a graphite anode.

The PEM was treated first by boiling for 1 hour each at 80°C in distilled water, 3% H<sub>2</sub>O<sub>2</sub> solution, 0.5M H<sub>2</sub>SO<sub>4</sub>, and distilled water in order to remove organic and metal ion contaminants and to hydrate the membrane. Then the PEM was placed on the catalyst-coated side of the carbon cloth, heated to 130°C in the hot press, and pressed together under 2.16MPa (58kgF) for 2 minutes. Kapton film was used to sandwich the cathode and prevent sticking to the plates of the hot press.

#### **7.4.1.3 Anodes**

The graphite anodes were graphite slabs (fuelcellstore.com), cut to size 3cm×3cm. The gold anodes were produced from a 2.05”×2.05” slab of polished glass (RMS roughness < 1nm), cut to size 3cm×3cm. The glass was placed in a gold evaporator, which was pumped down for over half an hour to < 10<sup>-6</sup> torr. The gold was evaporated by supplying between 120-140 A to a tungsten boat containing a 0.5cm shot of Au, while the substrate was attached to a stage about 20” above the boat and rotated. The rate of evaporation was determined by a crystal plate thickness monitor to be approximately 2Å/s for a fairly smooth (RMS roughness ~10nm) surface of 100nm thickness.

#### **7.4.1.4 Bacteria Culture**

The bacteria species *Geobacter sulfurreducens* was cultured under conditions described in Coppi *et al.* (2001), inoculating 2% culture anew every 5 days in anaerobic tubes of 10mL NBAF culture medium reduced with 100µL of the oxygen scavenger L-cysteine and growing in a 30°C incubator.

#### **7.4.1.5 Testing**

Chamber parts were autoclaved at 121°C for 30 min, with the exception of the cathode, which was sterilized with ethanol on the PEM side (the side facing the inside of the chamber), and the copper, which was not sterilized but does not touch the inside of the chamber. Parts were assembled under sterile conditions.

The medium used in the chambers was similar to the growth medium described in Bond and Lovley (2003), with the addition of acetate electron donors and the absence of fumarate electron acceptors, such that any electrons produced would be directly transferred to the anodes. 25mL of medium was injected into the sampling ports using syringes, leaving approximately 5mL air space for the degassing process.

Degassing was performed for 30min in each chamber, injecting a gas mixture of 80% N<sub>2</sub> and 20% CO<sub>2</sub> into one port while a plastic cannula in the second port maintained a flow of O<sub>2</sub> out and prevented the buildup of gas pressure inside the chamber. The remaining dissolved oxygen in the anode was decreased by the addition of 100µL of the oxygen



scavenger L-cysteine per 10mL medium, which increases Coulombic efficiency in the oxygen sensitive bacteria (Min *et al.* 2004), and the presence of oxygen was monitored by the addition of 0.5mL 0.1% resazurin per 1L medium, an oxygen indicator that changes color from blue to pink to clear when reduced.

5% of the most recent *G. sulfurreducens* culture was inoculated into each chamber. The chambers were sealed with RTV118 and the ports were closed with Parafilm, and the bacteria were left to grow at 30°C. A copper wire was used to close the circuit between anode and cathode, such that electrons produced in the chamber would not poison the organisms and could be siphoned out for recombination with protons and molecular oxygen.

#### **7.4.1.6 Current Status**

We have found that the chambers do not yet sustain continued growth over the growth cycle of *Geobacter*, preventing the bacteria from reaching a constant current steady state dependent only on continued replacement of depleted acetate electron donor. The reason for this is that the chambers are susceptible to evaporation of the liquid within the chamber, decreasing the amount of medium by about 4x within the 5-day growth period.

The major driving force for using an air-breathing cathode was to eliminate the need for constant aeration of the cathode solution in a two-chamber system, which requires extra equipment and energy. However, while largely selective to protons over electrons and gases like oxygen, Nafion is permeable to water molecules, and the carbon cloth does not prevent exchange of gases over time. A closer examination recognizes that, while this was not so much a problem in the experiments of Liu *et al.* (2004), where bacteria were grown under normal environmental conditions, the requirements of *Geobacter* to grow at the elevated temperature of 30°C proved problematic, in that it increased the rate of water evaporation within the chamber and drove the release of vapor molecules through the air-breathing cathode. The issues created by the more specific growing requirements of *Geobacter* over mixed bacterial cultures present small incompatibilities to the system employed by Liu *et al.* The evaporation issue may be mitigated through increased humidity settings within the incubator or growing *Geobacter* at sub-optimal room temperature conditions, but full containment within the chamber may require the addition of a second barrier to water loss.

### **7.4.2 Coupling Geobacter and Rhodopsin**

#### **7.4.2.1 Experiment Summary and Goal**

We performed a heterologous protein expression study of bacterial rhodopsin (bR) in *Geobacter sulfurreducens*, a bacterial species that uses metal ions in anaerobic sediments as the terminal electron acceptor in its metabolic processes; this species has been shown to generate current by transferring these electrons instead to an electrode within a microbial fuel cell (Reguera *et al.* 2005; Bond and Lovley, 2003). *G. sulfurreducens* is a fairly newly discovered species and to our knowledge, no group has attempted to alter its

electrical properties within a fuel cell by expressing proteins from other species. The coupling of br with *Geobacter sulfurreducens* constitutes an important first step in proving the viability of developing a space-power system based on a *limited set* of underlying biological parts.

Bacterial rhodopsins from archaea in the genus *Halorubrum* were chosen for expression for several reasons. They are simple photoactive membrane proteins that have been functionally expressed in other species, notably *Escherichia coli* and the eukaryotic yeast *Saccharomyces pombe* (Feng *et al.*, 2006; Hoffmann *et al.*, 1994) Interestingly, the expression of bR in the yeast mitochondrial membrane was able to decrease the need for energy by allowing the yeast to obtain some of its nourishment from light.

Cloning of the bR genes and functional expression in *Geobacter* should effect a measurable change in the electron transfer from *Geobacter* to electrodes while growing in a fuel cell, and might allow creation of semi-photosynthetic bacteria that derive energy both from chemical fuel and from light. Regardless of the magnitude of the change observed, this experiment represents a significant step in the engineering of this species towards an optimized bacterium for use in fuel cells.

#### **7.4.2.2 Materials and Methods**

##### **Obtaining bR genes**

Cultures of *Halorubrum xinjiangense* and *H. sodomense* were obtained from the Japan Collection of Microorganisms (JCM) and grown in JCM medium 168, made according to the instructions from JCM. Well-grown cultures were used to extract total DNA using the MasterPure Complete DNA purification kit (Epicentre Biotech, Madison, WI). Total DNA was used as the template in PCR reactions using primers specific for the bR genes. Primers for *H. xinjiangense* were those used by Feng, et al. (2004), while those for *H. sodomense* were designed by us. PCR was run using high-fidelity Vent DNA polymerase (New England Biolabs, Ipswich, MA) to avoid mutations in the gene sequences, and the resulting DNA products were run on an agarose gel to verify their size.

##### **Cloning of bR genes**

PCR products were cloned using the pCR-Blunt-II TOPO cloning kit (Invitrogen, Carlsbad, CA) according to the manufacturer's protocol. *E. coli* were transformed using the pCR-Blunt-II TOPO::bR plasmids and grown on selective plates. Single colonies from these plates were used to inoculate liquid cultures, and plasmids were isolated from the cells using the Plasmid Miniprep kit (Qiagen, Valencia, CA). Purified plasmids were digested using the EcoRI restriction enzyme (New England Biolabs) and analyzed on an agarose gel to verify the correct gene insertion. pCR-Blunt-II TOPO vectors have annealing sites for primers that allow sequencing of DNA products inserted into the vectors and sequencing is important to make sure the proteins, once expressed, will be functional.

##### **bR gene expression**

Two expression vectors, pRG5 and pRG6, were obtained (Kim, et al. 2005). These vectors grow in both *E. coli* and *Geobacter*, and will be used to express the bR genes in *Geobacter*. There are EcoRI recognition sites on both vectors, so genes excised from the pCR-Blunt-II TOPO::bR plasmids using these enzymes can be ligated into the expression vectors at these sites using T4 DNA ligase (New England Biolabs). Once pRG5::bR and pRG6::bR plasmids are obtained, they will be introduced to *G. sulfurreducens* using the electro-transformation protocols given by Coppi, et al. (2001). Cells will be grown in medium supplemented with all-*trans*-retinal (Sigma-Aldrich, St. Louis, MO) to induce chromophore formation and protein functionality.

### **Testing of protein expression**

Once the expression vectors have been introduced to *G. sulfurreducens* cells, expression of functional bR proteins will be tested in several ways. Cells expressing the proteins take on a bright red to orange color due to the absorbance properties of the proteins. This change can be detected visually and also by use of a spectrophotometer to compare the absorbance properties of cells expressing bR to wild type *G. sulfurreducens*.

Testing for changes in electrical properties of *Geobacter* will be carried out in fuel cells created for one of our other experiments. The current generated by *G. sulfurreducens* growing in these fuel cells will be recorded by use of an oscilloscope, and data from fuel cells growing wild type *G. sulfurreducens* will be compared to that from cells growing the bacteria expressing bR proteins.

#### **7.4.2.3 Results and progress**

*Halorubrum xinjiangense* and *H. sodomense* strains were obtained and successfully grown. Their DNA was extracted and used as the template in PCR reactions to amplify the bR genes. Using gel electrophoresis, the correct gene sizes of 780 bp for *H. xinjiangense* and 900 bp for *H. sodomense* were verified. These genes were ligated into pCR-Blunt-II TOPO vectors, yielding pCR-Blunt-II TOPO::bR insertion plasmids. These plasmids were used to transform *E. coli* cells for verification of the correct inserts by restriction digest analysis and sequencing.

We obtained the expression vectors pRG5 and pRG6 and have amplified these in preparation for insertion of the bR genes to create the final pRG5::bR and pRG6::bR expression plasmids. Due to time constraints and several setbacks in culturing *Geobacter* and obtaining supplies, the project has not yet progressed beyond this point. We are confident that with continued efforts we will be able to complete this expression project and begin to learn about the engineering of the electrical properties in *Geobacter*-fuel cell interactions.

#### **7.4.2.4 Discussion**

Bacterial rhodopsin (bR) proteins are just one of the many photoactive proteins, ranging from other simple ion transporters to the complex photosystem protein complexes used in photosynthesis by cyanobacteria and plants. bR proteins are a good initial choice because

they require no interaction with other proteins to function and have been shown to alter metabolic properties of other species when heterologously expressed. It is not entirely clear what affect the expression of the bR proton pumps will have on *Geobacter*. It is very likely that they will be functional, because the membrane properties of *Geobacter* are similar to the *Halorubrum* source strains and *E. coli*, in which they have already been functionally expressed.

bR allows bacteria to gain energy from sunlight because it uses the energy in photons to build up an electrochemical gradient of protons across the inner cell membrane. This gradient is then utilized by the enzyme ATP synthase in the membrane to store this energy in the high energy bonds of ATP, which the cell can use for metabolic processes. The cells also use the energy obtained from oxidizing reduced compounds to store energy in ATP, and in *Geobacter* the electrons released by these oxidative processes are what must be shuttled out of the cell. By using light to create ATP, the need for food may be decreased, leading to a decrease in electron transport to electrodes and electricity generation. While this is not the result we are ultimately seeking, this first attempt at electrically engineering *Geobacter* is still useful for several reasons.

Even if we learn that the expression of bR in *Geobacter* reduces its need for food, this could create an organism that would be able to grow well even if given intermittent chemical food. Growing photosynthetically would allow the cells to live through nutrient droughts without the need to restart the bacterial community. By learning that bR in the normal orientation decreases the need for food, it might be possible to reverse this effect by engineering bR to be inserted in the opposite orientation within the membrane. This has been successfully carried out with other membrane proteins, and it would be important to attempt with bR as well. Reversing the orientation of the bR proton pump would work against the gradient set up by oxidation of food molecules, and would require the cells to oxidize more of these—and generate more electrons to be transferred—in order to create the same necessary amount of ATP.

There are also other ways to try to increase the food intake and electron output of *Geobacter*. The ATP synthesis complex proteins could be engineered by mutating the genes to come up with a set of proteins that contained mutations. These could then be screened to find ones that are still functional, but are less efficient at converting the proton gradient into ATP; these less efficient proteins would require a larger gradient set up by the oxidation of more food compounds in order to supply the same amount of energy needed for the cell to live.

## **7.5 MFC Conclusions**

Microbial Fuel Cells have the potential to radically alter space systems design, by coupling advanced life support with power production, and also raising the possibility of “growable” in-situ fuel production on Mars. Development of a MFC for space will be an exercise in highly multi-disciplinary design optimization, including interdependent factors such as waste stream analysis, microbe selection, materials selection, bioreactor

design, and fuel cell geometry. During our Phase I study we have made significant progress in each of these areas.

Specifically, we have:

1. Created high-level mission scenarios for the use of microbial fuel cells
2. Calculated an upper bound for power output
3. Developed a systems dynamics model to test assumptions about various mission scenarios and calculate the power output as a function of in-situ resources and waste stream assumptions
4. Identified the critical areas that must be investigated for fuel cell optimization, and identified some pathways for such optimization
5. Identified potential fuel reduction pathways using cascading microbial fuel cells
6. Identified bioreactors that may be modified for MFC use
7. Created a fuel cell sizing model using baseline assumptions for bioreactor geometry
8. Create test microbial fuel cells for use of *G. sulf*
9. Conducted genetic tests to couple photo-active proteins *Rhodopsin* with electrigen microbe *Geobacter*

## 8 Conclusion

In our proposal we noted that Synthetic Bio-electric sources could:

- Radically extend exploration capability through higher-potency power storage and generation and scavenging techniques.
- Eliminate the need for nuclear generators and/or solar cells that degrade with time – instead, an organic system has the potential to improve with time.
- Provide the ability to fabricate or “grow” power generating capability in-space or at a planetary site, resulting in scalable and flexible long-duration missions.
- Be self-organizing and self-healing; provide increased reparability on site
- Simultaneously address other life-supporting functions like waste management, and material recycling, simplifying space system design.
- Lead to radically new system architectures.

Our investigation of electricity production in nature and its potential applications to space has confirmed and strengthened these hypotheses. The range of electricity production from proteins to organisms is astonishing. As importantly, we are now at a level of sophistication in biotechnology and materials and mechanical engineering that will allow the successful exploitation of these phenomena in working devices.

For the past seven months under this NIAC phase I project, we have had the unique opportunity to examine the problem of bio-electric power production from a practical perspective, rather than a narrow scientific perspective. In the process we have continuously linked the worlds of biotechnology, electrical engineering, and space systems design in order to lay the groundwork for a biological space power paradigm. This unique perspective has resulted in what we believe are important advances towards the creation of bio-synthetic power technologies. In particular, the ability to couple various electrically interesting biological entities such as Prestin, Rhodopsin, and Geobacter, holds enormous promise for the creation of working bio-machines. Further, our designs for the Power Skin and Bio-Electric Chambers are ready to move from conceptual design to detailed design and prototype.

The material in this report has summarized our historical, conceptual and experimental investigations into this fascinating area. We hope that it will provide a basis for continued and systematic analysis of space-power possibilities in the future.

# Appendix

## Appendix-I: Experimental Procedures for Power Skin

### Agarose Gel Electrophoresis

#### Casting agarose gels

##### Materials

- 1X TAE
- SYBR safe (10,000X stock)
- Agarose
- Microwave
- Stir plate and stir bar (optional)

##### Procedure

1. Add 300mL 1X TAE to a 500 mL bottle.
2. Measure out sufficient agarose to cast either a 1% (3 g) or 1.5% (4.5 g) gel.
3. Add the agarose to the TAE buffer in the 500 mL bottle.
4. Swirl to mix.
5. Microwave bottle with loosened cap on high until the gel starts to bubble and is transparent.  
*This generally takes just over two minutes for 300 mL. If you microwave too long, the gel will bubble over causing a big mess and you will need to start over.*
6. Remove from microwave and let cool by either sitting on bench top or adding stir bar and placing on stir plate.  
*The advantage of the stir plate is that, if you forget about your gel for a while, it is less likely to solidify accidentally.*  
*If you are in a hurry, you can place the bottle in a beaker of room temperature water on the stir plate to speed the cooling process significantly.*
7. While gel is cooling, assemble casting trays and gel combs and verify that the trays are level.
8. Once gel is cooled so that it can be touched comfortably with your gloved hand, add 30  $\mu$ L SYBR Safe (10,000X concentrate).
9. Pour gel into casting trays.  
*The height of the gel will depend on how much you wish to load. Diagnostic gels can be reasonably shallow since typically 10  $\mu$ L volumes are loaded. For gel purifications, the gel should be deeper to enable loading of large sample volumes.*
10. Let gels sit until they are solidified.  
*Gels are solid when they are cloudy in appearance and firm to the touch.*
11. Gels may be used immediately. Alternatively, gels may be individually sealed in 6 x 10 inch polyethylene bags, labelled with initials, date and percentage and stored at 4 °C.

*It is a judgement call as to whether a gel is too old to be used. If it takes on a shrivelled appearance, don't use it. If there is lots of condensation on the bag, only use it if your intended experiment isn't critical.*

## Running agarose gels

### Materials

- Prepared DNA ladder
- Precast gel with the appropriate percentage and well size/numbers for your samples (see above)
- 1X TAE
- Loading dye

### Procedure

1. Take a gel from the 4°C fridge.  
*If the number of gels is getting low, cast more gels as described above.*
2. Place your gel in gel box.
3. Add 1X TAE buffer to gel box such that buffer just covers the top of the gel.
4. Remove comb.
5. Load 12 µL prepared ladder  
*Typically load ladder in left-most lane and sometimes right-most lane as well depending on whether you have the space.*
6. Use 2 µL loading dye per 10 µL of sample.
7. Load samples left to right.  
*The capacity of the 8 well, 1.5mm wide well is approximately 45 µL. The capacity of the 15 well, 1.5mm well is approximately 15 µL.*
8. Place gel box cover on gel box such that your samples will run towards the positive, red electrode.
9. Run your gel at ~85 volts for 1 hr 20 mins. Use the timer to enable automatic shutoff of your gel.  
*If you are in a hurry the gel can be run faster at ~95 volts for less than an hour.*
10. Verify that bubbles are rising from the electrodes once you start your gel to ensure your gel is running properly.

## Visualizing agarose gels

### Materials

- FluorChem 8800 gel imager

### Procedure

1. Remove gel from gel box shaking gently to allow residual buffer to fall back into gel box.



2. Place in middle of UV box inside gel imager (you can leave the gel in gel tray).
3. Make sure that filter wheel is set to position 4 (SYBR gold).
4. Close the door and turn on reflective white light button.
5. In gel imager software, click the "Acquire" button such that gel displays on screen.
6. Adjust gel position on UV box so that the entire gel is within the frame.
7. Close the door, turn off reflective white light and turn on transilluminating UV light.
8. In gel imager software, click "Acquire image" button to capture gel image to the screen.  
*It is occasionally necessary to adjust exposure time to improved image.*
9. Increase filtering if bands are difficult to see.
10. Annotate gel as necessary.
11. Save a copy of gel picture in your user folder.
12. Print.
13. Remove gel and throw in trash.
14. Wipe down UV box if necessary.

## DNA from *Escherichia coli* cells

### Materials

For purifying plasmid DNA from *Escherichia coli* cells, the Qiagen Spin Miniprep Kit produces quite reliable results.

Buffer P1 (in case you need to make it yourself) is:

- 50 mM Tris-HCl pH 8.0
- 10 mM EDTA
- 10 µg/ml RNaseA

The buffer and RNaseA can also be ordered from Qiagen separately (catalog numbers 19051 and 19101).

### Protocol

#### QIAprep Spin Miniprep Kit Using a Microcentrifuge

This protocol is designed for purification of up to 20 µg of high-copy plasmid DNA from 1–5 ml overnight cultures of *E. coli* in LB (Luria-Bertani) medium. For purification of low-copy plasmids and cosmids, large plasmids (>10 kb), and DNA prepared using other methods, refer to the recommendations on page 37. Please read “Important Notes” on pages 19–21 before starting. Note: All protocol steps should be carried out at room temperature.

### Procedure

1. Resuspend pelleted bacterial cells in 250  $\mu$ l Buffer P1 (kept at 4 °C) and transfer to a microcentrifuge tube.  
Ensure that RNase A has been added to Buffer P1. No cell clumps should be visible after resuspension of the pellet.
2. Add 250  $\mu$ l Buffer P2 and gently invert the tube 4–6 times to mix.  
Mix gently by inverting the tube. Do not vortex, as this will result in shearing of genomic DNA. If necessary, continue inverting the tube until the solution becomes viscous and slightly clear. Do not allow the lysis reaction to proceed for more than 5 min.
3. Add 350  $\mu$ l Buffer N3 and invert the tube immediately but gently 4–6 times.  
To avoid localized precipitation, mix the solution gently but thoroughly, immediately after addition of Buffer N3. The solution should become cloudy.
4. Centrifuge for 10 min at 13,000 rpm (~17,900 x g) in a table-top microcentrifuge.  
A compact white pellet will form.
5. Apply the supernatants from step 4 to the QIAprep spin column by decanting or pipetting.
6. Centrifuge for 30–60 s. Discard the flow-through.  
*Spinning for 60 seconds produces good results.*
7. (Optional): Wash the QIAprep spin column by adding 0.5 ml Buffer PB and centrifuging for 30–60 s. Discard the flow-through.  
This step is necessary to remove trace nuclease activity when using endA<sup>+</sup> strains such as the JM series, HB101 and its derivatives, or any wild-type strain, which have high levels of nuclease activity or high carbohydrate content. Host strains such as XL-1 Blue and DH5 $\alpha$ <sup>TM</sup> do not require this additional wash step.  
*Although they call this step optional, it does not really hurt your yield and you may think you are working with an endA<sup>-</sup> strain when in reality you are not. Again for this step, spinning for 60 seconds produces good results.*
8. Wash QIAprep spin column by adding 0.75 ml Buffer PE and centrifuging for 30–60 s.  
*Spinning for 60 seconds produces good results.*
9. Discard the flow-through, and centrifuge for an additional 1 min to remove residual wash buffer.  
**IMPORTANT:** Residual wash buffer will not be completely removed unless the flow-through is discarded before this additional centrifugation. Residual ethanol from Buffer PE may inhibit subsequent enzymatic reactions. *They are right about this.*
10. Place the QIAprep column in a clean 1.5 ml microcentrifuge tube. To elute DNA, add 50  $\mu$ l Buffer EB (10 mM Tris·Cl, pH 8.5) or water to the center of each QIAprep spin column, let stand for 1 min, and centrifuge for 1 min.  
*If you are concerned about the concentration of the DNA, you can alternatively add 30  $\mu$ L water to the center of the column, incubate at room temperature on the bench for 5 mins and then centrifuge for 1 min. This will increase the concentration of DNA in your final sample which can be useful in some cases. See notes below for why you should elute in water rather than the Buffer EB they recommend if you plan to sequence your sample. Even if you are not sequencing, it may be beneficial to elute in water. For instance, if you elute in buffer EB and*

*you are using this DNA in a restriction digest, then the additional salts in your sample can affect the salt content of your digest. This may matter with some finicky enzymes.*

## Notes

- If you are doing more than ~10 minipreps simultaneously, it can save time to switch to the vacuum manifold version of this protocol since you eliminate having to load and unload samples into the centrifuge.
- The sequencing center has begun using new machines and as a result you may want to consider eluting in water rather than EB. See note from sequencing center.

The elution is dependent on pH, however measuring the pH of unbuffered water is difficult. However, anecdotally we have been able to get good yields using the water from the stock room. Eluting in deionized water from the Knight lab has also produced good results.

- I use the "mini-fuge" for the binding and washing steps. You still have to do the drying step after the **PE** wash in a "real" microfuge though.
- Passing the lysate over the column twice increases yield by about 20%.
- Contaminating salt from the initial lysate or the **PB** will ruin a sequencing reaction more frequently than eluting in the **EB** (10 mM Tris as a small component of the total sequencing reaction is negligible). I always elute with **EB** and my reactions sequence just dandy. There are two major sources of salt contamination: the inside upper edge of the spin column and the residual **PB** mixing with the **PE** wash. When you add the initial **PE**, it mixes with the leftover junk in the column. Spinning this through can only lower the salt to a level that was present after mixing. To get around these problems, I do two **PE** washes of about 300-500  $\mu$ L. For the the first, I dispense the liquid from the pipette tip along the inner ledge of the spin column in a circular motion to wash off the residue there. I follow the first **PE** wash with a second to further de-salt the sample before the drying spin. Yes, it adds a step, but the time spend here is far less than waiting three days only to find out your sequencing didn't work.

## Reagents

- T4 DNA ligase
- 10x T4 DNA Ligase Buffer
- Deionized, sterile H<sub>2</sub>O
- Purified, linearized vector (likely in H<sub>2</sub>O or EB)
- Purified, linearized insert (likely in H<sub>2</sub>O or EB)

## Procedure

### 10 $\mu$ L Ligation Mix

*Larger ligation mixes are also commonly used*

- 1.0  $\mu\text{L}$  10X T4 ligase buffer
- 6:1 molar ratio of insert to vector (~10ng vector)
- Add (8.5 - vector and insert volume) $\mu\text{L}$  ddH<sub>2</sub>O
- 0.5  $\mu\text{L}$  T4 Ligase

#### Calculating Insert Amount

$$\text{Insert Mass in ng} = 6 \times \left[ \frac{\text{Insert Length in bp}}{\text{Vector Length in bp}} \right] \times \text{Vector Mass in ng}$$

The insert to vector molar ratio can have a significant effect on the outcome of a ligation and subsequent transformation step. Molar ratios can vary from a 1:1 insert to vector molar ratio to 10:1. It may be necessary to try several ratios in parallel for best results.

#### Method

1. Add appropriate amount of deionized H<sub>2</sub>O to sterile 0.6 mL tube
2. Add 1  $\mu\text{L}$  ligation buffer to the tube.  
Vortex buffer before pipetting to ensure that it is well-mixed.  
Remember that the buffer contains ATP so repeated freeze, thaw cycles can degrade the ATP thereby decreasing the efficiency of ligation.
3. Add appropriate amount of insert to the tube.
4. Add appropriate amount of vector to the tube.
5. Add 0.5  $\mu\text{L}$  ligase.  
Vortex ligase before pipetting to ensure that it is well-mixed.  
Also, the ligase, like most enzymes, is in some percentage of glycerol which tends to stick to the sides of your tip. To ensure you add only 1  $\mu\text{L}$ , just touch your tip to the surface of the liquid when pipetting.
6. Let the 10  $\mu\text{L}$  solution sit at 22.5°C for 30 mins
7. Denature the ligase at 65°C for 10min
8. Dialyze for 20 minutes if electroporating
9. Use disks shiny side up
10. Store at -20°C

#### Restriction Digestion

##### Materials

- Restriction enzymes (EcoR I, Spe I, Xba I or Pst I) from NEB
- EcoR I buffer
- BSA
- Deionized, sterile H<sub>2</sub>O

##### Digest Mix

*Example - 50  $\mu$ L reaction. 100  $\mu$ L reactions are also common especially if your DNA to be cut is dilute.*

- 5  $\mu$ L EcoR I buffer (for all digests with BioBricks enzymes, we use EcoR I buffer. It keeps things simple and seems to work).
- X  $\mu$ L DNA (usually  $\sim$ 1  $\mu$ g depending on downstream uses).
- 0.5  $\mu$ L 100X BSA (added to all digests because BSA never hurts a restriction digest)
- 1  $\mu$ L BioBricks enzyme 1 (regardless of the volume of the reaction, 1  $\mu$ L enzyme is used because generally this represents a 10-25 fold excess of enzyme and is therefore sufficient for most digests. Also, it can be difficult to accurately pipet less than 1  $\mu$ L of enzyme since it is sticky due to the glycerol content.)
- 1  $\mu$ L BioBricks enzyme 2
- (42.5 - X)  $\mu$ L deionized, sterile H<sub>2</sub>O

#### Procedure

1. Add appropriate amount of deionized H<sub>2</sub>O to sterile 0.6 mL tube
2. Add restriction enzyme buffer to the tube.  
Vortex buffer before pipetting to ensure that it is well-mixed.
3. Add BSA to the tube.  
Vortex BSA before pipetting to ensure that it is well-mixed.
4. Add appropriate amount of DNA to be cut to the tube.  
Vortex DNA before pipetting to ensure that it is well-mixed.
5. Add 1  $\mu$ L of each enzyme.  
Vortex enzyme before pipetting to ensure that it is well-mixed.  
Also, the enzyme is in some percentage of glycerol which tends to stick to the sides of your tip. To ensure you add only 1  $\mu$ L, just touch your tip to the surface of the liquid when pipetting.
6. Place in thermal cycler (MJ Research, PT-200) and run digest protocol.
  1. 4-6 hour incubation at 37°C  
Use a longer incubation time if you have time or are worried about the efficiency of cutting. I think this time can be shortened to 2 hrs while still cutting to completion.
  2. 20 mins at 80°C to heat inactivate enzyme.  
This step is sufficient to inactivate even Pst I.
  3. 4°C forever (or until you pull the reaction out of the thermal cycler).
7. Generally, use some method of DNA purification to eliminate enzymes and salt from the reaction.

## Appendix II: Detailed MFC Experiment Review

The area of Microbial Fuel Cell is a rapidly advancing field. We conducted a detailed review of existing MFC architectures, in order to assess the state of the art and further develop our architectural model. Most of these fuel cells have been developed for experimentation. Power outputs and efficiency have been rising consistently over the past few years (two main metrics used to evaluate the fuel cells are coulombic efficiency and total power which is best measured as a power density). Most of the systems analyzed were either two-chamber experimental MFCs or single-chamber systems. It has been demonstrated that single-chamber systems can have high power densities. Some recent research has focuses on better flow-through systems. The experiments for the systems listed below are described where possible.

### Lovely two chamber Fuel Cell (2006)

**Goal:** Test single-strain MFCs

**Architecture:** Double-chamber, graphite anode

**Microbe:** *Geobacter sulfurreducens*

**Fuel:** Acetate

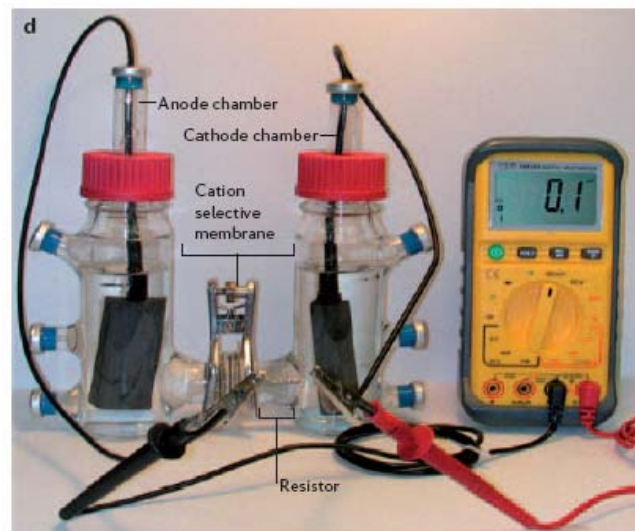


Figure 37: Example MFC in beaker (lovely, 2006) This is not optimized for electricity production but is used to test different bacteria strains.

### Min et al 2005:

**Goal:** Electricity from Swine Waste

**Architecture:** They tested both a two-chamber MFC using beakers (as in Lovely 2006) and a single-chamber MFC without a PEM exactly like Lui and Logan above. **Resistor:** 1000 Ohm

**Anode:** Carbon Paper from E-teck

**Cathode:** Carbon paper submerged in a phosphate buffer solution. (pH = 7;

2.75 g/L Na<sub>2</sub>HPO<sub>4</sub> + 4.22 g/L NaH<sub>2</sub>PO<sub>4</sub> + H<sub>2</sub>O)

**PEM:** For two chamber system Nafion 117; for single chamber, no PEM used

**Microbes:** Used only those present in swine-waste

**Results:** Max Power for two chamber system was: 45 mW/m<sup>2</sup> (1000 Ohm, 141 mA/m<sup>2</sup>); Max Power for Single Chamber system: 261 mW/m<sup>2</sup> (200 Ohm, 1.2 A/m<sup>2</sup>)  
The single chamber system was 6 times more powerful than the double chamber system. Swine waste was used pure but also tested *pretreated* by diluting it and then sonicating or autoclaving it. Sonicating it broke up the pieces which should have increased power output, but the effect was minima. Autoclaving should have killed anerobic bacteria. No significant difference resulting from this pre-treatment.

### Rabaey et al 2004

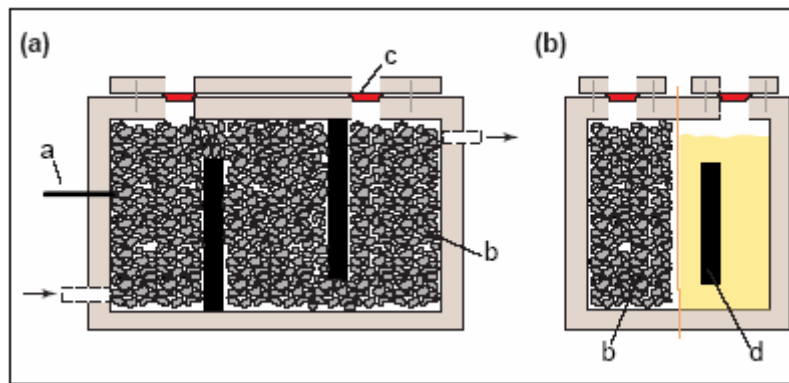


Figure 38: Carbon Gravel MFC [Rabaey 2004]

### Neissen, et al 2004

**Goal:** Using a polymer coated platinum anode to create electricity using hydrogen derived from biological sources.

**Microbe:** Clostridium butyricum and Clostridium beijernickii

**Architecture:** Simple 2-chamber MFC

**PEM:** Nafion

**Cathode:** Carbon paper in buffer solution

**Fuel:** Starch, Molasses

**Result:** Max power was about 2.6 W/M<sup>2</sup> this was a big increase at the time due to the platinum catalyst and hydrogen. Platinum can soil and poison the microbes. This was prevented using a special polymer coating.

### Lui and Logan 2004

**Goal:** Test absence of PEM

**Architecture:** Single-Chamber MFC with anode/cathode on opposite sides of the plexiglass cylinder (4cm by 3cm) used in batch mode. *Platinum wire* connected the circuit with a 1000  $\Omega$  resistor

**Input:** Domestic waste-water with no seed bacteria, input and bacteria allowed to grow.

**Anode:** made out of Toray carbon paper (E-Tek) and did not contain catalysts.

**Two cathodes**

- With PEM: PEM (nafion 117, dupont) attached to carbon cloth electrode which included .5 mg/cm Pt catalyst (E-tek)
- Without PEM: More rigid carbon paper with .35 mg/cm<sup>2</sup> of Pt.

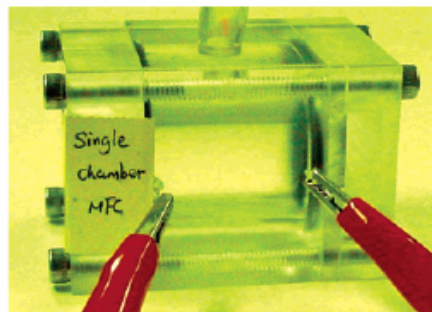
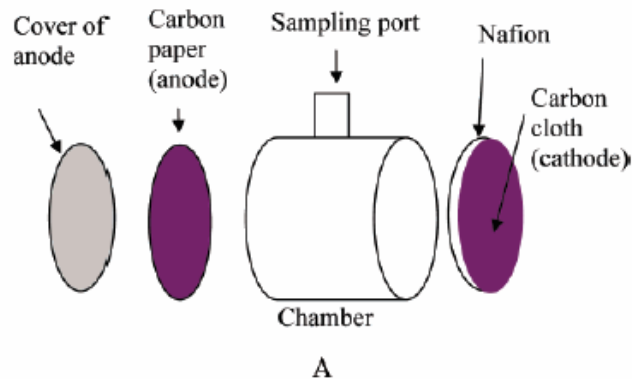


Figure 39: LIU 2004, Single Chamber MFC with anode and cathode on either side. (est 2.2 W/m<sup>2</sup>)

**Result:** The above fuel cell used an air cathode and was tested with and without a proton exchange membrane. Remove the PEM increased power density (2.2 w/M<sup>2</sup>), but allows oxygen to diffuse into the chamber which reduces Coulombic efficiency (it was estimated at 40-55% for glucose fed system with PEM but only 9-12% without PEM). Even with Nafion they estimate that oxygen diffuses into the chamber at a rate of 0.05 mg/L. They note that another reason for loss of Coulombic efficiency is simply the resistance used. Rabaey et al observed a Coulombic of 89% but used a very low 100  $\Omega$  resistor.

## 2. Lui et al 2004

**Goal:** Flow-Through MFC for waste remediation



**Architecture:** Single cylindrical plexiglass chamber tubular MFC for flow-through (15cm long by 6.5cmdiameter; empty bed volume of 388 mL)

**Input:** Domestic Waste Water, no seed bacteria.

**Anode:** Eight graphite rods (anode) each 6.15 mm in diameter and 150 mm long (Alfa Aesar, Ward Hill, MA) placed in a concentric arrangement about a single cathode. The graphite rods were abraded by sand paper to enhance bacterial attachment.

**Cathode:** air-porous cathode consisted of a carbon/platinum catalyst/proton exchange membrane (PEM) layer fused to a plastic support tube.

**PEM:** The PEM (Nafion 117, Dupont, Wilmington, DE) was sequentially boiled in H<sub>2</sub>O<sub>2</sub> (30%), deionized water, 0.5 M H<sub>2</sub>SO<sub>4</sub>, and then deionized water (each time for 1 h). The PEM was then hot pressed directly onto carbon cloth loaded with 0.5 mg cm<sup>-2</sup> of Pt (E-Tek, Miami, FL) by heating it to 140 °C at 1780 kPa for 3 min.

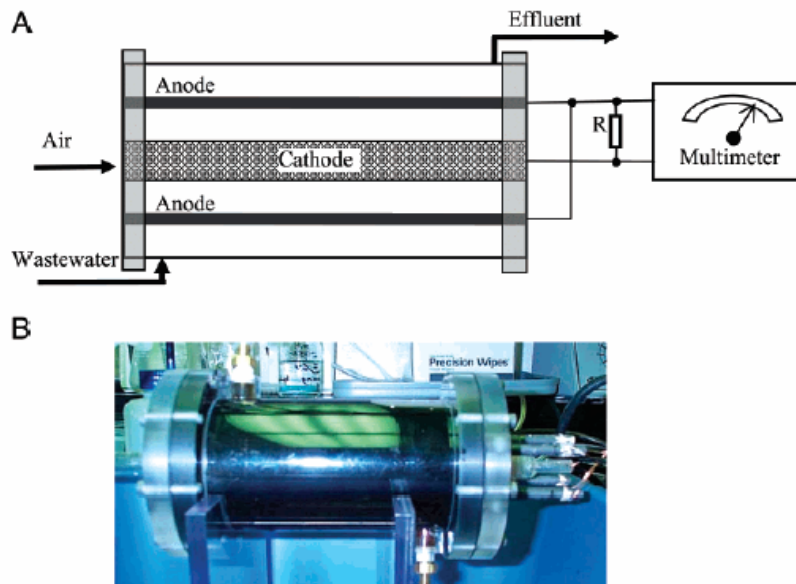


Figure 40: Cylindrical Flow-Through Fuel Cell [Lui et al 2004]

**Results:** Max Power Density: 26 mW/M<sup>2</sup> (varied with influent rates, and cathode issues); Waste-treatment: Removal of 80% of Chemical Oxygen Demand (COD); Coulombic Efficiency (based on COD removal and current): <12%

### Park et al 2001

**Goal:** Compare double and single compartment MFC and vary the anode material

**Microbe(s):** *E. coli*

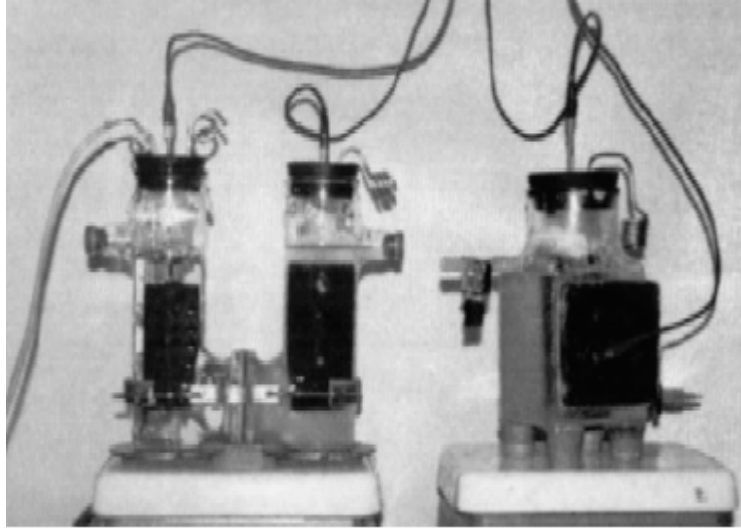


**Figure 41: Double and Single Compartment MFC (Park 2002)**

**Result:** The main results of this work are as follows: (1) a single compartment fuel cell produces nearly equivalent amounts of electricity as a more complex two-compartment system. (2) NR-graphite felt or Mn-graphite anodes are far superior to using normal graphite electrodes for bioenergy production. The Mn graphite electrode appears to perform as the best anode. (3) The Fe-graphite electrode is a superior fuel cell cathode when compared to graphite alone. (4) Using the single-cell fuel cell with the Mn-graphite anode and Fe-graphite anode can enhance the amount of electricity produced in microbial fuel cells and lower the cost of electricity production. [Park 2002]

## Appendix III: Microbes in Advanced Life Support

The concept of using biological systems for life support in space has a long history, dating back to as early as the 1950s [Myers, 1954; Krall and Kok, 1960; Golueke and Oswald, 1964; Krall and Kok, 1960, Golueke and Oswald, 1964; Eley and Myers, 1964; Miller and Ward, 1966]. Studies of closed-loop crop-growth were carried out by Russia in the early 1970s (BIOS project) and continue by various agencies to this day. These include the NASA-initiated the Controlled Ecological Life Support System (CELSS) program, NASA L/MSTP tests, the European Space Agency's Micro-Ecological Life Support System Alternative (MELISSA) Project, and the Canadian Space Agency Arthur C Clark Mars Greenhouse [MacElroy and Bredt, 1985; Galston, 1992; Gitelson et al., 1989; Tako, 1997; Salisbury et al., 1997; Barta et al., 1999; Lasseur and Savage, 2001; Bamsey, Silver et al, 2006].

Relevant studies on the use of biological organisms for waste remediation and recycling began seriously in the early to mid 1980s. This stream of research includes the use of fungus for cellulose degradation, the use of bioreactors for remediation and composting, and the use of aquatic ecosystems. Research in these areas is diverse and spans government, industry, and academic centers. Some specific projects with direct relevance to our proposal are highlighted below.

### NASA Lunar Mars Life Support Test Project (L/MSTP)

The L/MSTP was a large-scale test project run in three phases between 1995 and 1997 to verify the concept of bio-regenerative life-support. Early stages focused on atmospheric regeneration and water filtration, with human solid waste incineration and biological water filtration incorporated in phase III.

Phase III tests of combined biological and physiochemical processes for the treatment of wastewater for organic materials are directly relevant. These included two up-flow biological treatment compartments, the Immobilized Cell Bioreactor (ICB) and the Trickling Filter Bioreactor (TFB).

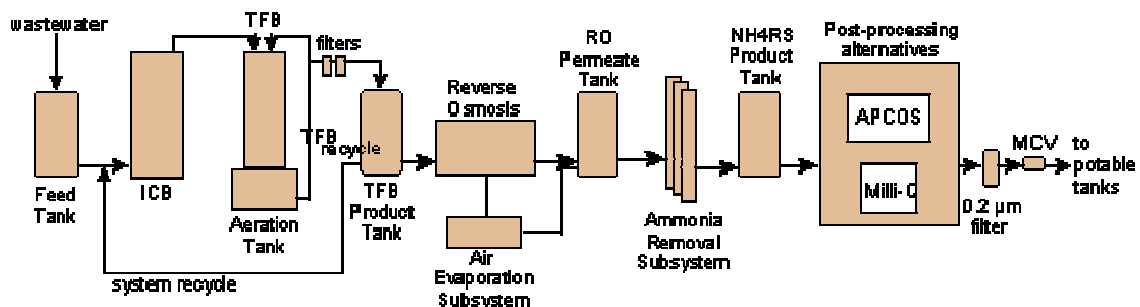


Figure 42: Water Filtration in the Phase III L/MSTP. (Courtesy: <http://advlifesupport.jsc.nasa.gov/>)

The ICB was an up-flow co-current reactor inoculated with a pre-mixed commercial inoculum of microorganisms. It has a nominal influent rate of 75 ml/min which was

mixed with recycled effluent flowing at 50 ml/min. Air was fed into this system and the flow rate adjusted twice Dailey. The *TFB* was designed for biological nitrification of wastewater ammonium. It is inoculated with microorganisms capable of converting ammonium ( $\text{NH}_4^+$ ) to nitrite ( $\text{NO}_2^-$ ) and nitrate ( $\text{NO}_3^-$ ) which are easier to remove.

### Breadboard Scale Aerobic Bioreactor (B-SAB)

Bioprocessing of wastes began at Kennedy Space center with the Closed Ecology Life Support System (CELSS) test bed, for which facilities and construction began in 1985. Objectives initially encompassed biological approaches for food and atmospheric regeneration (through crop production), biological waste treatment and recycling approaches. The breadboard Scale Aerobic Bioreactor was created at this time, including a continuously stirred tank bioreactor. During this project studies were run using grey water and simulated human waste as well as crop residues from the JSC LMSTP

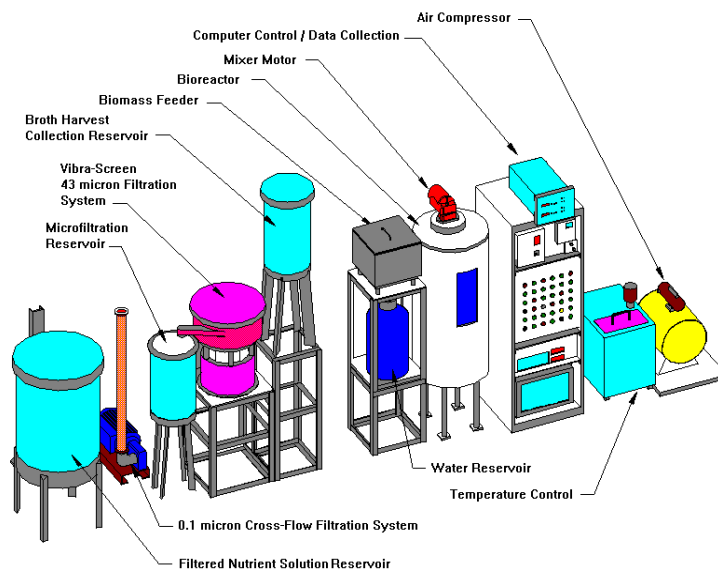


Figure 43: Components of the B-SAB (courtesy: <http://advlifesupport.jsc.nasa.gov>)

### European Space Agency Aquatic Ecosystem Regeneration

Another advanced example of relevant closed-loop life support systems is the European Space Agency's MELiSSA loop project. The main life support functions of MELiSSA are the recycling of waste (inedible biomass, feces, and urine),  $\text{CO}_2$ , and minerals, as well as the production of food, fresh water, and clean air. Based on the principle of an "aquatic" ecosystem, MELiSSA is comprised of four microbial compartments and a higher plant compartment (HPC).

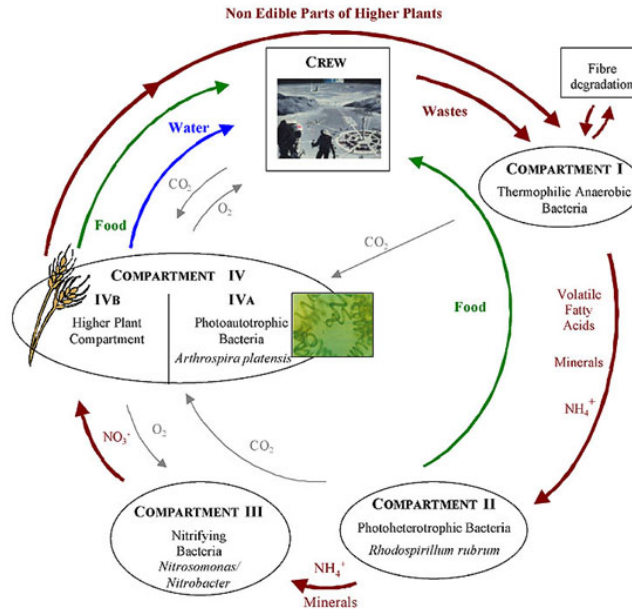


Figure 44: The "Melissa Loop" (source: <http://ecls.esa.int/>)

### Space ALS Research Conclusion

The results from these studies will inform our preliminary design. More detailed feasibility studies can use outputs from these experimental ALS systems as input assumptions about factors such as influent rates and organics and control of microbial growth. For example, simple theoretical extensions to these practical tests can be used to determine: the amount of electrical power that is generated, the amount of extra mass produced by introducing microbial fuel cell components and new microbial communities into advanced ICB designs, and how the up-flow configuration could be altered to increase anode area, and the affect on system functions.

## Appendix IV: Matlab Code for Sizing Model

```
% This Model calculates a cylinder fuel cell power output
% All units are centimeters unless otherwise stated

clear all
CellHeight = 25
CellLength = 25
CellWidth = 25

% Vary tube diameter, thickness, efficiency and determine output
effvary = 0:59 % input efficiency from 1 to 60 w/m^2 by 6
TubeIDvary = 0:.1:5.9 % Tube diameter from .5 to 3 by .25 centimeters

% Create a placeholder output array

Output = zeros (60)

%for this i is the row and j is the column so surface area increases
as you go down the matrix,
% and efficiency increases as you to the right in the matrix(up and
down)

for i = 1:60 %this varies the number of total rods based on their
diameter and calculates total surface area

    TubeID = TubeIDvary (i)
    TubeOD = TubeID + .5
    RodsHeight = floor(CellHeight/TubeOD) % Number of rods height-wise
    RodsLength = floor (CellLength/TubeOD)% Number of rods length-wise
    RodsTotal = RodsHeight*RodsLength
    RodSurface = pi*TubeID*CellLength % Surface area for one tube
    TotalSurface = RodSurface*RodsTotal/(100^2) % Total surface area in
m^2 the box

    for j = 1:60

        Efficiency = effvary (j) % This is the efficiency in
watts/meters squared
        TotalOutput = TotalSurface*Efficiency
        Output (i,j) = TotalOutput % i species how many row DOWN; j how
many columns OVER
    end
end

surf(effvary, TubeIDvary, Output) %creates a surface plot with diameter
on x, efficiency on y, value on z
```

## Bibliography

Allen, D. (1991). A Challenging Future for Improved Photovoltaic Systems. SDIO, 20-23.

Bailey, S. (2002). Photovoltaic Cell and Array Technology Development for Future Unique NASA Missions. IEEE, 799-804.

Beja O, Aravind L, Koonin EV, Suzuki MT, Hadd A, Nguyen LP, Jovanovich SB, Gates CM, Feldman RA, Spudich JL, Spudich EN, DeLong EF. (2000). Bacterial rhodopsin: evidence for a new type of phototrophy in the sea. *Science* 289 (5486): 1902-6.

Belyantseva I.A., Adler H.J., Curi R., Frolenkov G.I., Kachar B., 2000. Expression and localization of Prestin and the sugar transporter GLUT-5 during development of electromotility in cochlear outer hair cells. *J. Neurosci.* 20, RC116. (32)

Bertoncello, P. (2003). Bacteriorhodopsin-Based Langmuir-Schaefer Films for Solar Energy Capture. *IEEE Transactions on Nanobioscience*, 2(2), 124-134.

Bond, Daniel R., Derek R. Lovley. (2003) Electricity production by *Geobacter sulfurreducens* attached to electrodes. *Applied and Environmental Microbiology* 69:1548-1555.

Chaudhuri, S.K.; and Lovley, D.R. Electricity generation by direct oxidation of glucose in mediatorless microbial fuel cells. *Nature Biotechnol.* 21, 1229-1232 (2003).

Cheng, S.; Liu, H.; Logan, B.E. Increased power generation in a continuous flow MFC with advective flow through the porous anode and reduced electrode spacing. *Environ. Sci. Technol.* 40, 2426-2432 (2006).

Coppi, Maddalena V., Ching Leang, Steven J. Sandler, Derek R. Lovley. (2001) Development of a Genetic System for *Geobacter sulfurreducens*. *Applied and Environmental Microbiology.* 67:3180-3187.

Dallos P, Fakler B, 2002 Prestin, A new type of motor protein. *V3, Nature molecular cellular biology*, 104-111.

Eley, J.H. and J. Myers. 1964. Study of a photosynthetic gas exchanger. A quantitative repetition of the Priestley experiment. *Texas Journal of Science.* 16:296-333.

Energy and Power. *IEEE Aerospace and Electric Systems Magazine*, October 2000, 18-26.

Esper, Berndt, Adrian Badura and Matthias Rogner. (2006). Photosynthesis as a supply for (bio)-hydrogen production. *Trends in Plant Sci.* 11(11): 543-549

Feng, Jie, Hong-Can Liu, Jin-Fang Chu, Pei-Jin Zhou, Ji-An Tang, Shuang-Jiang Liu (2006) Genetic cloning and functional expression in *Escherichia coli* of an archaeorhodopsin gene from *Halorubrum xinjiangense*. *Extremophiles* 10:29–33

Flood, D. (1997). *Satellite Solar Energy Systems*. IEEE, 12.

Forge A. 1991, Structural features of the lateral walls in mammalian cochlear outer hair cells. *V265 Cell Tissue Res*, 473–83

Francis, R. (1988). *Issues and Opportunities in Space Photovoltaics*. IEEE, 1-13.

Golueke, C.G. and W.J. Oswald. 1964. Role of plants in closed systems. *Ann. Rev. Plant Physiol.* 15:387-408.

Hampp, NA. (2000) Bacteriorhodopsin: mutating a biomaterial into an optoelectric material. *Applied Microbial Biotech.* 53: 633-639.

Hoffmann, A. (2004). Photoactive Mitochondria: In vivo Transfer of a Light-Driven Proton Pump Into the Inner. *PNAS*, 91, 9367-9371.

Hoffmann, Astrid, Volker Hildebrandt, Joachim Heberle, Georg Boldt. (1994) Photoactive mitochondria: In vivo transfer of a light-driven proton pump into the inner mitochondrial membrane of *Schizosaccharomyces pombe*. *Biochemistry* 91:9367-9371.

Ikeda, T. 1990. *Fundamentals of Piezoelectricity*. Oxford University Press.

Iwasa K. H. 2001. A Two-State Piezoelectric Model for Outer Hair Cell Motility, *Biophysical Journal* Volume 81 November 2001 2495–2506

Jiang, Z. (1999). Bacterial Photoreceptor with Similarity to Photoactive Yellow Protein and Plant Phytochromes. *Science*, 285, 406-551.

Jones, P.A. (1998). *Spacecraft Solar Array Technology Trends*. IEEE, 141-153.

Kalinec F, Holley MC, Iwasa KH, Lim DJ, Kachar B. 1992, A membrane-based force generation mechanism in auditory sensory cells. *Proc Natl Acad Sci USA* 1992; 89: 8671–8675. (27)

Kim, Byoung-Chan, Ching Leang, Yan-Huai R. Ding, Richard H. Glaven, Maddalena V. Coppi, and Derek R. Lovley. (2005) OmcF, a Putative c-Type Monoheme Outer Membrane Cytochrome Required for the Expression of Other Outer Membrane Cytochromes in *Geobacter sulfurreducens*. *Journal of Bacteriology* 187:4505-4513.



Klodal Anna and Martinac Boris (2001). Common evolutionary origins of mechanosensitive ion channels in Archaea, Bacteria and cell-walled Eukarya. *Archaea* Vol 1, 2002, 35-44.

Korneel Rabaey and Willy Verstraete. "Microbial fuel cells: novel biotechnology for energy generation" *Trends in Biotechnology*, Volume 23, No 6. June 2006

Krall, A.R. and B. Kok. 1960. Studies on algal gas exchangers with reference to space flight. *Dev. Indust. Microbiol.* 1:33-44.

Kurland, R. (1989). Advanced photovoltaic Solar Array Program Status. IEEE Report, 829-835.

Lam, K (2005). Biological Self-Assembled Monolayers for Photosynthetic Solar Cell and Sensing Applications. 13th International Conference on Solid-State Sensors, Actuators and Microsystems, 1772-1780.

Lam, K. (2004). A Bio-Solar-Cell Powered by Sub-Cellular Plant Photosystems. IEEE, 220-224.

Lam, K. (2006). A MEMS Photosynthetic Electrochemical Cell Powered by Subcellular Plant Photosystems. *Journal of Micromechanical Systems*, 5(17), 1243-1252.

Lingler, S., Rubinstein, I., Knoll, W., Offenhäusser, A. (1997), Fusion of small unilamellar lipid vesicles to alkanethiol and thiolipid self-assembled monolayers on gold, *Langmuir*, 13, 7085-91

Liu, H.; Cheng, S.A.; Logan, B.E. Power generation in fed-batch microbial fuel cells as a function of ionic strength, temperature and reactor configuration. *Environ. Sci. Technol.* 39, 5488-5893 (2005).

Liu, H.; Logan, B.E. Electricity generation using an air-cathode single chamber microbial fuel cell in the presence and absence of a proton exchange membrane. *Environ. Sci. Technol.* 38, 4040-4046 (2004).

Lodish, H, A Berk, P Matsudaira, CA Kaiser, M Krieger, MP Scott, SL Zipursky, J Darnell. (2004). *Molecular Cell Biology*, 5<sup>th</sup> edition. New York: W. H. Freeman and Co.

Lovley, Derek R., Professor of Microbiology at University of Massachusetts, Amherst. Teleconference. November 1, 2006.

Lu, Yidong, Jingjing Xu, Baohong Liu, Jilie Kong. (2007). Photosynthetic reaction center functionalized nano-composite films: Effective strategies for probing and exploiting the photo-induced electron transfer of photosensitive membrane protein. *Biosensors and Bioelectronics* 22(7):1173-85.

Ludwig J. et al (2001). Reciprocal electromechanical properties of rat Prestin: the motor molecule from rat outer hair cells. *Proc. Natl Acad. Sci. USA* 98, 4178–4183.

Miller, R.L. and C.H. Ward. 1966. Algal bioregenerative systems. In: E. Kammermeyer (ed.) *Atmosphere in space cabins and closed environments*. Appleton-Century-Croft Pub., New York.

Min, B.; Cheng, S.; Logan, B.E. (2005) Electricity generation using membrane and salt bridge microbial fuel cells. *Water Res.* 39, 1675-1686.

Myers, J. 1954. Basic remarks on the use of plants as a biological gas exchangers in a closed system. *J. Aviation Med.* 25:407-411.

Naumann, R., Schmidt, E.K., Jonczyk, A., Fendler, K., Kadenbach, B., Liebermann, T., Offenhäusser, A., Knoll, W., (1999), The peptide-tethered lipid membrane as a biomimetic system to incorporate cytochrome c oxidase in a functionally active form, *Biosens. Bioelectr.* 14, 651-662

Oliver D. et al (2001). Intracellular anions as the voltage-sensor of Prestin, the outer hair cell motor protein. *V292 Science*, 2340–2343. (29)

Rabaey, K.; Boon, N.; Hofte, M.; and Verstraete, W. Microbial phenazine production enhances electron transfer in biofuel cells. *Environ. Sci. Technol.* 39, 3401-3408 (2005).

Rabaey, K.; Boon, N.; Siciliano, S.D.; Verhaege, M.; and Verstraete, W. Biofuel cell select for microbial consortia that self-mediate electron transfer. *Appl. Environ. Microbiol.* 70, 5373-5382 (2004).

Randal B. Bass, Pavel Strop, Margaret Barclay Douglas C. Rees. Crystal Structure of *Escherichia coli* MscS, a Voltage-Modulated and Mechanosensitive Channel. *Science* 22 Nov 2002 Vol 298

Reguera, G; Nevin, K.P.; Nicoll, J.S.; Covalla, S.F.; Woodard, T.L., Lovley, D.R. Biofilm and nanowire production leads to increased current in *Geobacter sulfurreducens* fuel cells. *Appl. Environ. Microbiol.* 72, 7345-7348 (2006).

Reguera, Gemma, Kevin D. McCarthy, Teena Mehta, Julie S. Nicoll, Mark T. Tuominen, Derek R. Lovley. (2005) Extracellular electron transfer via microbial nanowires. *Nature* 435:1098-1101.

Rittman, Bruce. “Environmental Biotechnology: Principals and Applications.” McGraw Hill Inc. NY, NY. 2001

Roundy, Shad. Energy scavenging for wireless sensor networks : with special focus on vibrations / by Shad Roundy, Paul Kenneth Wright, Jan M. Rabaey. Boston : Kluwer Academic Publishers, 2004.

Rupa Das, Patrick. (2004). Integration of Photosynthetic Protein Molecular Complexes in Solid-State Electronic Devices. *Nano Letters*, 4(6), 1079-1083.

Santos-Sacchi J., Shen W., Zheng J. & Dallos P (2001). Effects of membrane potential and tension on Prestin, the outer hair cell membrane protein. *V531, J. Physiol. (Lond.)*, 661–666

Senft, D. (2005). Opportunities in Photovoltaics for Space Power Generation. *IEEE*, 536-542.

Skulachev, V.P. (1976). Conversion of Light Energy by Bacteriorhodopsin. *FEBS Letters*, 64(1), 23-26.

Skulachev, V.P. (1982) A Single Turnover Study of Photoelectric Current-Generating Proteins. *Methods in Enzymology*, 88, 35-46.

Stella, P. (1990). Mission Applications for Advanced Photovoltaic Solar Arrays. *IEEE*, 1362-1368.

Sukharev, S. I., Blount, P., Martinac, B., and Kung, C. (1997). Mechanosensitive channels of *Escherichia coli*: The MscL gene, protein, and activities. *Annual Review of Physiology* 59, 633-657.

Sukharev, S. I., Blount, P., Martinac, B., Blattner, F. R., and Kung, C. (1994). A Large-Conductance Mechanosensitive Channel in *E. Coli* Encoded by MscL Alone. *Nature* 368, 265-268.

Sukharev, S. I., Schroeder, M. J., and McCaslin, D. R. (1999a). Stoichiometry of the large conductance bacterial mechanosensitive channel of *E.coli*. - A biochemical study. *Journal of Membrane Biology* 171, 183-193.

Sukharev, S. I., Sigurdson, W. J., Kung, C., and Sachs, F. (1999b). Energetic and spatial parameters for gating of the bacterial large conductance mechanosensitive channel, MscL. *Journal of General Physiology* 113, 525-539. Wood, J. M. (1999). Osmosensing by bacteria: Signals and membrane-based sensors.

Sukharev, S., Durell, S. R., and Guy, H. R. (2001). Structural models of the MscL gating mechanism. *Biophysical Journal* 81, 917-936.

Trinca, M. (2000). Bacteriorhodopsin: An All Natural, Organic Optical Computing Protein. *IEEE Potentials*, April/June.

Wheeler R.M., Mackowiak C.L, Stutte G.W, Yorio N.C., Ruffe L.M., Sager J.C., Prince R.P., Berry W.L, Peterson B.V., Goins G.D., Hinkle C.R., and Knott W.M. “Crop Production for Advanced Life Support Systems – Observations From the Kennedy Space Center Breadboard Project”

Wise, K. (2002). Optimization of Bacteriorhodopsin for Electronic Devices. Review: Trends in Biotechnology, 20(9), 387-345.

Zhang, L. (2003). High-Performance Behavior of Oriented Purple Membrane Polymer Composite Films. Biophysical Journal, 84, 2502-2507.

Zheng J., Long K.B., Robison D.E., He D.Z., Cheng J., Dallos P., Madison L.D. (2002). Identification of differentially expressed cDNA clones from gerbil cochlear outer hair cells. V7, Audiol. Neurootol, 277-288.

Zheng J., Long K.B., Shen W., Madison L.D., Dallos P., 2001. Prestin topology: localization of protein epitopes in relation to the plasma membrane. NeuroReport 12, 1929-1935.

Zheng J., Shen W., He D.Z.Z., Long K.B., Madison L.D., Dallos P., 2000. Prestin is the motor protein of cochlear outer hair cells. V405, Nature, 149-155. (3)